AN INVESTIGATION OF IMPROVEMENTS TO ELECTROCHEMICAL PRECIPITATION OF STRUVITE FROM SOURCE SEPARATED URINE

By Nicole Mulenga Malanda

Dissertation submitted in fulfilment of the requirements for the degree of Master of Science in Engineering

Department of Chemical Engineering

Faculty of Engineering and Built Environment

University of Cape Town

23 November, 2016

Declaration: I know the meaning of plagiarism and declare that all the work in this document, save for that which is properly acknowledged, is my own.

Signed digitally by Nicole Mulenga Malanda (22/11/2016)

Email: mlnnic004@myuct.ac.za

Signed by candidate

Acknowledgements

Praises be unto the LORD that has completed the good work that He started!

This research was funded by the Water Research Commission of South Africa. The financial support from the University of Cape Town, the Environmental and Process Systems Engineering Research Group and the Max and Lillie Sonnenburg Scholarship is also gratefully acknowledged.

I would like to thank my supervisors; Professor Harro von Blottnitz and Dr Dyllon Randall. Their support throughout this project was remarkable. I would like to thank them especially for their guidance and constant encouragement at every stage of this project even when I felt lost. Thank you for making me fall in love with my topic and the need to create a sustainable future for the upcoming generations. Thank you also for allowing me to own this project but always being there to share your wisdom. Harro, thank you for the funding, the support and all the hard work over the holidays and for making sure that I hand in a good dissertation. Dyllon, thank you for pushing me to get my submissions in on time. Finally, I sincerely appreciate the opportunity that you gave me to travel overseas for the first time in my life.

I would also like to thank EAWAG for availing their facilities and Dr Kai Udert for sharing his expertise and for allowing me the opportunity to collaborate with him on this project. I would also like to thank Brian Sinnet, Bettina Sterkele, Hanspeter Zöllig for the many scientific discussions and crazy ideas that we threw around and joked about. Thank you also to the laboratory staff; Karin Rottermann and Claudia Bänninger for assisting me with the analysis of samples. My appreciation also goes to Ms Carol Carr and Ms Ariane Eberhardt for making sure that all my funding and administrative issues were sorted out on time.

Most importantly, I would also like to thank my dear mother, Kretie Malanda. Your love and strength always amazes me. May this dissertation and qualification be your own accomplishment! I would also like thank my family and friends for the moral support that they gave me throughout the project. Thank you for the love. God bless.

Finally, I would also like to thank my dear friend Muziwami! You've held my hand throughout this journey; when I felt like giving up, you were always there to remind to keep my eyes on the "ultimate prize".

Access to decent sanitation remains a problem in developing countries. At the same time, sanitation technology is constantly evolving specifically regarding resource recovery solutions. Some chemical elements found in human excreta derived from non-renewable resources, and the recycling of phosphorous from sewage in particular is a possible solution to the growing issue of resource scarcity. A potential way to recover phosphorous from urine or water-borne sewage is through struvite precipitation. Struvite ($MgNH_4PO_4.6H_2O$) is a mineral that can be used as a slow-release magnesium, ammonium and phosphate based fertilizer and can be produced from urine by adding magnesium to the ammonium and phosphate rich urine. Usually, magnesium is dosed chemically using salts such as $MgCl_2$, MgO, $MgSO_4$ or bittern, together with pH regulating agents but these reactants produce unfavourable chemical by-products and the process tends to be expensive. Previous studies have proven that electrochemical dosing of magnesium is a feasible and reliable method of struvite precipitation. It not only produces high grade struvite that is valuable and marketable, but it also eliminates the need for alkalinity dosing in order to create a suitable pH environment for struvite precipitation. Further to that, electrochemical precipitation does not produce any harmful chemical by-products. Previous work shows that one main challenge that is associated with this method is the formation of a mineral layer on the magnesium anode called nesquehonite ($MgCO_3 \cdot 3H_2O$). This leads to increased electrode potentials and hence high energy consumptions and may also lead to system failures of the reactor. Further to that, struvite generally precipitates as small crystals that are difficult to separate from the solution, leading to low mass recoveries of the product. These small crystals are formed as a result of the high supersaturation, which generally occurs for most processes that are employed to make struvite.

In view of these problems, this dissertation presents an investigation of the potential improvements to the electrochemical precipitation of struvite from source-separated urine. The main aim is to minimise or eliminate the formation of mineral precipitates on the anode surface. It also looks into ways of increasing the crystal sizes of the struvite being precipitated in the electrochemical system. The methodology for this investigation involved modelling and experimental work. The specific objectives for this study were to:

a) Investigate how thermodynamic modelling of struvite precipitation compares to the experimental results from an electrochemical precipitation reactor,
b) Employ the aspect of seeding in an electrochemical reactor for struvite production and determine the technical feasibility of the proposed process,
c) Establish how to minimise the formation of nesquehonite so that the quality of struvite produced in the electrochemical reactor is not compromised,

d) Investigate how the crystal sizes of the struvite particles produced in the seeded electrochemical precipitation batch reactor setup compare to those produced in the continuously stirred reactor setup with a recycle that gives the particles a longer residence time,
e) Investigate the economics and energy requirements of the SEP (Seeded electrochemical precipitation reactor).

The results of the thermodynamic model suggested that the Mg:P molar ratio (magnesium to phosphorous molar ratio), the pH of the reaction environment and the presence of the constituent ions in adequate quantities play a critical role in the precipitation of struvite with regards to yield and purity. The model predicted that phosphorous conversion to struvite from stored urine can reach up to 98 % at Mg: P molar ratio of 1.2 and at a pH of 9.5. Complete P recoveries were obtainable at higher Mg:P molar ratios of up to 21, in a pH range of 9 to 10. However, nesquehonite also started to form at Mg: P molar ratios greater than 7.8 and between pH values of 6 and 12 due to excess magnesium ions and the presence of carbonate ions in the urine. Theoretically, the implication of this was a compromise on the quality of the struvite produced and, practically, also the likelihood of the formation of a passivation layer of nesquehonite on the sacrificial magnesium anode. As such, the magnesium concentration in the model was kept high enough to recover most of the orthophosphate present in the urine but low enough to avoid the formation of nesquehonite.

The optimum Mg:P molar ratio and pH range were tested experimentally using an electrochemical precipitation batch reactor with struvite seeds. A Mg:P molar ratio of 1.2 and pH of 9.5 proved to provide good operating conditions for phosphorous recovery of up to 96 % instead of the 98% that had been predicted by the thermodynamic model. The results of the seeded electrochemical precipitation experiments, at different seeding and stirring conditions, showed that seeding does not affect the rate and extent of phosphate recovery and the rate at which equilibrium is reached. This was due to the fact that the precipitation of struvite occurred extremely rapidly owing to its sparingly soluble nature and the degree of supersaturation of the solution, which also led to the fast precipitation of numerous small struvite crystals. Results of the thermodynamic model and those of the seeded electrochemical precipitation experiment were comparable with regards to the recovery of the orthophosphate from the source separated urine and the conversion of magnesium from the sacrificial anode. However, there were notable discrepancies with regards to the final pH and the conversion of the carbonate ions and thus the likelihood of the formation of nesquehonite.

The formation of the passivation layer of nesquehonite on the anode surface over time led to an increase in the magnesium electrode potential which translated to an increase in the cell potential by 130% from 1 V to 2.3 V. It was postulated that this was due to the relatively high level of magnesium supersaturation at the anode surface compared to the rest of the system which favoured the formation of nesquehonite. This was not computed in the thermodynamic model which assumed the system to be well mixed, however the simulations did show that nesquehonite does indeed form at high magnesium concentration. The precipitates that were collected in suspension were analysed for magnesium, orthophosphate and ammonium ions and the results also showed that these ions were present in a 1:1:1 ratio. Further to this, XRD results confirmed that the layer on the anode was indeed nesquehonite. This led to the conclusion that the precipitates that formed in suspension were struvite and most of the nesquehonite that formed only built up on the anode surface and did not affect the quality of the struvite collected.

Analysis of the size of the crystals that were produced in the electrochemical precipitation batch reactor over 2 hours showed that there was only a slight increase in the size of the resultant struvite particles after seeding. Two extreme stirring rates were also investigated and it was observed that high stirring rates produced larger particles than the lower stirring rate. This implies that the high stirring rate resulted in a decrease in the local supersaturation at the anode surface. This promotes particle size enlargement through a growth mechanism in the bulk solution rather than the formation of smaller particles through nucleation. Also, higher stirrer speeds could result in higher rate of particle-particle collisions and increased particle shear which would result in the formation of smaller particles. However, this appears not to be the case for this research. When the system was run continuously, i.e. by recycling the struvite particles back into the reactor with fresh urine in order to increase their residence time in the reactor, there was some growth of the crystals after 8 hours. The general shape exhibited by the particles was coffin like in all the images with other spherical and randomly shaped particles.

This dissertation has thus shown that the electrochemical precipitation of struvite from source separated urine can be improved in terms of the functionality of the system and the quality of product by i) seeding ii) stirring.

The cost of struvite precipitation in the seeded electrochemical precipitation reactor using a magnesium sacrificial anode was evaluated and compared against the cost of struvite precipitation by chemical dosage of magnesium with $MgCl_2$. The electricity and magnesium electrode costs were evaluated for the seeded electrochemical precipitation method while only the chemical costs for the chemical dosage method

were considered. Transport costs were neglected as they were assumed to be the same for both. The economic evaluation showed that the electrochemical precipitation method costs about ZAR 3.47 per kilogram of struvite while the chemical dosing method costs about ZAR 3.87 per kilogram of struvite produced. Since these costs are similar, it is recommended that this technology be investigated further. It is also important to note that chemical precipitation is an already proven technique for struvite production while electrochemical precipitation of struvite is relatively new, even though the core technology has existed for some time now. Therefore, there is likely more room for improvement and optimization in an electrochemical precipitation process while this might not be the case for chemical precipitation of struvite.

Also, since it is difficult to control the magnesium concentration on the anode surface, it is recommended that in order to suppress the formation of nesquehonite on the anode surface, the urine should be pre-treated in order to remove the carbonate ions which leads to the formation of nesquehonite. Pre-treatment could involve acidifying the solution in order to convert the carbonate slowly into unstable carbonic acid and then to carbon dioxide gas. This would be beneficial especially when the system is run continuously in order to influence crystal growth and essentially avoid system failures which would be caused by the build-up of the nesquehonite layer.

Table of Contents

Table of Contents

List of Tables

List of Figures

List of Figures

a	activity (mol/dm3)
A	sphere particle radius (m)
a*	activity at equilibrium (mol/dm3)
AH	Hamaker constant (J)
C	concentration (mol/dm3)
c	number of ions per m3
D	dielectric constant
e	elementary charge (C)
E	electric field (V/m)
G	Gibbs energy (J)
H	shortest distance between two stern layers (m)
k	boltzmann's constant (J/molecule.K)
kd	mass transfer coefficient
kr	reaction rate constant
Ksp	solubility product
J	mass flux ($kg/m^2.s$)
NA	Avogadro's constant (mol-1)
pHiep	iso-electric point
R	universal gas constant (J/mol.K)
S	supersaturation
T	temperature (kelvin)
z	valence

1 Introduction

1.1 Background

The recovery of plant nutrients such as phosphorous and nitrogen from waste streams is increasingly becoming a sustainable solution in both developing and developed countries. There is still a strong need to provide proper sanitation in developing countries and adherence to effluent nutrient concentration limits may be synergistic with nutrient recovery in both developed and developing countries. Nutrient recovery is important, particularly that of phosphorous, because natural phosphorous rock is predicted to be depleted in 50–100 years (Cordell et al., 2008). Dominant, amongst other uses, phosphorus is an essential plant nutrient and thus constituent in fertilizers. Over the years, research has focused on developing ways of recovering phosphorous from water-borne waste streams, *inter alia* by struvite precipitation.

Struvite ($\mathrm{MgNH_4PO_4.6H_2O}$), also known as MAP (magnesium ammonium phosphate), is a slow-release magnesium, ammonium and phosphate-based fertilizer and it can be produced from urine by dosing the ammonium and phosphate rich urine with magnesium. Struvite was first discovered in sewer systems and rendered problematic as it would build-up around the pipes, reducing their diameters and eventually blocking them, particularly on the walls of the anaerobic digestion system (Borgerding, 1972). Acid treatment would disintegrate the build-up but over time the problem resurfaced particularly in curves and bends of local high pH areas. This triggered an interest in the compound responsible for this, leading to the discovery of benefits of struvite as a fertilizer.

In order to produce struvite, ammonium and phosphate rich streams are dosed with magnesium compounds such as $\mathrm{MgCl_2}$, MgO or $\mathrm{MgSO_4}$, as well as pH regulating agents (Etter et al., 2011). However, these processes tend to release harmful chemical by-products and are generally expensive (Hug & Udert 2013; Kruk et al., 2014). Recent research has looked at the electrochemical dosage of high purity magnesium ions as a means of producing high quality struvite from waste water streams such as urine or the supernatant of fermented sludge from waste water treatment plants (Hug and Udert 2013; Kruk et al., 2014). These studies proved that electrochemical dosing of magnesium is a feasible and reliable method for struvite precipitation. It not only produces high grade struvite that is valuable and marketable, but it also eliminates the need for alkalinity dosing in order to create a suitable pH environment for struvite precipitation. Further to that, electrochemical precipitation does not produce any harmful chemical by-products.

Previous work by Bourgeois (2010) shows that one main challenge that is associated with this method is the formation of a mineral layer on the magnesium anode called nesquehonite ($MgCO_3 \cdot 3H_2O$). This leads to increased electrode potentials and hence high energy consumptions and may also lead to system failures of the reactor. Further to that, struvite generally precipitates as small crystals that are difficult to separate from the solution, leading to low mass recoveries of the product. These small crystals are formed as a result of the high supersaturation of the system, which generally occurs for most processes that are employed to make struvite.

1.2 Problem statement

Struvite, a phosphorous rich compound is a slow-release fertilizer that can be produced from urine by dosing with magnesium. Electrochemically dosing an ammonium and phosphorous rich stream with magnesium released from a high purity magnesium alloy leads to the production of high quality struvite that is free of by-products that would otherwise exist if magnesium is dosed as a chemical compound. Electrochemical precipitation of struvite from urine, however, may be accompanied by the formation of a layer of nesquehonite mineral on the magnesium anode which results in increased electrode potentials that may lead to high energy consumptions and system failures of the reactor. Additionally, struvite normally precipitates as small particles that are difficult to separate due to the high supersaturation of the system. For electrochemical struvite production to be useful in practise, these challenges need to be overcome.

1.3 Objective

This dissertation thus presents an investigation of the potential improvements to the electrochemical precipitation of struvite from source-separated urine. It is believed that seeding might help to achieve high struvite recoveries by influencing the crystal growth by secondary nucleation so that the struvite product can be easily separated from the solution (Söhnel and Garside, 1992), hence seeding and other ways of increasing the crystal size of the electrochemically precipitated struvite are investigated. The other aim is to minimise or eliminate the formation of nesquehonite on the anode surface. The methodology for this investigation involved modelling and experimental work to understand the conditions under which nesquehonite is formed.

The specific objectives for this dissertation were to:

a) Investigate how thermodynamic modelling of struvite precipitation compares to the experimental results from an electrochemical precipitation reactor,
b) Investigate how to minimise the formation of nesquehonite so that the quality of struvite produced in the electrochemical reactor is not compromised,
c) Investigate the aspect of seeding in an electrochemical reactor for struvite production and determine the technical feasibility of the proposed process,
d) Investigate how the crystal characteristics (size, quality and morphology) of the struvite particles produced in the seeded electrochemical precipitation batch reactor setup compare to those produced in the continuously stirred reactor setup with a recycle that gives the particles more residence time,
e) Investigate the economics and energy requirements of the SEP (Seeded electrochemical precipitation reactor).

1.4 Scope of Research

The electrochemical precipitation of struvite from source-separated urine has been proposed as a new method of recovering pure struvite from source separated urine, with high yields. In this study, the reactor that was developed by Hug and Udert (2013) was modified to include the concept of struvite seeding. Thermodynamic modelling was carried out to determine the experimental conditions necessary to produce struvite of the highest purity possible in the seeded electrochemical precipitation reactor (SEP). Its feasibility was tested by running the reactor for different set times, hence the struvite purity and particle sizes were determined based on those set times. The presence of nesquehonite was also measured qualitatively and not quantitatively. This dissertation did not extensively investigate other methods of reducing the formation of nesquehonite beyond reporting on experiments carried out under specific operating conditions that are predicted to be ideal towards reducing the formation of nesquehonite based on the thermodynamic model. It also did not investigate the functionality of the reactor over longer operating times. This was due to time and resource constraints.

1.5 Outline of dissertation

From this introductory chapter, the dissertation proceeds into Chapter two, which assembles the relevant theories on the fundamentals of precipitation, electrochemistry and thermodynamic modelling. The literature review in Chapter three is a study of the literature and work that has been done and is pertinent to this study on the various ways of producing struvite, thermodynamic modelling and electrochemical precipitation of struvite. After the literature review, Chapter four details a combined

methodology of the modelling and experimental investigation for this study. The details of the description of the apparatus, experimental procedures and the analytical techniques that were used are covered in this chapter. Chapter five presents all the results that were obtained and the corresponding discussions on the results. Chapter six and seven cover the conclusions and the recommendations of the study, respectively. Finally, Chapter eight lists all the references that have been used in this dissertation.

The appendices are also included in Chapter nine and contain the raw data obtained from thermodynamic modelling, additional experimental results including particle spectra and SEM images, information on databases used and as well as sample calculations. The Assessment of Ethics in Research Projects form is also attached in the Appendices.

1.6 Context for the dissertation

This research was carried out as part of the WRC funded project K5/2218 “Nutrient and energy recovery from sewage”. Some of the findings included in this dissertation were also presented in a report to the Water Research Commission of South Africa which was authored by myself, Nicole Malanda, with contributions from my supervisors, Dyllon Randall and Harro von Blottnitz. Care has been taken to ensure that this dissertation is reflective of my own work, with contributions by others clearly identified.

2 Precipitation and electrochemistry theory

This chapter looks into the fundamentals of precipitation, electrochemistry and thermodynamic modelling. The theories in this chapter have been used for the formulation of the approach and the experiments of this study. They were also used to aid the electrochemistry calculations and draw logical conclusions from the results that were developed. The contents of this chapter have been derived from a couple of standard textbooks.

2.1 Chemical Precipitation

Chemical precipitation is a form of a crystallisation process whereby crystallisation occurs rapidly to form a sparingly soluble solid. Due to the high levels of supersaturation during precipitation, the process is less prone to secondary nucleation caused by the presence of solute material. The resultant particles are thus usually numerous and small in size; typically less than 10 μm. This also leads to difficult solid-liquid separation characteristics. Particles formed through precipitation are usually indistinctive amorphous particles which are difficult to separate however the extent to which secondary processes such as aggregation occur can influence the morphology of the particle (Söhnel and Garside, 1992).

Precipitation is a very important process in industry and post precipitation processes are very essential in determining the properties (size and morphology) of the resultant particles. The process is widely used in the food industry and also in the recovery valuable components from waste water streams such as dissolved metals and nutrients such as phosphorous. Precipitation can also be problematic in the case of spontaneous chemical precipitation which may occur within wastewater and water systems causing pipe blockages (Kroiss et al., 2011). The process of precipitation in industry involves the dosing of chemicals to prompt the process of precipitation, coagulation, co-precipitation and flocculation (the formation of separable macro-flocculants formed alongside particles and flocculants bound to organic matter) then finally the separation by either sedimentation, filtration, floatation and adsorption (deBarbadillo et al., 2012).

2.1.1 Supersaturation

The thermodynamic driving force behind all crystallisation processes is supersaturation and is evaluated by considering the chemical reaction that occurs between two soluble reactants to form a sparing soluble product. A solution with respect to supersaturation can be: undersaturated (solubility of the solids is not exceeded and therefore spontaneous nucleation will not occur), metastable or

oversaturated (solute concentration exceeds the equilibrium value and spontaneous nucleation will occur). The level of supersaturation governs particle rate processes such as nucleation, growth and aggregation. Saturation is defined as the difference, Δμ, between the chemical potential of the solute in solution μ, and the chemical potential of the solution in equilibrium with the solid phase, μ*, as shown in Equation 1:

$$\Delta\mu = \mathrm{RT}\ln(\mathrm{S}) \tag{1}$$

For the chemical precipitation reaction represented by Equation 2, at equilibrium, its solubility product is defined by Equation 3:

$$\mathrm{xA^{z+}} + \mathrm{yB^{z-}} \leftrightarrow \mathrm{A_xB_y} \tag{2}$$

$$\mathrm{K_{sp}} = (\mathrm{a_A^*})^{\mathrm{x}}.(\mathrm{a_B^*})^{\mathrm{y}} \tag{3}$$

Where a and $\mathrm{K_{sp}}$ are the activity of the ionic species and the equilibrium solubility product respectively. According to Mersmann (2001) and Söhnel and Garside (1992), the supersaturation of an aqueous solution expressed in ion activity is given in Equation 4:

$$\mathrm{S} = \left(\frac{(\mathrm{a_A})^{\mathrm{x}}(\mathrm{a_B})^{\mathrm{y}}}{\mathrm{K_{sp}}}\right)^{\frac{1}{\mathrm{x+y}}} \tag{4}$$

2.1.2 Nucleation

Nucleation is the initial formation of the first solid in the solution. It is as a result of the build-up of induced or spontaneous supersaturation. Supersaturation may be derived from change in temperature, pH, pressure and any appropriate strain to the system (Söhnel& Garside, 1992). When nucleation occurs in systems that do not already have precipitating matter and are at higher supersaturation levels; it is termed primary nucleation and if it occurs in the presence of already existing precipitating matter and at lower supersaturation levels, it is termed secondary (Mullin, 2001). The latter takes place when seeding material is introduced and reduces the nucleation energy requirements as the crystal growth starts on the seeding surface (Nieminen, 2010; CEEP, 2013). Primary nucleation is further subdivided into homogeneous and

heterogeneous nucleation whereby the latter is initiated by the presence of a foreign solid phase and former is not (Mullin, 2001). Figure 1 shows the nucleation pathways.

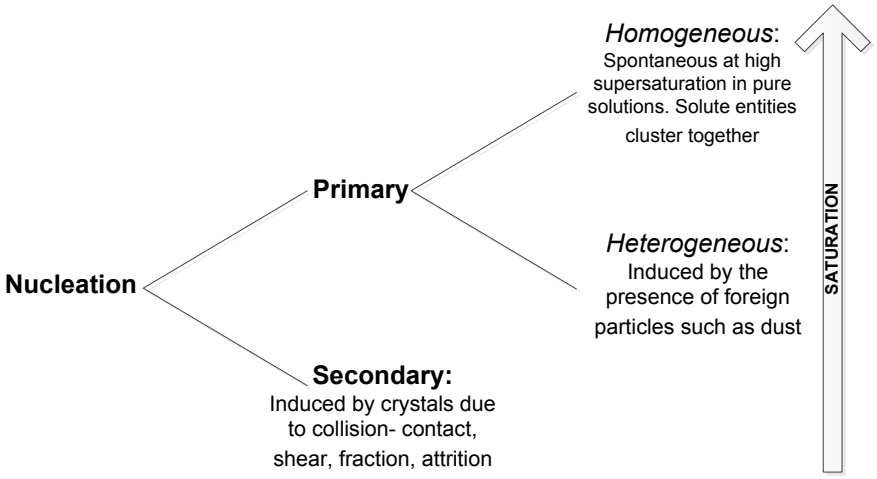

Figure 1: Nucleation mechanisms, modified from (Mullin, 2001).

2.1.3 Growth

After the formation of nuclei in a supersaturated solution, they begin to grow into crystals; first by mass transportation (bulk diffusion) of solutes from the bulk solution to the crystal interface. This is then followed by the arrangement of the growth units into the crystal lattice through surface integration (Mullin, 1972).

The concentration gradient which makes the system supersaturated, defined as:

$\Delta C = C - C^*$, can be divided into two parts i.e. the diffusive-convective transport, defined as: $C - C_1$ and $C_1 - C^*$, with the latter being the most influential for the integration reaction within a reaction boundary layer (Mullin, 1972). Equation 5 defines the scenario when growth is determined by diffusion and convection and Equation 6, when it is defined by the integration step:

$$\frac{C_I - C^*}{C - C_I} \leq 1 \tag{5}$$

$$\frac{C - C_I}{C_I - C^*} \leq 1 \tag{6}$$

$$\dot{m} = k_d (C - C_I) = k_r (C_I - C^*)^r \tag{7}$$

Equation 7 defines the flux density, $(\dot{m})$, where I represents interfacial conditions, * represents conditions at equilibrium, k_d is the mass transfer coefficient, k_r is the rate

constant, r is the order of integration and C is the concentration. Temperature dependence of the reaction rate constant is generally defined by the Arrhenius equation (Mullin, 2001).

2.1.4 Aggregation

This is the coming together of particles with or without their consequent cementation by crystal bridges (Mersmann, 2001). The particles are held together by weak cohesive forces such as van der Waals forces that can be easily broken. Aggregate formation does not require supersaturation to form and is sometimes regarded as the intermediate process prior to agglomeration. Aggregation commences with the collision of particles due to mechanisms such the Brownian motion and diffusion in a process called perikinetic aggregation. When the collision is influenced by hydrodynamic motions such as convective currents and mechanical stirring, orthokinetic aggregation takes place. The orientation of the particles also plays a major role in dictating the collision efficiency and the particles. After the collision of the particles, the staying together of these particles is determined by the magnitude of the repulsive and attractive forces between them. The solution chemistry may be altered to influence attraction or repulsion (Söhnel, et al., 1988).

2.1.5 Agglomeration

The process whereby many small particles are attracted to each other, aggregate successfully and cement to one another to form larger and fewer particles is called agglomeration. They are usually harder to disperse than aggregates. Particles do this by the formation of inter-particle crystalline bridges which requires growth and supersaturation (Hartel et al., 1986). Strong agglomerates are thus formed in highly supersaturated solution. The process of agglomeration is favoured when the inner particle distance is smaller than 20 particle diameters (Karpinski, 2002).

2.1.6 Seeding

Seeding is the introduction of small crystals of the crystallising solid into a supersaturated solution to initiate nucleation. Seeding provides a surface for crystal growth and prevents spontaneous nucleation (Yu, 2007). When seeding is implemented, the surface of the seeds should be large enough to prevent additional nucleation at the moment crystallisation is started in order to prevent large size distributions. A good saturation control strategy and seeding procedure can influence the quality of the resultant crystals formed as a result of seeding. Parameters that ought to be considered when seeding are the seed loading, seeding time, size of the seeds, the state of the seed material (dry or in suspension), the quality of the seed and the point of addition in the crystalliser (Ulrich and Jones, 2006). It is also

recommended that the seeds that are used be small enough and of a quantity that results in high yields and of a desirable size distribution.

2.2 Electrochemistry

2.2.1 Electrochemical cells

Electrochemistry is the branch of chemistry that examines the combination of chemical and electrical effects of a process. Electrolytic processes are reactions in which chemical changes occur on the passage of an electric current. The typical electrochemical cell consists of two electronic conductors which are also called electrodes and an ionic conductor, called the electrolyte. The charge transport in the electrodes occurs via the motion of electrons whilst that in the electrolyte occurs via the motion of both the positive and the negative ions. Figure 2 shows the setup of a typical electrolysis cell.

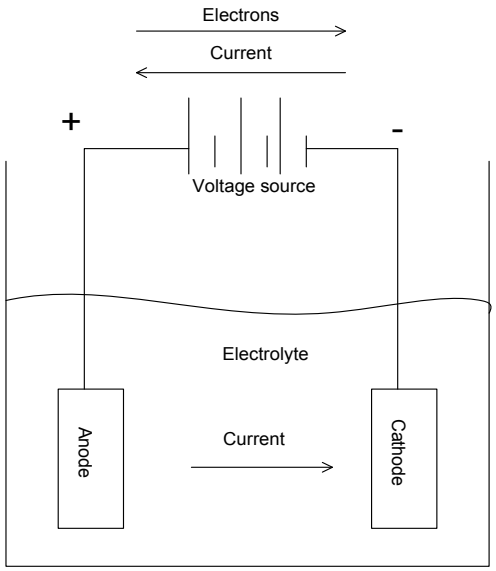

Figure 2: Typical electrolysis cell setup. The anode and the cathode are immersed in the electrolyte and a voltage is supplied to drive the current from the anode to the cathode.

Half-cell electrochemical reactions occur at each electrode and the combination of the two individual half-cell reactions makes up the overall chemical reaction of the cell.

In this study, the magnesium and steel electrode made up the anode and cathode respectively and the urine made up the electrolyte. The chemical reactions at each of the electrodes involve: the oxidation of the magnesium anode, allowing for the release of magnesium ions into the electrolyte; whilst at the steel cathode, water is reduced to elemental hydrogen and hydroxide.

The half-cell reactions that occur at the electrodes as follows:

Anode: $\mathrm{Mg} \rightleftharpoons \mathrm{Mg^{+}} + 2\mathrm{e^{-}}$ $-E^0 = 2.362$ V

Cathode: $2\mathrm{H_2O} \rightleftharpoons \mathrm{H_2} + 2\mathrm{OH^{-}}$ $-E^0 = 0.00$ V

$\Delta E^0 = 2.363$ V

The larger the E^0, the greater the tendency for the reaction to proceed in the forward direction i.e. from left to right. The overall reaction has a positive electromotive force hence the reaction will occur spontaneously at standard conditions (25 ^{o}C, 101.3 kPa, pH= 0, ion activity =1).

Oxidation involves the loss of electrons and occurs when the energy of the electrode dips below the highest occupied molecular orbital of the compound. Reduction is the gain of electrons and occurs when the energy of the electrode increases above the lowest vacant molecular orbital of the compound. The oxidation reaction occurs at the anode whilst the reduction reaction occurs at the cathode.

2.2.2 Electrochemical cell configurations

The electrode at which the reaction of interest occurs is called the working electrode whilst the other would be called the counter electrode in a two-electrode configuration. A third electrode called the reference electrode may also be used in a three electrode configuration. The reference electrode is an ideal non-polarizable electrode of known potential such as a $\mathrm{Ag/AgCl}$ placed in potassium chloride solution, and is usually placed close to the electrode on which the reaction of interest will take place in order to minimise the solution resistance between the two electrodes which is sometimes termed the ohmic potential drop in the solution. A reference is used to determine the potential of the working electrode. For that purpose, the potential of the reference needs to be constant and this can only be achieved if no current flows in the reference. The potential difference between the working electrode and the reference electrode can thus be accurately monitored. A reference electrode can be placed very close to the working electrode by the use of a fine capillary tip called a Luggin-Haber capillary even though some uncompensated solution resistance still remains (Bard and Faulkner, 1980).

2.2.3 Electrode potentials

The electrode potential for a reaction is derived directly from the free energy change for that reaction and thus thermodynamics predicts which reaction proceeds as the oxidation and which will proceed as the reduction reaction. The standard oxidation

potential is equal in magnitude and opposite in sign to the standard reduction potential. The reaction with the lower standard reduction potential proceeds as an oxidation reaction and the other as a reduction reaction. In this study magnesium is oxidised whilst the water is reduced. The cell potential or voltage is evaluated using Equation 8 and if the difference of the reduction potential is positive then it means that the reaction is feasible.

$$\mathrm{E_{cell}} = \mathrm{E_{cathode}} - \mathrm{E_{anode}} \quad (8)$$

The current and the electrode reaction rate is governed by the rates of processes such as mass transfer (movement of the species from the bulk solution to the electrode surface), electron transfer at the electrode surface, chemical reactions preceding the electron transfer and other surface reactions such as adsorption, desorption or crystallisation (electrode position).

Factors affecting electrode reaction rate and current

Figure 3 shows the pathways of a general electrode reaction and the mass transport that occurs during the reaction. The overall electrode reaction $\mathrm{O} + \mathrm{ne} \leftrightarrow \mathrm{R}$ made up of a series of steps including mass transfer, adsorption and desorption that cause the conversion of the dissolved oxidised species, O, to be reduced to R. According to Bard and Faulkner (1980) the current or the electrode reaction are generally governed by processes such as:

1. Mass transfer, for example, of O from the bulk solution to the electrode surface,
2. Electron transfer at the electrode surface,
3. Chemical reactions that precede the electron transfer,
4. Other surface reactions such as adsorption, desorption and crystallisation (electrodeposition).

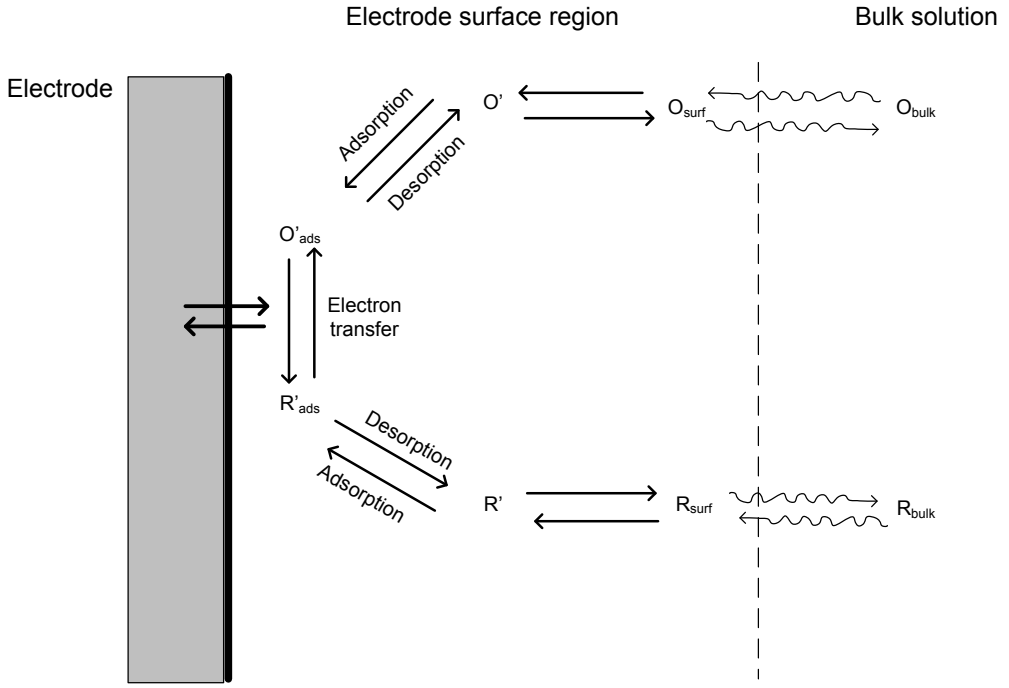

Figure 3: The pathway of a general electrode reaction (Bard and Faulkner, 1980).

The simplest reactions in electrochemical cell involve only mass transfer of a reactant to the electrode, electron transfer and mass transfer of the product to the bulk solution. More complex reactions involve additional series of electron transfers and protonation, branching mechanisms, parallel path and modification of the electrode surface (Bard and Faulkner, 1980). There are three fundamental modes of mass transport in solution and they are:

1. Migration- this is the motion of a charge body such as an ion under the influence of an electrical potential gradient.
2. Diffusion- this is the motion of species under the influence of a chemical potential gradient.
3. Convection- this is the hydrodynamic transport either due to density gradients known as natural convection or due to external means such stirring (forced convection).

The rates of all the reaction steps in the electrochemical system generally reach steady state when a steady state current is obtained. There are some inherent reactions which may occur and limit the magnitude of the current passed and these reactions are called rate determining reactions.

Figure 4 is a summary of the factors that affect the processes that occur in the electrochemical cell and will inevitably affect the reactions at the electrode and overall performance of the entire electrochemical cell.

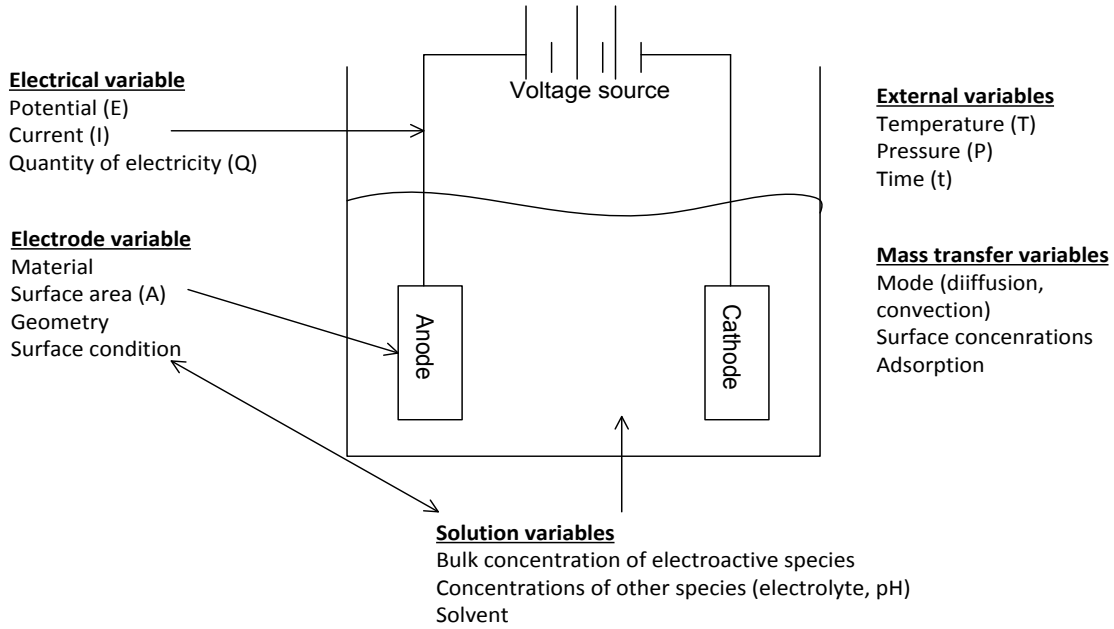

Figure 4: Summary of variables that affect the activities that occur in the electrochemical cell (Hamann et al, 2007).

2.2.4 Faraday's law, current densities and efficiencies

Faraday's law is the relationship between the quantity of current (charge) that is passed through a system and the quantity of chemical change that occurs due to the passage of the current. The amount of chemical change is proportional to the amount of current passed. Equation 9 shows how the mass of the chemical substance is released due to the passage of current.

$$\mathrm{m_{Faraday}} = \frac{\mathrm{M}}{\mathrm{z}} . \frac{\mathrm{Q}}{\mathrm{F}} \tag{9}$$

Where $\mathrm{m_{Faraday}}$ is the mass of the substance(g), M is the molar mass of the substance $(\mathrm{gmol^{-1}})$, Q is the electric charge(C), z is the number of electrons transferred and F is the Faraday constant which is 96485 $(\mathrm{Cmol^{-1}})$. According to

Faraday's law, the greater the current, the faster the rate of mass transfer from the electrode. It then follows in Equation 10:

$$Q = \int_0^t I dt \tag{10}$$

Electric energy can also be calculated from voltage, current and time according to Equation 11:

$$W = \int_0^t V_{cell} I dt \tag{11}$$

Where t is the time of current passage and I and V_{cell} is the current passed and cell voltage respectively, both as a function of time.

The current density is defined as the current per unit area (Am^{-2}) proportional to the Mg^{2+} that are liberated into the solution according to Faraday's laws that describe the dependency of electric charge and dissolved mass by means of electrolysis and the columbic efficiency (%). Coulombic efficiency or current efficiency is the current that is invested in a targeted process. A rate describes the kinetics of a process and always has a unit that is per time. Equation 10 describes how Coulombic efficiency is determined.

$$\text{Coulombic efficiency} = \frac{m_{Mg,dissolved}}{m_{Mg,Faraday}} \times 100 \tag{12}$$

For the electrochemical precipitation of struvite, the following efficiencies can be evaluated

- Overall dissolution rate (determined by the measured phosphate and magnesium concentrations in the solution and assuming that phosphate precipitates with magnesium at a 1:1 molar ratio),
- Electrochemical dissolution rate (determined by Faraday's law) and
- Non-electrochemical dissolution rate (the difference between overall dissolution and the electrochemical dissolution). This is because magnesium undergoes self-dissolution (corrosion mechanism) due to the high reactiveness of the metal.

The mass dissolved is calculated:

$$m_{Mg,dissolves}(t) = (m_p(t_0) - m_p(t)).\frac{M_{Mg}}{M_p} + m_{Mg}(t) - m_{Mg}(t_0) \quad (13)$$

Where $m_p(t_0)$ and $m_p(t)$ is the measured mass of phosphate initially and at time t in the reactor, respectively. Likewise, $m_{Mg}(t_0)$ and $m_{Mg}(t)$ is the measured mass of magnesium initially and at time t in the reactor respectively. M_{Mg} is the molar mass of magnesium which is 24.3 $(gmol^{-1})$, M_p is the molar mass of phosphorous which is 31 $(gmol^{-1})$.

2.2.5 Thermodynamic modelling

For struvite, saturation, β is defined as:

$$\beta = \frac{f_1.[NH4+].f_2.[Mg2+].f_3.[PO_4^{3-}]}{K_s^o} \quad (14)$$

Where $[NH_4^+]$, $[Mg^{2+}]$, $[PO_4^{3-}]$ are the concentrations of NH_4^+, Mg^{2+} and PO_4^{3-}, f_1, f_2 and f_3 are their fugacities and K_s^0 is the standard solubility product (Stumm and Morgan, 1996). High supersaturation leads to an increased degree of primary-nucleation resulting in the formation of numerous tiny particles of struvite. The temperature and the pH of the solution directly affect the solubility of the struvite. Low temperatures and minimal solubility pH leads to high supersaturation.

The solubility product of struvite is defined in Equation 15 and 16 as:

$$K_{sp} = \{Mg^{2+}\}\{NH_4^+\}\{PO_4^{3-}\} \quad (15)$$

$$= \gamma_{Mg^{2+}}[Mg^{2+}]\,\gamma_{NH_4^+}[NH_4^+]\,\gamma_{PO_4^{3-}}[PO_4^{3-}] \quad (16)$$

Where { } denotes activity, γ denotes the activity and [ ] denotes concentration.

The concentration solubility product is defined as:

$$K_c = [Mg^{2+}][NH_4^+][PO_4^{3-}] \quad (17)$$

Where K_{sp} denotes the gamma-activity, K_c denotes concentration and β expresses the relationship between *f* in eq. 14 and *γ* in eq. 16 (alternative way of defining saturation).

Temperature corrections of the solubility product are performed with the Van't Hoff equation (Strumm and Morgan, 1996):

$$\frac{K_s(T_2)}{K_s(T_1)} = e^{\frac{\Delta H}{R}(\frac{1}{T_1}-\frac{1}{T_2})} \quad (18)$$

Work has been done to experimentally determine the solubility product of struvite at different temperatures and the most commonly used pK_{sp} value is 12.6 (Snoeyink and Jenkins, 1980; Stumm and Morgan, 1981). The activities of the ions are determined by thermodynamic modelling of activity effects (Bhuiyan et al., 2008).

For solubility studies of struvite, the equilibrium relationships of ionic species such as $H_2PO_4^-$, HPO_4^{2-}, PO_4^{3-}, $MgH_2PO_4^+$, $MgHPO_4$, $MgPO_4^-$, Mg^{2+}, $MgOH^+$, NH_4^+, H^+, OH^- and NH_3 (aq) are usually considered (Ohlinger et al., 1998; Buchanan et al., 1994).

The estimations of the solubility product and the enthalpy of struvite formation are important and work has been done to determine these parameters experimentally in various streams such as source separated urine, wastewater, water and synthetic supernatant streams (Bhuiyan et al., 2008; Ronteltap et al., 2007). It is important to understand the thermodynamic processes that occur when struvite forms and to predict as accurately as possible the solubility of struvite and also what happens when the activity product of the struvite constituent ions exceeds the thermodynamic solubility product (K_{sp}) (Bhuiyan et al., 2008).

Magnesium phosphate complexes such as $MgHPO_4$, $MgH_2PO_4^+$ and $MgPO_4^-$ and $[MgCO_3]_{aq}$ reduce the concentration of magnesium ions and phosphate ions that are available in solutions for the formations of struvite (Ali and Schneider, 2008; Doyle and Parsons, 2002; Seckler et al., 1996; Pastor et al., 2008). The pK_{sp} value increases when more magnesium complexes are considered; a study showed that when three magnesium complexes ($MgHPO_4$, $MgH_2PO_4^+$ and $MgPO_4^-$) were considered, the pK_{sp} value was 13.27 and when one magnesium complex ($MgHPO_4$) was considered it was 13.15 (Ohlinger et al., 1998).

Additionally, previous studies on the investigation of the thermodynamics of struvite precipitation from source separated urine found that, because of the high amounts of calcium, carbonate, ammonium and sulphate in source separated urine, other various complex compounds are likely to form such as calcium phosphates and magnesium carbonates, also limiting the formation of struvite (Bhuiyan et al., 2008; Ronteltap et

al., 2010) and ultimately reducing the extent to which phosphorous is recovered. In their study, Ben Moussa et al. (2006) postulated that during the formation of struvite, it is inevitable for calcium carbonate not to form in a urine stream thus; it is very likely that the purity of the struvite collected is compromised in the event that only pure struvite is needed. Other ions such as sodium and chloride did not have substantial influence (Ronteltap, 2010) thus are usually allowed to vary in thermodynamic modelling simulations in order to balance the charge of the resultant solution (Mehta and Batstone 2013).

2.2.6 Activity coefficients

The precise determination of the solubility product involves the correct calculation of the activity coefficients and the consideration of other parallel equilibrium reactions that may occur due to the presence of other ions in solution (Ronteltap et al., 2007). Solubility coefficients are consequently influenced by activity coefficients and must be considered for all chemical reactions (Ronteltap et al., 2007). This can be supported by the fact that the solubility product of struvite is approximately 80 times higher (ionic strength = 0.4 M) than the calculation without activity coefficients would predict (Ronteltap, 2009).

$$\prod_{i=1}^{n} \gamma_i = \frac{K_{sp}}{K_c} \tag{19}$$

The typical ionic strength values for undiluted urine lie between 0.3 and 0.6 M. Davies approximation is amongst the numerous methods for approximating activity coefficients but it applies the same coefficient to all the ions with the same charge and is a suitable approach for diluted urine with I < 0.5 M.

$$\log \gamma_i = -Az_i^2 \left(\frac{\sqrt{I}}{1+\sqrt{I}} - BI\right) \tag{20}$$

Where I is the ionic strength, z_i is the charge of ion i, A = 0.509 for water are 25 ^oC, B = 0.2 or 0.3.

The ionic product is defined as:

$$I = 0.5 \sum_{i} (c_i z_i^2) \quad (21)$$

Where c_i and are the concentration of ion i.

The B. Dot approach is another approach for (ionic strengths from 0.3 to 1) that can be implemented to approximate the activity coefficient and is widely applied in geochemical models such as PHREEQCI (Parkhurst and Appelo, 1999).

2.2.7 Saturation Index

The saturation index is an index showing whether water will dissolve or precipitate out a particular mineral. Its value is negative when the mineral may be dissolved, positive when it may be precipitated, and zero when the water and mineral are at chemical equilibrium. In modelling software such as PHREEQCI, the target saturation index is specified by the user; a positive, zero, or negative value specifies supersaturation, equilibrium, or undersaturation for the mineral with respect to the solution. The saturation index (SI) is calculated by comparing the chemical activities of the dissolved ions of the mineral (ion activity product, IAP) with their solubility product (K_{sp}).

$$SI = \log\left(\frac{IAP}{K_{sp}}\right) \quad (22)$$

2.2.8 Ionic imbalance

In all modelling cases, it is important to ensure that the ionic imbalance in the aqueous solution is minimised as much as possible in order to produce accurate thermodynamic modelling results. This is done by measuring the relative amounts of anions and the cations in the solution and using one of the following ions (although not limited to only these) to balance the system: H^+ and OH^- for adjusting the pH, SO_4^{2-}, NO_3^-, Cl^-, Na^+, Ca^{2+}, Mg^{2+}, $K^+$and NH_4^+ (Murray and Wade, 1996; Noguchi and Hara 2004).

There are numerous causes for an ionic imbalance and work has been done to evaluate the causes of ionic imbalance depending on each unique case and solution composition. In their work Murray and Wade, (1996) determined that at extremely low and high pH, resultant concentration errors of up to 100 % were obtained. They also found that in simple water systems, the high H^+ or OH^-, the protonation of ligands and the hydrolysis of metal cations led to a significant ionic balance hence postulated that

the effect would be pronounced in complex multi-component streams such as urine. Thermodynamic modelling tools and software packages enable the user to predict the interaction of ions in solution that contribute to the ion imbalance (Murray and Wade, 1996). Equation 23 and 24 shows how ionic imbalance is calculated.

$$\sum \text{cations} = \sum \text{anions} \tag{23}$$

$$\%\ \text{difference} = 100 \times \frac{|\sum \text{cations} - \sum \text{anions}|}{\sum \text{cations} + \sum \text{anions}} \tag{24}$$

2.2.9 The effect of pH on ionic speciation

The pH of the solution affects the saturation index by changing the speciation of the struvite reactants and other competing precipitates. Studies show that the precipitation of struvite in municipal wastewater and sludge dewatering liquor occurs when the pH is higher than 7.5 and continues to increase until pH 10.5 (Doyle et al., 2001). This is looked at in more detail in the Literature Review section in chapter three.

3 Literature Review

The Literature Review chapter is an assessment of the literature pertaining to this dissertation mainly to identify the gaps that exist and to motivate the reason for this study. The main sources of this information are: published journal papers and theses of work in the field of struvite precipitation and electrochemistry. The main aspects that are addressed are the factors that influence struvite precipitation in Section 3.1, and electrochemical processes in waste water treatment systems in Section 3.2. This chapter concludes by highlighting studies that have been done in the field of electrochemical precipitation of struvite, suggests what still needs to be done and how this dissertation can fill certain gaps in this field of research.

3.1 Struvite

It is estimated that 75–90% of phosphate in urban inflows ends up in sewage (Cordell et al., 2011). The use of untreated sewage sludge has been restricted in the recent years due to the health concerns (Werner, 2006; Adam, 2009). According to the study by Etter et al., (2011), urine could be a reliable source of new phosphorous, could even alleviate sanitation challenges in developing countries and offer a low cost fertilizer in the form of a mineral called struvite.

Struvite (MAP) is a phosphate based mineral of the orthophosphate group (readily available for biological uptake). It is made up of magnesium, ammonium and orthophosphate in a 1:1:1 molar ratio and typically surrounded by six water molecules. Struvite crystals generally assume an orthorhombic structure of a PO_4^{3-} and a $Mg(H_2O)_6^{2+}$ octahedral and NH_4^+ groups bound together by hydrogen bonding which break at high temperatures (Abbona and Boistelle, 1979). Struvite is generally in the form of a white powder and is insoluble in water with a solubility of 0.018g.100 ml^{-1} in water at 25°C but soluble in acidic solutions with a solubility of 0.018g.100 ml^{-1} in 0.01M hydrochloric acid at 25°C; Bridger et al., 1962).

Struvite was first discovered as a problematic compound as it would scale in pipes and other equipment in wastewater treatment plants and sludge treatment facilities. This was also true in urine collecting systems where urine pipe blockages by struvite were reported (Udert et al., 2003b). Consequently, much research went into solving these problems and the use of struvite as an inorganic fertilizer was suggested. Struvite is commonly used as a slow releasing phosphate based fertilizer that is derived from waste water and is a good replacement for rock phosphate. Struvite derived from human waste is likely to pass any regulations associated with toxicity, pathogen and metal content and may be compared to most phosphate fertilizers on the market (Sikosana et al., 2014). Some studies however, have been conducted and

confirmed that struvite contains low concentrations of heavy metals and other pollutants (VUNA, 2013) thus its slow releasing nature minimises the risk of leaching and root damage and is favoured in grasslands and forests where application is minimal (Trenkel, 1997).

3.1.1 Thermal stability of struvite

The constituent ions of struvite as aforementioned are held together by hydrogen bonding which can be easily broken in high temperatures. Struvite is thus thermally unstable in temperatures over 50 ^{o}C (Sarkar, 1991). The ammonium and the water tend to evaporate when the mineral is subjected to high temperatures for certain periods of time, leading to the formation of magnesium hydrogen phosphate trihydrate ($\mathrm{MgNPO_4 \cdot 3H2O}$). The prolonged heating of struvite leads to the formation of magnesium hydrogen phosphate monohydrate ($\mathrm{MgNH_4PO_4 \cdot H_2O}$) and eventually, magnesium hydrogen phosphate ($\mathrm{MgHPO_4}$) and forms bobierrite ($\mathrm{Mg_3(PO_4)_2 \cdot 8H_2O}$) if heated in excess water, (Iqbal et al., 2008).

3.2 Production of struvite from source separated urine

Comprehensive studies have been conducted to assess the technical and economic feasibility of producing struvite from source separated urine. The determination of the phosphate content in the influent (urine), the economics of the magnesium source for the precipitation process, the efficiency of the technology implemented for crystal recovery, the potential of flocculants to improve the recovery of phosphates, the role of filter cake on the recovery of struvite and the production of user-friendly granulated struvite fertilizer (Etter et al., 2011; Sikosana et al., 2014).

Struvite can be produced successfully from source separated urine using different methods and various magnesium sources. Projects have been carried out successfully in Nepal and South Africa to produce struvite from source separated urine (Etter et al., 2011; VUNA, 2013). The formation of struvite occurs in the form of stable white orthorhombic crystals according to Equation 25:

$$\mathrm{Mg^{2+} + NH_4^+ + HPO_4^{2-} + 6H_2O \rightarrow MgNH_4PO_4.6H_2O} \qquad (25)$$

3.2.1 Source separated urine

A method of separating waste streams at the source offers many benefits because each stream has different levels of pollution and nutrients. This means that each stream can be treated differently and efficiently to recover these pollutants and nutrients. Additionally, separation of end products from by-products usually requires a

lot of energy. One of the growing areas of interest in waste treatment is the separation of the urine stream from faeces and flush water at source. Urine makes up only less than 1 % of the total volume of waste water and is a very nutrient rich stream. It contains about 80 % of the nitrogen and 50 % of the phosphorous that the human body excretes (Ronteltap, 2009). Source separated urine can be collected by implementing the “No-Mix technology” which allows urine to be collected via a valve, which opens when pressure is exerted on toilet seat and closes when the pressure is released and the toilet is flushed. This valve is in the front compartment of specially designed toilet chambers and drains almost undiluted urine with very little flush water. This technology was studied at Eawag in their award winning project NOVAQUATIS and this system proved to have many advantages on top of providing the nutrient rich urine (Larsen, 2004). An added advantage of this system was that the load in waste water treatment plants was lessened especially with regards to removing hormones and pharmaceuticals which most waste water treatment facilities failed to do (Larsen and Lienert, 2007). The well-known urinals which are implemented in most male lavatories also provide this separate stream. Also, in Nepal the use of Urine Diversion Dry Toilets (UDDT) was also investigated and found to be a reliable way of collecting concentrated urine for struvite production (Etter et al., 2011).

3.2.2 Struvite particle characterisation

One of the most important factors in precipitating struvite is to monitor the quality of the product. It is beneficial to produce large particle sizes so that they are easily separable and will not breakup up into smaller particles (Ronteltap et al., 2009). Crystals formed in batch experiments with hydrolysed urine were shown to have an average size of >90 µm at a pH of 9 and a temperature of 20 ^{o}C.

The parameters that affect the size of the particles include the degree of agitation and saturation of the solution, temperature and pH. The type of the stirrer and stirrer speed affects the intensity of agitation (Ronteltap et al. 2010). Particles size increases with supersaturation and decreases with decreasing temperature. However, this is only up to a certain point because at higher degrees of supersaturation, nucleation is the predominant particle formation mechanism, which results in smaller particles. Furthermore, studies show that stored urine has an optimum pH for struvite production (Hug & Udert 2013). Ronteltap et al. (2010) also postulated that the size of the particles is also affected by the rate of mixing.

Typical shapes for struvite particles vary from coffin-like structures (Wierzbicki et al. 1997), to needle-like structure but are assumed to be spherical when the crystal size measurements is measured with a laser diffraction particle size analyser, Mastersizer

X (Malvern Instruments Ltd., Worcestershire, United Kingdom), (Ronteltap et al., 2009).

3.2.3 Factors that influence the crystallisation process in source separated urine

Literature suggests that the most important factors that affect struvite precipitation are the substrate molar ratios $(\mathrm{Mg^{2+}}:\mathrm{NH_4^+}:\mathrm{PO_4^{3-}})$, pH as well as its inhibition caused by other ions such as $\mathrm{Ca^{2+}}, \mathrm{K^+}, \mathrm{CO_3^{2-}}$ (Stratful et al., 2004; Doyle et al., 2002; Le Corre et al., 2009). Struvite precipitates spontaneously in the presence of orthophosphates, ammonium and magnesium (in a minimum molar ratio of 1:1:1) thus wastewater treatments plants with a magnesium concentration of between 3-10 mg/L coupled with favourable pH results in struvite precipitating in the pipes (OSTARA, 2013).

3.2.3.1 pH

When urine is stored for long periods of time after having been collected from No-Mix toilets, the urea is microbially degraded, resulting in a strong pH increase to values around 9. Previous work shows that the pH of stored urine is already adequate for the relatively good production of struvite by only dosing $\mathrm{Mg^{2+}}$ in the form of salts. At high pH levels, such as 9, struvite and calcium phosphate precipitation is spontaneous (Hug and Udert, 2013). Studies on the production of struvite show that pH is a major influencing factor because the speciation of both the $\mathrm{PO_4^{3-}}$ and $\mathrm{NH_4^+}$ is strongly affected by pH; with increases in pH increasing the activity of $\mathrm{PO_4^{3-}}$ whilst decreasing that of $\mathrm{NH_4^+}$. In source separated urine, $\mathrm{NH_4^+}$ ions are in abundance compared to $\mathrm{PO_4^{3-}}$ hence fluctuations in pH mainly affect $\mathrm{PO_4^{3-}}$ (Ronteltap et al. 2007). The optimum range for struvite production is between 7 and 11 (Doyle and Parsons, 2002). Studies by Le Corre et al. (2006) also showed that an increase in pH from 8 to 11 significantly reduced the size of the resultant crystals formed in synthetic solutions due to the interference of the formation of agglomerates. This is because of the relationship between pH and the zeta potential of struvite.

In a study of the electrochemical coagulation of struvite from source separated urine, i.e. by dosing $\mathrm{Mg^{2+}}$ with the electrical dissolution of the sacrificial magnesium anode, the chemistry at the magnesium electrode increased the resultant pH of the solution due to the formation of the hydroxyl ions at the cathode (Hug and Udert, 2013). The work done by Ben Moussa et al. (2006) and Wang et al. (2010) on the electrochemical coagulation of struvite, by dosing external magnesium sources for the electrochemical precipitation of pure struvite with inert anodes further confirms that, due to the reactions that occur at the cathode, there was no need for alkalinity dosing when using an inert anode. The hydroxide ions that are produced at the cathode surface increase

the interfacial pH up to 1.5 units in comparison to the bulk solution (Ben Moussa at al., 2006).

As aforementioned, the pH affects many aspects in the production of struvite even the speciation of struvite substrates and may influence the extent to which competing precipitates such as nesquehonite ($MgCO_3.3H_2O$) and magnesium phosphate form (Hug and Udert, 2013; Kruk et el., 2013). As a result, the purity of struvite may start to decrease after pH 9 especially when there are competing ions in the solution such as Ca^{2+},K^+ and CO_3^{2-} because the precipitation of other magnesium and calcium complexes is favoured (Wang et al., 2010).

The speciation of the carbonate, phosphate and ammonium ion is illustrated below:

Speciation of the carbonate ion

TIC (Total inorganic carbon) species such as carbon dioxide dissolves in water to form carbonic acid which further dissociates to hydrogen and bicarbonate ions with increase in pH according to Le Chatelier's principle and this shown in Equation 26.

$$CO_2(l) + H_2O \leftrightarrow H_2CO_3 \leftrightarrow H^+ + HCO_3^- \leftrightarrow H^+ + CO_3^{2-} \quad (26)$$

Figure 5 shows the speciation curve of carbonate. During the storage of urine, urea is microbially degraded resulting in strong pH values of around 9. For a stored urine stream, the total inorganic carbon is modelled as the bicarbonate ion and is most abundant and active at pH values of 8-9.

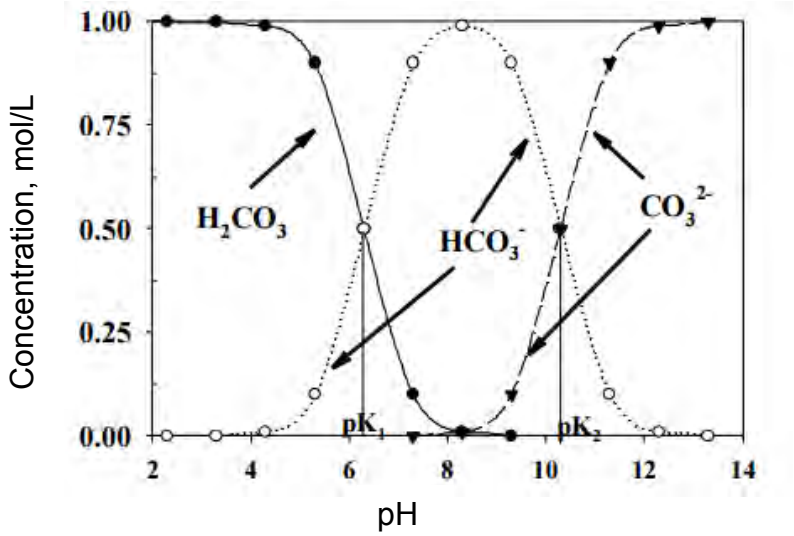

Figure 5: Carbonate speciation diagram (from OLI ™ modelling).

Speciation of phosphate ion

Aqueous phosphate exists in four forms: in strongly basic conditions, the phosphate ion (PO_4^{3-}) predominates, whereas in weakly basic conditions, the hydrogen phosphate ion (HPO_4^{2-}) is prevalent. In weakly acidic conditions, the dihydrogen phosphate ion $(H_2PO_4^-)$ is most common. In strongly acidic conditions, trihydrogen phosphate (H_3PO_4) predominates. Phosphoric acid (H_3PO_4) dissociates in water according to Equation 27 and eventually releases the phosphate ion with increase in pH. Figure 6 shows the speciation of the phosphate ion.

$$H_3PO_4 \leftrightarrow H^+ + H_2PO_4^- \leftrightarrow H^+ + HPO_3^{2-} \leftrightarrow H^+ + PO_4^{3-} \quad (27)$$

Previous experimental work on struvite production shows that pH has a significant effect on the phosphate conversion due to the fact that an increase in pH causes an increase in the availability of free ortho-phosphate. This usually resulted in the formation of compounds such as magnesium phosphate and calcium phosphate which sometimes resulted in the decrease of the yield of struvite (Ali and Schneider 2008; Doyle and Parsons 2002; Seckler et al., 1996; Pastor et al., 2008).

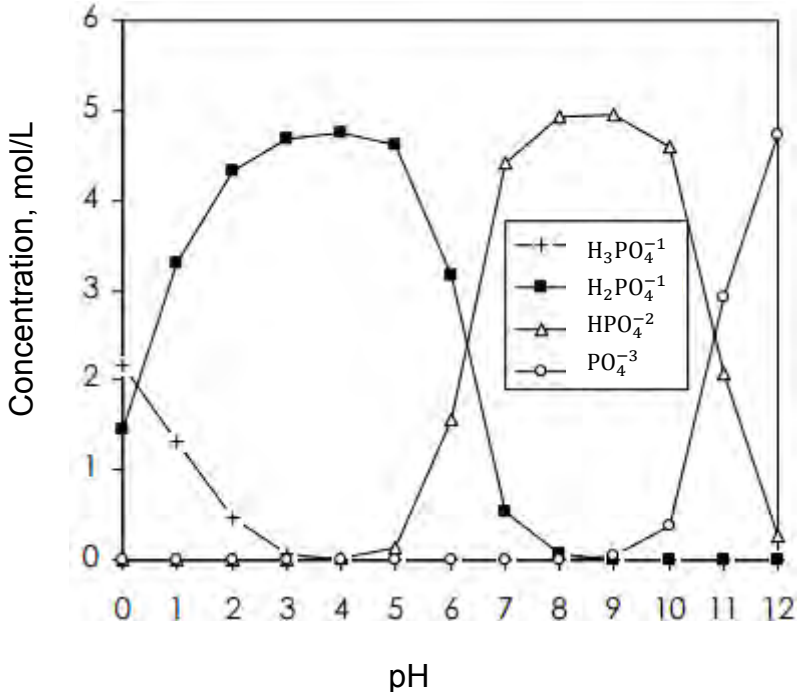

Figure 6: Phosphate speciation diagram as a function of pH (from OLI ™ modelling).

Speciation of ammonium ion

Inorganic nitrogen is made up of ammonia (NH_3) and the ammonium ion (NH_4^+). The equilibrium of ammonia in water is represented in Equation 28.

$$NH_3 + H_2O \leftrightarrow NH_4^+ + H_3O^- \quad (28)$$

The equilibrium equation of ammonium is a function of pH, temperature and ionic strength.

Figure 7 shows the speciation of ammonia and at pH values greater than 11, the concentration of ammonia is zero. Ammonium concentrations are fairly high at pH values greater than 8.

Stored urine is usually at a higher pH value than fresh urine due to the hydrolysis of the urea to ammonium (Ramaru, 2009) so the ammonium concentration could actually be higher than measured depending on the storage system. This is because ammonia evaporates and fills up any excess space that is above the urine level in the container. Urease decomposes urea into ammonia and bicarbonate causing a pH increase according to Equation 29:

$$NH_2(CO)NH_2 + 2H_2O \rightarrow NH_3 + NH^+ + HCO_3^- \quad (29)$$

The release of ammonia and bicarbonate, as well as the pH increase, promotes precipitation. Ureolysis is the initial trigger for precipitation, but dilution with flushing water determines the precipitate composition (Udert et al., 2003).

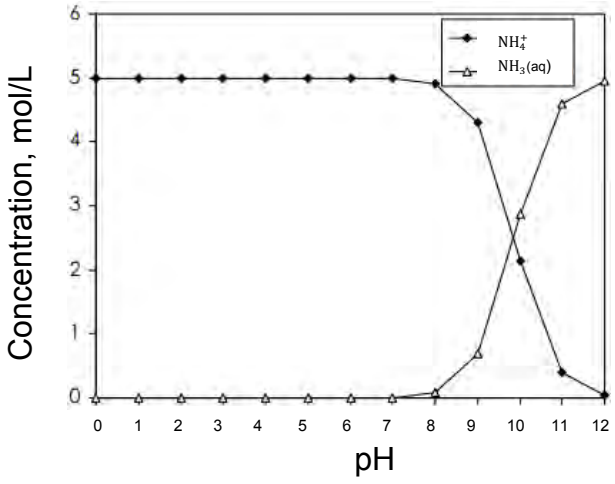

Figure 7: Ammonia speciation diagram as a function of pH (from OLI ™ modelling).

3.2.3.2 Stirring rate in struvite precipitation

Stirring creates turbulence which is reported to be a contributor to the formation of struvite because carbon dioxide is stripped thus increasing the pH in the system and the rate of mass transfer in the ionic transport system (Stratful et al., 2004; Kim et al., 2009). The effect of stirring however, can lead to scaling on the walls of the reactor (Wilsenach et al., 2007).

The stirring rate influences the supersaturation of the solution and allows for thorough mixing so that there are no localised points of over high oversaturation which leads to primary nucleation and precipitation of numerous small struvite crystals. In their work to investigate the factors that affect the size of struvite crystals that can be formed by dosing $\mathrm{MgCl_2}$, Ronteltap et al. (2010) discovered that the particles produced under conditions of vigorous stirring were significantly bigger than those produced under conditions of gentle stirring.

On the other hand, the work that Le Corre, (2006) did, showed that high stirring rates not only accelerated nucleation but limited crystal growth and Durrant et al. (1999) showed that high stirring rates may lead small crystal sizes due to crystal shearing and breakage.

The work that Bourgeois, (2010) did in investigating the effects of stirring in a struvite electrochemical precipitation cell showed that stirring influences the hydrodynamics that take place in the electrochemical cell and leads to the formation of a layer on the anode hindering the easy release of the $\mathrm{Mg^{2+}}$ into the solution. It was then postulated that at lower stirring speeds, the struvite settled and did not coagulate on the anode surface. The precipitation of struvite, just in this study, was carried out in an electrochemical cell (reactor) where $\mathrm{Mg^{2+}}$ was added in the form of a sacrificial magnesium anode by electrical dissolution.

Ronteltap et al. (2010) compared the particle sizes produced when a two blade propeller was used and when a magnetic stirrer was used for stirring the solution during struvite production. The larger particle sizes were achieved when the two propeller stirrer was used. This is because of the greater turbulence achieved by the two blade propeller leading to proper mixing. Poor mixing leads to slower dissipation of the precipitates which in turns leads to increase in supersaturation which favours nucleation over crystal growth. In that study, magnesium was dosed chemically. The effect of secondary nucleation by particles present in an unfiltered sample of urine was also investigated by Ronteltap et al. (2010) and the results show that there was no significant influence in the resultant size of the particles.

From the above mentioned pieces of literature, it can thus be proposed that the effect of stirring has different influences on different factors that affect the production of struvite i.e. the article size and the efficiency of magnesium dissolution. The efficiency of magnesium dissolution is dependent on the magnesium source. With respect to this study, a compromise thus, needs to be reached where the rate of stirring is ideal for the right level of supersaturation and thus production of large particles but no too turbulent so that high levels of supersaturation occur due to magnesium anode dissolution.

3.2.3.3 The residence time

The precipitation of struvite is extremely fast with introduction of Mg^{2+} (Stratful et al., 2001; Lee et al., 2003) thus an increase in the residence time does not particularly affect the extent to which phosphate is recovered. Within the first four minutes, the recovery of phosphate reaches up to 92 % (Yoshino et al., 2003) then slowly goes up a little with time. Crystals do however grow significantly in 3 hours (Battistoni et al., 2000). Statful et al. (2001) showed that the struvite crystal length increases from 0.1 mm to 3 mm if the residence time is increased from 1 minute to 180 minutes. Similar observations were made by Yoshino et al. (2003) where the crystal diameter increased to 0.6 mm within 18 hours.

3.2.3.4 The effect of seeding

Struvite has a low solubility hence very high supersaturation levels can be achieved leading to the formation of tiny struvite particles via primary homogenous nucleation. Secondary nucleation could be influenced by lowering the supersaturation and seeding could be implemented to lower the activation energy needed and possibly produce larger struvite crystals (Ramaru, 2009).

Ronteltap et al. (2010) further postulated that the presence of foreign particles found in unfiltered urine, once left in suspension as nuclei for secondary nucleation had no major effect on the resultant size of the struvite crystals formed. Other studies however, also show that seeding with struvite crystals proved to improve the recovery of phosphorus and also the settling characteristics (Wang, 2010). Both these cases were evaluated after carrying out experiments with the Mg^{2+} dosing in the form of a salt. Work by Ali and Schneider, (2006) also showed that seeding with quartz sand particle and struvite particles gave different results in that there was more particle growth when struvite particles seeding was implemented. The SEM images of the quartz sand particles showed that there was no precipitation of the struvite on the sand particles at all; the struvite particles homogeneously nucleated out instead.

Studies have also suggested that the negative zeta-potential struvite particles may be a limitation to struvite tendency for agglomeration (Le Corre et al., 2007). It can thus be postulated that the highly negative struvite crystals readily and strongly attract to the positively charged surface of the anode. This agrees with the observations that Bourgeois, (2010) made in the electrochemical precipitation of struvite using magnesium sacrificial anode. Bourgeois, (2010) observed the formation of a struvite layer when struvite crystals were left in suspension in an electrochemical cell. The struvite crystals were attracted to the surface of the anode and this layer increased with thickness when the reaction cycle was run for longer periods of time (Bourgeois, 2010). It is thus re-affirmed that when considering the aspect of seeding, the seed loading, seeding time, size of the seeds, the state of the seed material (dry or in suspension), the quality of the seed and the point of addition in the crystalliser is very important (Ulrich and Jones, 2006).

The work done by Hirasawa et al. (2008) showed that the size of the seeds plays a significant role. They concluded that using 1.2 mm sized seeds was more preferable than using 2 mm sized particles because of the larger specific surface area with the smaller particles. Literature also suggests that the mass of struvite particles used as seeds is also important. In the work done by Yoshino et al. (2003), they showed that the rate of recovery of phosphate decreased significantly by doubling the loading of the seeds.

The feasibility of precipitating struvite from dewatering liquors in a fluidised bed reactor was also investigated by Ramaru, (2009). The struvite particles were recycled to the reactor and used as seeds, they provided favourable nucleation sites for struvite precipitation hence high conversion rates were achieved at higher recycle ratios.

3.2.3.5 Magnesium sources and molar ratios

The optimum molar ratio of the substrates ($\mathrm{Mg:N:P}$) for the formation of struvite was found to be 1.2:3:1 (Krähenbühl, 2012). Adult human beings excrete about 0.3 g of phosphate per day and during storage of source separated urine, at least 28% of the phosphate precipitates until all the magnesium and calcium in the urine has been consumed (Udert et al., 2003b). The addition of magnesium ions in the form of $\mathrm{MgCl_2}$, MgO, $\mathrm{MgSO_4}$ or bittern can trigger the precipitation of remaining phosphate in the form of struvite (Etter et al., 2011). This dosage of the $\mathrm{Mg^{2+}}$ as above-mentioned can be controlled via the current and works well for decentralised reactors (Hug and Udert, 2012; Kruk et al., 2014). Ideally, the source of the magnesium has to be affordable, soluble in alkaline conditions i.e. in hydrolysed urine and not contain a lot of impurities

that may affect the purity of the struvite product. It must also be cheap to transport thus must have a reasonable magnesium content (Gantenbein and Khadka, 2008).

Table 1: Summary of the factors that influence struvite production (Sikosana et al., 2010).

Factor	Effect
pH	Solubility decreases from 3000 mg/L to 100 mg/L with a rise in pH 5-7.5 Affects the uptake of ammonia and hence the Mg: N: P ratio (Le Corre et al., 2009) Optimum pH for maximum yield between 8.5 and 9.5 (Green et al., 2004)
Supersaturation ratio	Affects crystal growth
Temperature	Affects the saturation and hence the solubility constant Optimal conditions: 25 to 35 °C (Le Corre et al., 2009)
Mixing	High turbulence releases $CO_2$and increases pH High mixing quickens nucleation and results in brittle crystals
Impurities	Sodium, sulphate and bicarbonates and calcium have adverse effects $CaCO_3$ increase the induction time for crystal formation (Le Corre et al., 2009) Sludge liquors have high Ca levels and will have a high selectivity for calcium carbonate instead of struvite. (Crutchik and Garrido, 2011) Ratios of Ca: Mg of 1:1 inhibits struvite and induces calcium phosphate growth Sodium, sulphate bicarbonates and calcium have adverse effects Inhibited by TSS over 1000 ppm (Green et al., 2004)
Concentrations of Mg and N	High ammonia concentrations increase struvite production (1: 9.4) When Mg is adequate and the levels of Ca are high and N low, the precipitation of calcium phosphate is favoured Mg: Ca must be less than 1:1 High levels of ammonia affects struvite kinetics

3.3 Electrochemistry

3.3.1 Current density

The rate of release of the Mg^{2+} into the solution influences two main factors; the supersaturation of the solution and the pH at the surface of the anode and inevitably the pH of the solution in the whole reactor. The higher the current density, the higher the rate of release of the Mg^{2+} into the solution, assuming that there are no resistances on the anode. The purity of struvite is also higher at higher current densities (Kruk et al., 2013) however, it does not make sense to increase the current density nor to run the electrochemical cell for unnecessarily long periods of time only to have a large Mg^{2+} concentration in the solution after all the $PO_4 - P$ has been precipitated out. Also in the presence of inhibiting ions such as K^+, Ca^{2+} and CO^{3-} there is a possibility of other compounds like nesquehonite and calcium phosphate forming in solution if other conditions such as pH and temperature are favourable. At pH levels above 9, nesquehonite starts to form (Hug and Udert, 2013). For molar ratios of Ca: Mg above 1.1, calcium ions compete with magnesium to form an amorphous calcium phosphate, hence inhibiting struvite formation (Kruk et al., 2013). At pH from 10.0 to 10.5 the formation of $Mg_3(PO_4)_2.22H_2O$ is favoured over that of struvite (Le Corre et al., 2007).

The work done by Kruk et al., (2013) showed that a phosphorous removal rate of 4.0 mgPO_4-Pcm^{-2}h^{-1} from supernatant of fermented waste activated sludge, was attained at electric current density of 45 Am^{-2}. The work done by Hug and Udert, (2012) showed that a phosphorous removal rate of 3.7 mgPO_4-Pcm^{-2}h^{-1} from electrochemical struvite precipitation from source separated urine was attained at electric current density of 55 Am^{-2}. They also realised high current efficiencies of above 100 % and low energy consumption of 1.7 WhgP^{-1} at a potential of -0.6 V vs NHE.

3.3.2 Magnesium electrodes

Magnesium is a highly reactive metal which readily interacts with atmospheric components in the air. In their work on the investigation of electrochemical behaviour of magnesium electrodes, Lu et al. (1999) postulated that magnesium surfaces are always covered by surface films which compromise the extent of the reactions that occur on the surface of the electrode thereafter. Components such as $MgCO_3, Mg(HCO_3)_2, Mg(OH)_2$ and Mg form (passivate) on the surface and decrease the interaction between the active magnesium metal electrode surface and the environment (electrolyte) in which it is placed. It is thus important to prevent the extent to which passivation occurs in order to minimise the resistance on the surface of the electrode. As part of the development of the reactor for the electrochemical precipitation of struvite reactor Hug (2010) did voltammetry and batch experiments to

determine the optimal magnesium electrode potential range. The results showed that a nearly constant rate of magnesium dissolution was reached for applied potentials of -790, -590 and -190 mV. It was concluded that in order to reduce the extent to which passivation occurred and achieve high reaction speeds at minimum energy, magnesium electrode potentials greater than -800 mV were found to be appropriate for their sequencing batch reactor with a 2 h cycle. The magnesium electrode dissolution rates in solution have also been reported greater than 100 % due to the high reactivity of the metal. The Mg^{2+} ions are easily self-liberated from the electrode to the solution and the overall dissolution rate is determined by the magnesium concentrations in the solution and those that react with the ions in the solution. The electrochemical dissolution rate (determined by Faraday's law) and non-electrochemical dissolution rate is the difference between overall dissolution and the electrochemical dissolution (Hug, 2010; Bourgeois, 2010).

3.3.3 The principle of a seeded electrochemical precipitation crystalliser

Electrochemical precipitation of struvite is a safe practice that does not require dosing of chemicals that may cause harmful by-products (Kruk, 2013). It is also a high speed and low reactor volume system. Hug and Udert (2012) cover the technical feasibility and economic viability for the process of phosphate removal from source separated urine by struvite precipitation. Hug and Udert (2012) conducted well controlled electrochemical batch experiments at constant anode potentials and compared the costs of electrochemical magnesium dissolution with the costs for precipitating struvite with magnesium salts. They demonstrated that the process was technically simple and economically feasible and thus interesting for decentralized reactors. They achieved phosphate removal in the 13 batch cycles that lasted 2 hours each varied between 59 and 84 % which was mainly due to the variation of the initial phosphate content (between 180 and 226 mgL^{-1}). The average current density for all the experiments was about 5.5 mA cm^{-1} (Hug and Udert, 2012). From the results, Hug and Udert (2012) concluded that electrochemical magnesium dosing is a feasible process for precipitating struvite at specific electrode potentials, provided that the batch experiments are carried on a solution that has been stored for several hours before filtration. They also concluded that a fairly simple reactor design can achieve high yield of struvite.

A similar study by Kruk et al. (2013) showed that using high purity magnesium sacrificial anode as the only source of magnesium was very effective in the recovery of high quality struvite from wastewater solutions. They also determined that struvite purity was strongly dependent on the pH and current density. With a current density

of 45 Am^{-2} and pH ranging between 7.5 and 9.3, a struvite purity exceeding 90% was achievable.

The use of iron electrodes was implemented by Zheng et al. (2009) and they concluded that it was possible to achieve 100 % recovery of phosphate. In their study, the urine sample was electrolyzed for 15 minutes in a system that had an electrode to solution ratio of 160 cm^2L^{-1} and energy consumption of 3.2 kJ. The main aspect addressed in their research was the effect of pH on the system and the results concluded that a urine sample with a pH below 9 achieved nearly 100 % removal of phosphate could be reached in 30 minutes at a stirring speed of 150 revolutions per minute (rpm).

In another study, Hasson et al. (2010) looked at the implementation of seeding such that the precipitation surface was shifted from the electrode onto small calcium carbonate seeds. These researchers came up with a quantitative comparison of the yield of calcium carbonate with and without seeding and it was concluded that the yield increased when seeding was employed and the overall current densities required were much lower than without seeding. They were able to achieve a reduction in the specific cathode area by a factor of more than 10 without altering the specific energy requirement.

From the work done by Hasson et al. (2010); Kruk et al. (2013) and Hug and Udert (2012), implementing the aspect of seeding to the electrochemical precipitation of struvite could possibly be effective feasible way to recover more phosphate from source separated urine and also produce large particles of struvite.

3.4 Summary of Literature Review

The discussion in section 3.1 showed that struvite precipitation is a feasible and reliable method of recovering phosphorus from waste water streams. It is can be used as a valuable and marketable fertilizer that is easy to produce. Source separated urine is a waste stream that contains almost 50 % of the phosphorous that is excreted from the human body and is thus a good resource for struvite precipitation. Waste water treatment systems researchers have development novel designs such as a “No-Mix technology” which allows urine to be collected via a valve, which opens when pressure is exerted on toilet seat and closes when the pressure is released and the toilet is flushed. This valve is in the front compartment of specially designed toilet chambers and drains almost undiluted urine with very little flush water. This way, urine can be collected separately as a rich concentrated solution. This technology was studied at

Eawag in their award winning project NOVAQUATIS and this system proved to have many advantages on top of providing the nutrient rich urine (Larsen, 2004).

The characteristics of struvite as a mineral include thermal stability at temperatures less than 50 °C. Crystals are typically coffin like shaped. The factors that affect the precipitation of struvite include pH, stirring rate, residence time, seeding and magnesium dosing. Chemical dosing of magnesium is the most common method of producing struvite and electrochemical dosing is also a growing area of study. Fairly recent studies show that electrochemical precipitation of struvite is a safe practice that does not require dosing of chemicals that may cause harmful by-products. It is also a high speed and low reactor volume system and is both technically feasible and economically viable.

The implementation of seeding in an electrochemical precipitation of calcium carbonate by Hasson et al. (2010) showed that the precipitation surface was shifted from the electrode onto small calcium carbonate seeds. It was concluded that the yield increased when seeding was employed and the overall current densities required were much lower than without seeding. From the work done by Hasson et al. (2010); Kruk et al. (2013) and Hug and Udert (2012), seeded electrochemical precipitation of struvite could possibly be an effective and cheap way to recover phosphate from source separated urine.

Hug and Udert (2013) assessed the feasibility of the electrochemical precipitation reactor initially, by running voltammetry and batch experiments to conclude on the sensitivity of the magnesium anode. They postulated an optimum magnesium electrode potential based on reaction rates and energy consumptions. They also discovered the formation of nesquehonite on the layer of the anode and recommended that further studies be done to improve the energy requirements and the settling properties of the produced crystals.

4 Approach, materials and methods

This chapter develops the hypotheses and key questions, and then details the thermodynamic modelling procedure developed to study the precipitation of struvite from source separated urine. All the experiments that were carried out to validate the model and the test the seeded electrochemical systems are also included in this chapter.

4.1 Research hypotheses and key questions

As stated in Chapter 1, the broader aim of this dissertation is to improve electrochemical precipitation of struvite from source-separated urine. In line with this aim, and informed by the findings from the literature review, it is thus hypothesised that:

1. Given a long enough reaction time (in batch mode), the recovery rates of phosphorous for the electrochemical precipitation processes with and without seeding will be the same, and can be predicted by a thermodynamic model. This is because seeding influences the rate at which phosphorous is consumed and not the extent to which it is consumed, in other words phosphorus conversion depends on the kinetics of the process and not the thermodynamic equilibrium of the process.
2. Nearly all the phosphorous in urine can be recovered electrochemically by introducing magnesium ions under conditions that avoid the formation of nesquehonite, an unwanted side reaction that consumes magnesium and contaminates the struvite product.
3. Seeding can help to make larger struvite particles of high purity. The average size of produced struvite particles will become smaller if the current density is increased (as supersaturation is increased thus leading to more spontaneous nucleation), but larger if the reactor is seeded and well mixed.

The following key questions guide the development of the remainder of this chapter, as well as the interpretation of the results and drawing of conclusions.

1. Can thermodynamic modelling adequately predict experimental results obtained under the same conditions?
2. What is the minimum concentration of magnesium ions and the ideal pH necessary to recover most of the phosphorous from source separated urine without triggering the precipitation of nesquehonite?
3. Does the size of the of struvite particles increase as a result of seeding?

4. How do the struvite seed characteristics change with change in the residence time and stirring?
5. How do the economics of the electrochemical process compare with the conventional process?

In order to answer these questions, the approach taken involved first developing a thermodynamic model of struvite precipitation in order to come up with optimum conditions for the prototype. Next, precipitation experiments were carried out in order to validate the model before the optimum conditions could be implemented in the SEP reactor. The second part was the investigation of the SEP to produce struvite and determine the technical feasibility of the proposed process. It is the aim of the third part of the investigation to investigate how the reactor residence time and the level of magnesium ion supersaturation influence the product characteristics. Particle size distributions were measured and images of the crystals were analysed under the Scanning Electron Microscope (SEM).

4.2 Thermodynamic Modelling

To answer key questions 1 and 2, and thus to help substantiate hypotheses 1 and 2, a thermodynamic analysis was carried out. The approach to this analysis, the modelling techniques used and the choices made are discussed later in this section.

Further, to answer key question 1 and substantiate hypothesis 1, a kinetic understanding of struvite precipitation is also necessary. In their study of the kinetics of struvite precipitation, Le Corre et al., (2007) showed that the magnesium concentration had a major impact on struvite kinetics, with higher concentrations leading to shorter induction times, hence faster rates of precipitation leading to production of fine crystals. They also showed that pH measurements correlated well with magnesium concentrations, especially at laboratory scale. Investigations at both laboratory and pilot scale demonstrated that struvite precipitation in synthetic liquors corresponded to a first order kinetic model. In addition, precipitation of struvite from urine reactions are very fast and therefore for the purpose of this study we only focused on the thermodynamic aspects of the system.

In this research, kinetics of the struvite precipitation were not theoretically analysed or predicted. Instead, in the experimental work, samples were taken after different time

periods to confirm that enough time had passed for equilibrium to be reached. Conditions affecting the successful removal of P and recovery as struvite and their consequences on thermodynamics of precipitation have been widely investigated (Ronteltap, 2009, Doyle and Parsons, 2002, Jaffer et al., 2002, Bouropoulos and Koutsoukos, 2000). Solution supersaturation and pH value are the predominant parameters of controlling struvite precipitation.

The average composition of the source separated urine stream that was used for the thermodynamic modelling is shown in Table 2. Urine was collected from the source separated urine storage tanks at the Eawag main building (Forum Chriesbach) and analysed for its initial composition. This urine was collected in these tanks by an already installed No-Mix system which consists of source separating toilets and waterless urinals.

A chemical equilibrium-based computer model, PHREEQCI (Version 3.1.4.8929, August 2014, Parkhurst and Appelo) was used to perform the thermodynamic modelling. The urine composition was used in the PHREEQCI simulations as initial concentrations before changing the magnesium concentration or the pH of the solution. PHREEQCI can access thermodynamic data from well-established database or rely on user provided data. The database that was used for the modelling in this study is called wateq4f.dat (Appendix V) and was used to simulate the saturation of struvite and nesquehonite. The database was extended for acetate which was used to model the Chemical Oxygen Demand (COD) in sources separated urine.

Table 2: Average composition of the source separated urine. This composition was used for the thermodynamic modelling.

Initial urine composition			Standard deviation
Chemical Oxygen Demand (COD)	mg/L	1078	67
Total Inorganic Carbon (TIC)	mg/L	948	250
Mg	mg/L	2.0	0.5
PO_4-P	mg/L	99	16
NH_4-N	mg/L	1360	300
Cl	mg/L	1062	90
SO_4	mg/L	200	20
Na	mg/L	557	20
K	mg/L	501	20
Ca	mg/L	24	2
pH		8.90	0.04
Temperature	K	298.15	-

4.2.1 Modelling technique

Thermodynamic modelling was performed to predict the yields of struvite and nesquehonite at varied magnesium concentrations and pH levels. The system that was simulated was such that it closely simulated the system for the electrochemical precipitation of struvite although it neglected the kinetic effects. In the electrolytic reactor, the chemistry at the magnesium electrode influences the resultant pH of the solution. Previous work showed that the pH of stored urine was already adequate for a good production of struvite provided additional Mg was added, in the form of salts (Hug & Udert 2013). The sequential dissolution of the Mg anode occurs according to the following reactions:

$$\mathrm{Mg} \rightarrow \mathrm{Mg^{+}} + \mathrm{e^{-}} \tag{30}$$

$$\mathrm{Mg^{+}} + \mathrm{H_2O} \rightarrow \mathrm{Mg^{2+}} + \mathrm{OH^{-}} + 0.5\mathrm{H_2} \tag{31}$$

Equation 31 is assumed to be the rate determining step in the chemical reaction.

The work done by Ben Moussa et al. (2006) and Wang et al. (2010) with the dosing of external magnesium sources for the electrochemical precipitation of struvite with inert anodes further confirms that, due to the reactions that occur at the cathode, there is no need for alkalinity dosing when using an inert anode. This is because oxygen is

reduced and hydrogen is evolved on the cathode surface according to the equation 32 and 33. The hydroxide ions that are produced at the cathode surface increase the interfacial pH up to 1.5 units in comparison to the bulk solution (Ben Moussa et al., 2006).

Cathode reactions when using an inert anode:

$$O_2 + 2H_2O + 4e^- \rightarrow 4OH^- \quad (32)$$

$$2H_2O + 2e^- \rightarrow H_2 \uparrow + 2OH^- \quad (33)$$

Parameters such as temperature, initial pH and the chemical composition of the urine were defined for different concentrations of magnesium ion ranging from a Mg:P molar ratio of 0.02 to 28. This range was selected based on the work conducted by Hug and Udert (2013) on the investigation of the saturation index of struvite and nesquehonite as a function of pH. The input concentrations were then converted to units of molality or, equivalent moles of elements and element valence states and mass of water. Speciation calculations were performed on each solution so that each solution was then available for subsequent batch-reaction, transport, or inverse-modelling calculations. The pH in the simulation was allowed to vary for different magnesium concentrations at constant temperature of 25°C in order to balance the charge of the resultant solution.

Four solutions were thus selected to further investigate by modelling, how the recovery of phosphate is affected by keeping the Mg:P molar ratio constant whilst varying the pH of the solution from 6 to 14.5. Sodium or chloride ions were selected to balance the charge of the resultant solution. This is because ions such as sodium and chloride ions do not have substantial influence on the process (Ronteltap, 2010) thus are usually allowed to vary in thermodynamic modelling simulations in order to balance the charge of the resultant solution (Mehta and Batstone 2013). The precipitation (equilibrium phases function) of only struvite and nesquehonite was activated in all the cases that were investigated, although the saturation indexes of all possible compounds were monitored to account for the mass balance of the system. These are given in Appendix I.

Previous studies in the modelling of struvite eliminated compounds such as hydroxylapatite ($Ca_5(PO_4)_3OH$) and calcium carbonate ($CaCO_3$) in their database due

to the fact that the precipitation kinetics of hydroxylapatite are extremely slow and the presence of Mg^{2+}, PO_4^{3-} and dissolved organics inhibits the precipitation of calcium carbonate (Ramaru, 2009). For this study, these components were also excluded as the focus was on the precipitation of struvite and nesquehonite only.

4.3 Experimental design for batch experiment to verify thermodynamic modelling

After modelling the precipitation of struvite and nesquehonite for the various Mg:P molar ratios and pH ranges, the thermodynamic modelling results were validated by running a simple batch experiment (non-electrochemical with magnesium ion source in the form of $MgCl_2 \cdot H_2O(aq)$) under the conditions defined in the simulations and comparing the results.

In the simple batch experiment, Mg:P molar ratios of 1.2 and 21 were investigated experimentally in treatment E1 and E2 respectively by dosing urine with $MgCl_2 \cdot H_2O(aq)$ and $NaOH(aq)$ as sources of Mg^{2+} and Na^+ respectively. From the thermodynamic model, the Mg:P molar ratio determined the amount of $MgCl_2 \cdot H_2O(aq)$ needed and the resultant Na^+ charge difference determined the amount of $NaOH(aq)$ required in the experiment. The molar ratios were chosen in order to investigate two distinctive conditions according to the thermodynamic modelling results. The first condition being one in which only struvite forms and the second being one in which both struvite and nesquehonite form. Treatments E1 and E2 were performed three times to minimise error and to ensure reproducible results. These repeats are denoted by a, b and c for the first, second and third run respectively.

4.3.1 Solution preparation

The urine samples for the validation experiment (treatment E1 and E2), was collected from the source separated urine storage tanks at Eawag. The same urine source was used for the electrochemical experiment. The method of urine sample analysis involved filtration of the urine through a coffee filter to remove any solid residues followed by filtration through Nanocolor filter paper of 0.45 µm pore size. The measurement of the samples was carried out with the following instruments and methods for the respective ions:

- FIA (Flow injection analysis- reaction with bromocresol purple, Foss FIA star 5000 Analyser Gerber Instruments): NH_4^+, PO_4^{3-};

- IC (Ion Chromatography- Metrohm, column IonPac® AS12A, Dionex Corporation, Sunnyvale, Ca, USA): Cl^-, SO_4^{2-};
- ICP (Inductively coupled plasma- Optical Emission Spectrometer, Spectro Analytical Instruments, Kleve, Germany): $Na^+, K^+, Mg^{2+}, Ca^{2+}$;
- HATCH LANGE cuvette tests: COD (LCK 114), PO_4^{3-} (LCK 349).

The same procedure was carried out to determine the final composition of the urine after the experiments.

As aforementioned, $MgCl_2.6H_2O\,(aq)$ and $NaOH\,(aq)$ were added in the relevant quantities according to the thermodynamic model. These chemicals were of analytical grade and obtained from Merck standard solutions (Switzerland). Table 3 shows the quantities of $MgCl_2 \cdot H_2O\,(aq)$ and $NaOH\,(aq)$ that were added in the two treatments.

Table 3: Volumes of $MgCl_2 \cdot H_2O$ (aq) and $NaOH$ (aq) added in batch experiment

	1M $MgCl_2 \cdot H_2O$ (aq) (ml)	**1M $NaOH$ (aq) (ml)**
Treatment E1 (Mg:P=1.2)	0.374	1.60
Treatment E2 (Mg:P=21)	6.54	28

4.3.2 *Experimental setups*

The setup for Treatment E1 and E2 consisted of a 500 ml glass beaker placed on a magnetic stirrer (IKA RCT classic). A pH probe (WTW PH 196) and a stop watch which was used to determine the pH and duration of the respective experiments as shown in Figure 8.

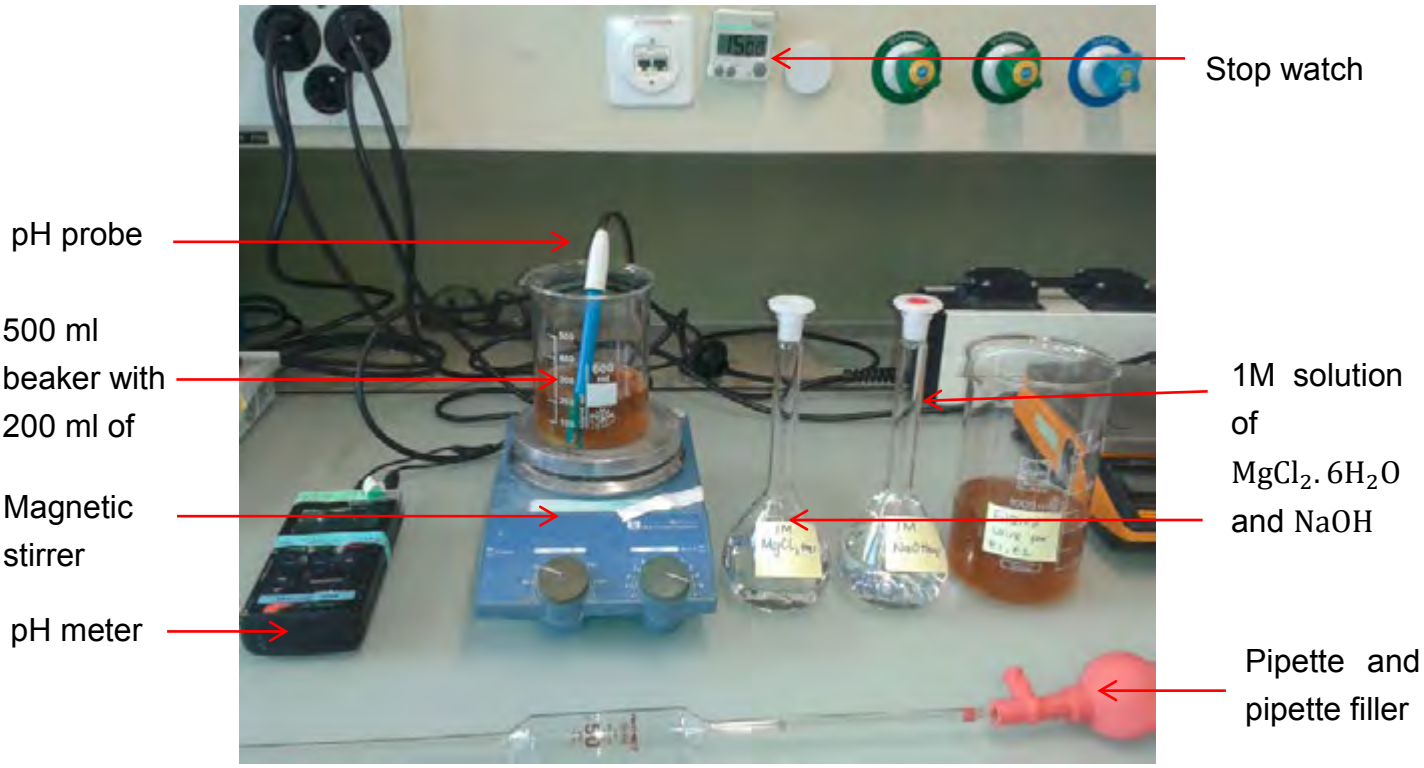

Figure 8: Experimental setup of the simple batch reactor for the validation of the thermodynamic model.

4.3.3 *Experimental procedure*

For the batch experiment, treatments E1 and E2, 200 ml of urine were placed in a 500 ml beaker followed by the addition of $NaOH$ (aq) then $MgCl_2 \cdot H_2O$ (aq). The solution was then stirred at 120 rpm for 30 minutes after which 15 ml of the final solution was withdrawn in order to determine the final urine composition. The final pH of the solution was also measured using the pH probe (WTW PH 196). The precipitates were separated from the urine in a centrifuge and analysed by x-ray diffraction (XRD) to qualitatively identify the precipitates. Each of these steps was done in triplicate. Table 4 shows a summary of the batch experiments that were carried out and the conditions under which they were carried out.

Table 4: Summary of the simple batch experiment carried out for the validation of the thermodynamic model.

Experiment	**Brief description**	**Justification**	**Magnesium dosage**	**Treatment conditions**	
Simple batch experiment	Two Mg:P molar ratios were investigated and for each treatment, three repeats were performed: E1[a], E1[b], E1[c] E2[a], E2[b], E2[c]	For the validation of the thermodynamic model.	$MgCl_2 \cdot H_2O(aq)$	$MgCl_2 \cdot H_2O(aq)$ was used for magnesium dosing and $NaOH$ added to 200 ml of urine and stirred at 120 rpm.	
				E1[a], E1[b], E1[c]	• Molar ratio of Mg:P = 1.2 • Stirring rate of 120 rpm • Final urine concentration results compared to simulation S1 which was simulated at Mg:P =1.2.
				E2[a], E2[b], E2[c]	• Molar ratio of Mg:P = 21 • Stirring rate of 120 rpm • Final urine concentration results compared to simulation S1 which was simulated at Mg:P =21.

4.4 Experimental design for electrochemical precipitation experiment

Further to the validation of the thermodynamic model with the simple batch experiment as outlined in section 3.3; seeded and non-seeded electrochemical experiments were carried out at the optimum conditions for struvite precipitation as suggested by the simulation results of the thermodynamic model. The 2 h electrochemical batch experiment was carried out to answer the question of how the yield of struvite experimentally, compares to the yield predicted by the thermodynamic model under the same conditions. It was also carried out to verify the modelled minimum concentration of magnesium ions and ideal pH necessary to recover most of the phosphorous from source separated urine without triggering the precipitation of nesquehonite. Treatments E3 (control), E4, E5, E6 and E7 were performed twice to minimise error and ensure reproducibility of results. Two instead of three runs were done due to resource and time constraints. The first and repeat runs are denoted by ^{a}, ^{b} respectively.

4.4.1 Solution preparation

The preparation of the urine samples was performed as outlined in section 3.3.1.

4.4.2 Experimental setups

The apparatus setup for the electrochemical precipitation of struvite is shown in Figure 9. The 1 L isothermal glass reactor was placed on the magnetic stirrer kept at 25 ^{o}C by running a warm water bath in the jacket of the reactor for the duration of each treatment. The three electrode configuration as shown in Figure 9 was implemented such that the reference electrode (Ag/AgCl) in a Luggin-Haber capillary was placed as close as possible to the anode (magnesium electrode) in order to minimise the solution resistance between the anode and the reference electrode. The potentiostat (PGU 10V-1-IMP-S) was used to supply the voltage for the dissolution of the magnesium electrode and the data logger captured the data from the pH and temperature meter for the duration of each treatment

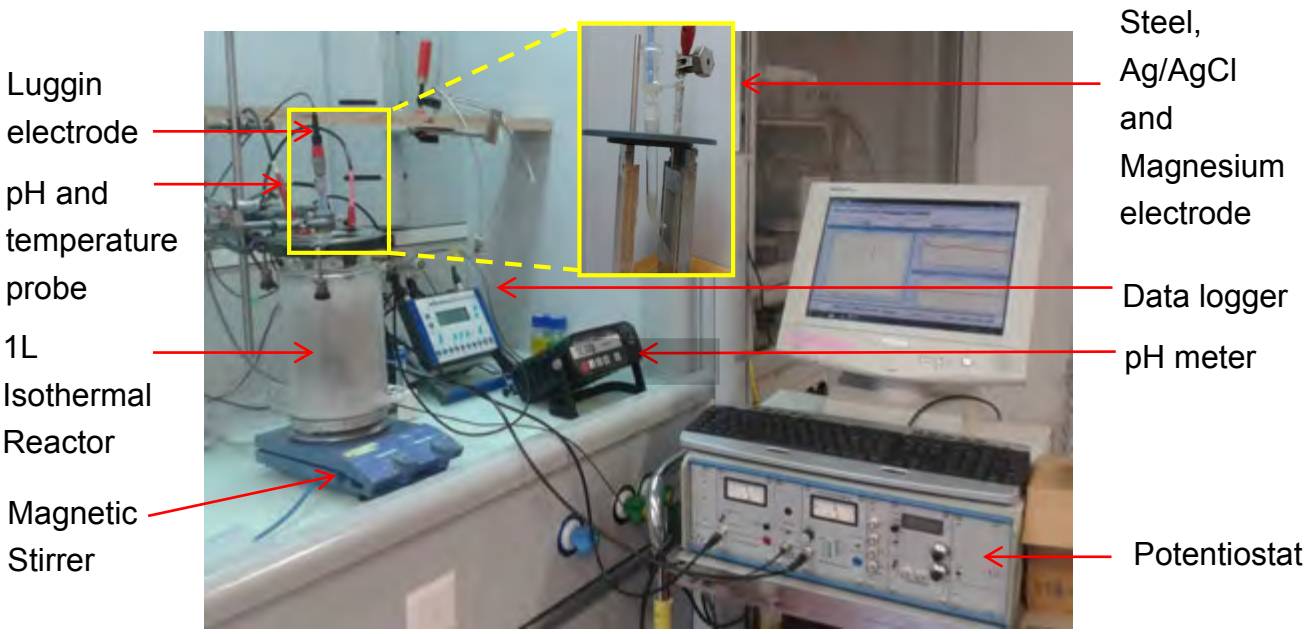

Figure 9: Experimental setup of the electrochemical precipitation batch reactor with the electrode setup shown in detail. The potentiostat was run at constant current density of 70 Am^{-2}. A power source was used for operating the data logger, magnetic stirrer, the pH meter and the potentiostat.

4.4.3 Experimental procedure

For the electrochemical precipitation experiments, non-seeded batch experiments and seeded batch experiments were carried out under the conditions shown in Table 5. The VUNA struvite used in Treatments E4 and E5 was obtained from the VUNA project (Appendix III describes the characterisation of the VUNA struvite seeds) and sieved in a 63 µm sieve to remove any agglomerates that had been formed in the powder. Seeds for treatments E6 and E7 were the seeds produced electrochemically in treatment E3.

The aspect of seeding was implemented at the optimum conditions as suggested by the thermodynamic model (Mg:P molar ratio of 1.2 at pH 9.5). It should also be noted that a current density of 70 Am^{-2} was chosen in order to avoid passivation (Hug and Udert, 2012) for all four electrochemical experiments. To determine the magnesium dosing, Faraday's law of electrolysis was employed. An area of 15 cm^2 on the anode was demarcated and the potentiometer was operated galvanostatically for two hours; the duration of the experiment. This kept the current through the electrolytic cell constant, disregarding changes in the load itself and also in order to achieve the

correct current density and a Mg:P molar ratio of 1.2. The following parameters were measured and recorded by the data logger (RSG40):

- Current
- Voltage for the three electrode configuration (Steel, Ag/AgCl and Magnesium electrode)
- Electrode potential for the two electrode configuration (Mg-steel)
- pH (WTW PH 196)
- Temperature (WTW PH 196)
- Conductivity (WTW LF 96-B)

The quantitative analysis of the precipitates was carried out by dissolving 0.4 g of the sample in 1 ml of 3.2 % HCl and then diluted to 10 ml with nanopure water. The sample was then filtered and measured for $\mathrm{NH_4^+}$ and $\mathrm{Mg^{2+}}$ in the ICP and the $\mathrm{PO_4^{3-}}$ in the FIA. Table 5 shows a summary of the experiment to further explain the experimental techniques that were implemented.

Table 5: Summary of the electrochemical experiment carried out for the development of the seeded electrochemical batch reactor.

Experiment	**Brief description**	**Justification**	**Magnesium dosage**	**Treatment conditions**	
Electrochemical batch experiment	Five electrochemical treatments at Mg:P molar ratio of 1.2 were carried out including a control treatment to investigate how seeding influences the yields of struvite. Each treatment was repeated twice: E3[a], E3[b] (control treatment) E4[a], E4[b] E5[a], E5[b] E6[a], E6[b] E7[a], E7[b]	To aid in the development of the seeded electrochemical batch reactor	Magnesium electrode	Magnesium electrodes were used for magnesium dosing in a 1 L reactor. Seeded and non-seeded experiments	
				E3[a], E3[b] (control treatment)	• Molar ratio of Mg:P = 1.2 • No seeds • Stirring rate of 120 rpm • Final urine concentration results compared to simulation S1 which was simulated at Mg:P =1.2.
				E4[a], E4[b]	• Molar ratio of Mg:P = 1.2 • 0.8 g VUNA struvite used as seeds • Stirring rate of 120 rpm • Final urine concentration results compared to simulation S1 which was simulated at Mg:P =1.2.

				E5[a], E5[b]	• Molar ratio of Mg:P = 1.20.8 g VUNA struvite used as seeds • Stirring rate of 500 rpm • Final urine concentration results compared to simulation S1 which was simulated at Mg:P =1.2.
				E6[a], E6[b]	• Molar ratio of Mg:P = 1.2 • 0.8 g of electrochemically precipitated struvite used as seeds • Stirring rate of 120 rpm • Final urine concentration results compared to simulation S1 which was simulated at Mg:P =1.2.
				E7[a], E7[b]	• Molar ratio of Mg:P = 1.2 • 0.8 g of electrochemically precipitated struvite used as seeds • Stirring rate of 500 rpm • Results compared to simulation S1 which was simulated at Mg:P =1.2.

4.5 Experimental investigation of the struvite product particle characteristics

Two experiments were carried out to investigate how the reactor residence time and level of magnesium ion supersaturation influence the product particle characteristics. The influence of the residence time was investigated by running the SEP in continuously stirred mode for 8 hours. That of the level of magnesium ion supersaturation was investigated by running the SEP in batch mode at various current densities. The product particle characteristics were determined by measuring the particle size and morphology.

4.5.1 Solution preparation

The preparation of the solutions for both experiments was performed as outlined in section 3.3.1.

4.5.2 Experimental setup for the continuously stirred seeded electrochemical reactor

The setup for the continuously stirred seeded electrochemical precipitation reactor is shown in Figure 10. The 1 L reactor was placed on the magnetic stirrer which stirred the urine at 700 rmp. The urine was pumped (Heidolph Pump drive 5001) into the reactor from a storage tank at a rate of 0.5 L/h. The effluent of the reactor was sent to a settling tank where the struvite was collected. The three electrode configuration, as shown in Figure 10, was applied such that the reference electrode (Ag/AgCl) in a Luggin-Haber capillary was placed as close as possible to the anode (magnesium electrode) in order to minimise the solution resistance between the anode and the reference electrode. The potentiostat (PGU 10V-1-IMP-S) was used to supply the voltage for the dissolution of the magnesium electrode and the data logger captured the data from the pH and temperature meter. Table 6 shows the specifications of the SEP run at continuously stirred mode.

Table 6: Specifications of the seeded electrochemical continuously stirred struvite reactor.

Type of reactor	Continuously stirred reactor
Flow rate of urine (L/h)	0.5
Volume of reactor (L)	1
Residence time in the reactor (hours)	2
Stirring rate, magnetic stirrer (rpm)	700
Mg:P molar ratio	1.2
Electrode specifications: Current density (A/m^2) Area (m^2)	 70 0.0015

The following assumptions were made for initial design:

- Only struvite precipitates from the urine;
- The concentration of magnesium in the initial urine is zero;
- 99% conversion of struvite can be reached;
- At a current density of 70 A/m^2, the level of passivation is low. This is because the electrode potential is greater than -800mV;
- Steady state of the CSTR is attained after six hydraulic retention times.

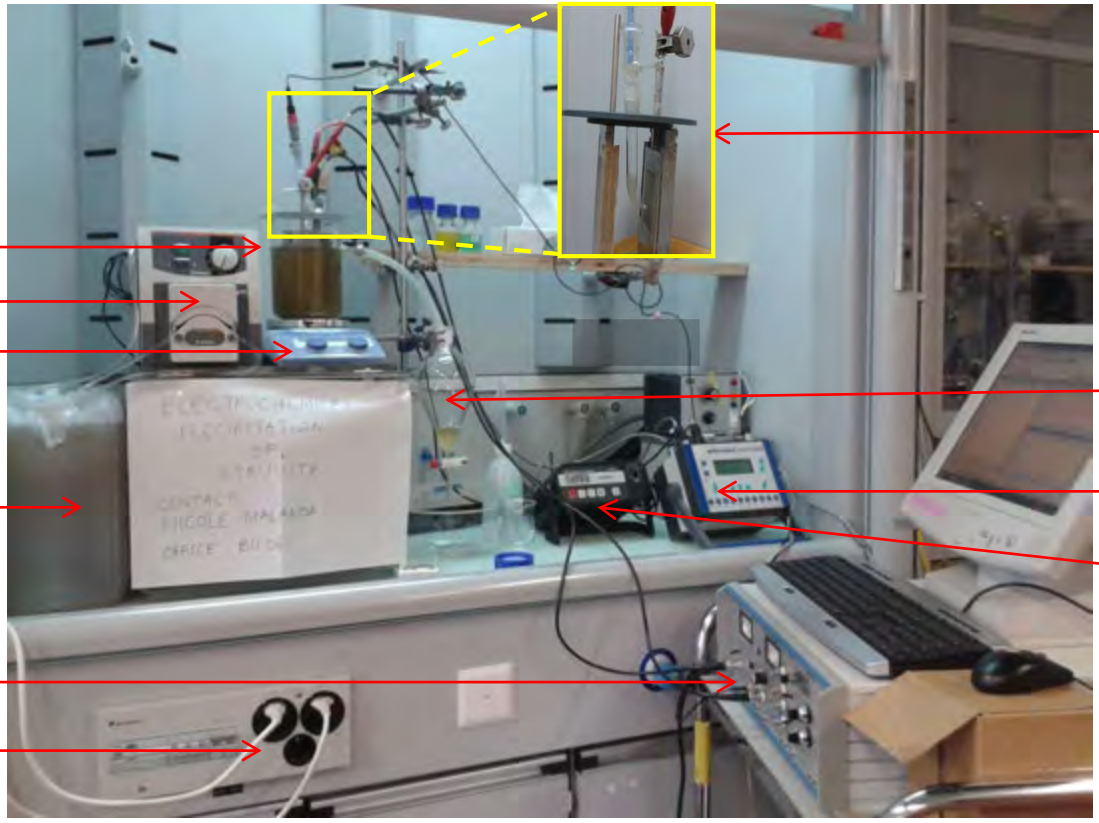

Figure 10: Experimental setup of the seeded continuously stirred electrochemical precipitation of struvite reactor with the electrode setup shown in detail. The potentiostat was run at constant current density of 70 Am^{-2}. The power source was used for operating the pump, the data logger, magnetic stirrer, the pH meter and the potentiostat.

4.5.3 Experimental procedure for running the continuously stirred electrochemical precipitation struvite reactor

The urine was diluted in order to achieve a concentration of 100 mg/L of phosphate in the urine in order to maintain the Mg:P molar ratio of 1.2 in the reactor. The pump (Heidolph Pumpdrive 5001) was tested before and after every treatment to ensure that the flowrate remained constant at the flow rate of 0.5 L/h. The pH probe (WTW PH 196) was also calibrated before every run. The stirring rate was kept at 700 rpm throughout the entire experiment.

The seeded experiment was then run for a period of 8 hours for each run. A total of four treatments were carried out: the first one, continuous without a recycle loop (treatment E8) and the second one carried out with a recycle loop was repeated twice (treatment E9). The recycle loop ensured that the struvite that was collected in the settling tank could be used as seeds in the reactor. Samples of the seeds from the

reactor in treatment E9 were taken for size distribution and SEM analysis after every 2 hours.

The following parameters were measured and recorded by the data logger (RSG40):

- Current
- Voltage for the three electrode configuration (Steel, Ag/AgCl and Magnesium electrode)
- Electrode potential for the two electrode configuration (Mg-steel)
- pH (WTW PH 196)
- Temperature (WTW PH 196)
- Conductivity (WTW LF 96-B)

The precipitates were analysed using a Malvern Mastersizer (Malvern Instruments Ltd., Worcestershire, United Kingdom) for particle size distribution and SEM (NovaSEM230 FEG from FEI with an Oxford EDX system) for the morphology and the particle size. It is important to note that the results from the Mastersizer are volume based and expressed in terms of equivalent spheres. Table 7 shows a summary of the SEP experiment in continuously stirred mode.

Table 7: Summary of the electrochemical experiment carried out in the continuously run SEP to investigate the effect of residence time on the product particle characteristic.

Experiment	**Brief description**	**Justification**	**Magnesium dosage**	**Treatment conditions**	
Electrochemical continuous experiment	Two electrochemical treatments at Mg:P molar ratio of 1.2 (current density of 70 Am^{-2} and surface area 0.0015 m^2) were carried out including a control treatment to investigate how residence time influences the characteristics of the struvite particles. Treatment E8 was run continuously without a recycle loop as the control treatment whilst E9 was run continuously with a recycle loop and repeated twice : E8 (control treatment) $E9^a$, $E9^b$, $E9^c$	To discover how the residence time influences the product characteristics of the struvite	Magnesium electrode	Magnesium electrodes were used for magnesium dosing in a 1 L reactor	
				E8 (control treatment)	• Molar ratio of Mg:P = 1.2 • No seeds • No recycle loop • Stirring rate of 700 rpm • Particle size distribution measured
				$E9^a$, $E9^b$, $E9^c$	• Molar ratio of Mg:P = 1.2 • Recycle loop of seeds produced in the reactor • Stirring rate of 700 rpm • Particle size distribution measured and compared to that of the seeds produced in treatment E8

4.5.4 Experimental setup and procedure for the batch seeded electrochemical reactor at varied levels of magnesium ion supersaturation

The effect of the level of magnesium ion supersaturation on the struvite product particle characteristics was investigated by varying current densities in the SEP in batch mode. The experimental setup was as shown in Figure 9. The residence time was set to 2.5 h and the current density was varied between 30 and 90 Am^{-2}. Table 8 shows a summary of these treatments.

Table 8: Summary of the electrochemical experiment carried out in the SEP reactor in batch mode at varied current densities to investigate the effect of the level of magnesium ion supersaturation on the product particle characteristics.

Experiment	**Brief description**	**Justification**	**Magnesium dosage**	**Treatment conditions**	
Electrochemical run in batch mode at varied current densities	Five treatments were run at current density 30, 35, 45, 55, 60 and 90 Am^{-2}	To discover how the level of magnesium ion supersaturation influences the struvite product particle characteristics in the electrochemical experiment	Magnesium electrode	Magnesium electrodes were used for magnesium dosing in a 1 L reactor	
				Current density 30, 35, 45, 55, 60 and 90 Am^{-2}	• No seeds • Stirring rate of 120 rpm • Particle size distribution measured

5 Results and discussions

This chapter covers the results and the discussion of the experiments that are outlined in Chapter 3, namely the thermodynamic modelling and the validation of the model by the simple batch experiment. The results and discussion of the unseeded and seeded electrochemical precipitation of struvite experiments in batch and continuous mode are also covered. The final sections of the chapter cover the analysis of the particles produced in the above mentioned electrochemical precipitation at Mg:P molar ratio of 1.2 and those produced in the SEP in batch mode at varied levels of magnesium ion supersaturation. This chapter concludes with an economical assessment of the seeded electrochemical precipitation process.

5.1 Thermodynamic modelling and validation

5.1.1 Effect of magnesium ion concentration on theoretical recoveries of struvite and nesquehonite

In the simulation, the pH was not manually controlled and left to vary for different magnesium concentrations at a constant temperature of 25 ^{o}C. This was done in order for the resultant solution to achieve a resultant charge of zero. This is similar to the process that would occur in the electrolytic cell as explained by electrochemistry theory in Appendix VI. Figure 11 shows how the pH and yields of struvite and nesquehonite respond to an increase in the Mg:P molar ratio for the range of 0 to 11.

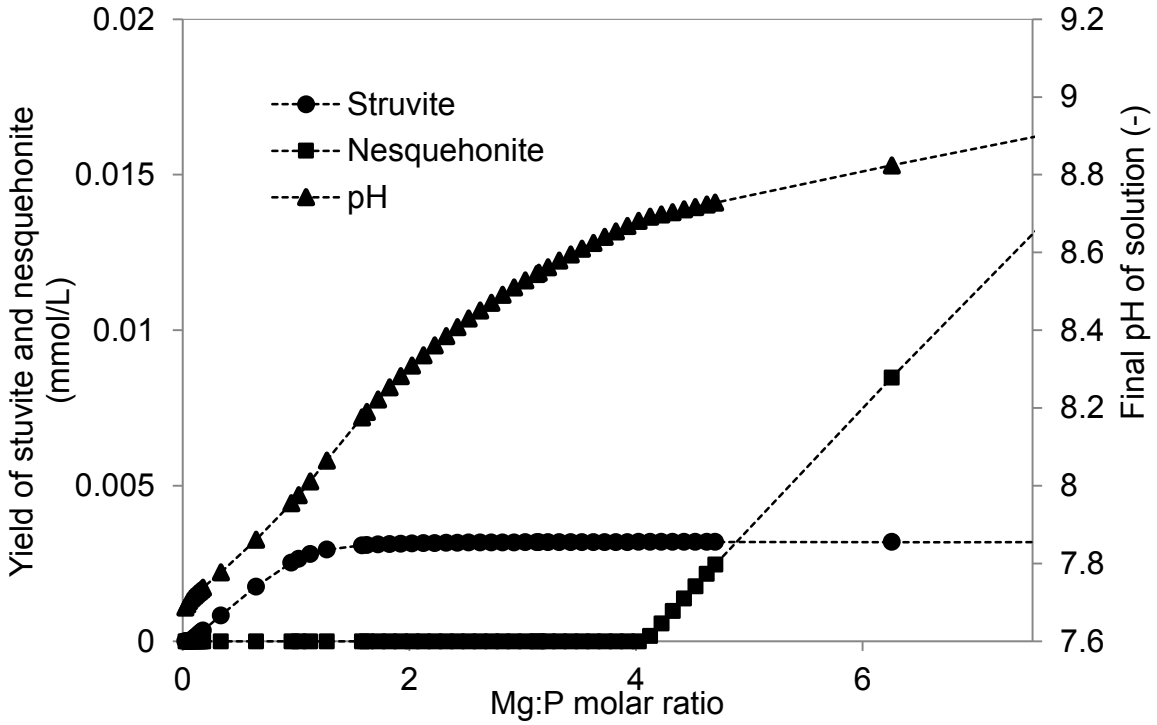

Figure 11: Yields of struvite and nesquehonite and the final solution pH with increase in Mg:P molar ratio.

The pH increases gradually to a value of 8.7 at Mg:P molar ratio of 4 and thereafter increases gradually to pH 8.9 at Mg:P molar ratio of 7. The yield of struvite increases linearly to 0.0029 at Mg:P of 1.3 at pH 8.1. Thereafter it starts to increase gradually to 0.0030 mol/L at Mg:P molar ratio of 2.1. The yield of struvite remains at that level until nesquehonite starts to form at a Mg:P molar ratio of 4 and pH of 8.7. The yield of nesquehonite increases linearly as the Mg:P molar ratio and pH increases.

The increase of the Mg:P molar ratio is directly related to the increase in concentration of magnesium ions in the solution. The increase in the concentration of magnesium ions inevitably results in the formation of hydroxide ions as illustrated in Equations 29 and 30, leading to the increase in pH. As the concentration of magnesium ions increases, the position of equilibrium shifts to the right leading to the release of more hydroxide ions according to le Chatelier's law of dynamic equilibrium. As the concentration of magnesium ions increases in the solution, struvite starts to precipitate. When more magnesium is added, it Mg ceases to be the limiting agent, the ideal Mg:P molar ratio for maximum struvite yield is achieved (Mg:P molar ratio greater than 2.1) and thereafter with further addition of magnesium, phosphorous starts to become the limiting reagent. The yield of struvite reaches its maximum which, for this simulation, is 0.0032 mol/L at pH range 8.5 to 9. At this pH range the speciation

of the phosphate and ammonium ion favours the formation of struvite as shown in Figure 6 and

Figure 7. Nesquehonite forms due the increase pH as well as the supersaturation of the magnesium ions. This is expected as the speciation of the carbonate ion at pH of 8.7 in accordance with Figure 5, favours the formation of the carbonate ion because nesquehonite contains HCO_3^{2-}.

Figure 12 shows the percentage conversion of ortho-phosphate, magnesium and carbonate ions with increase in the Mg:P molar ratio in the solution for the same system represented in Figure 12. The conversion of phosphate increases sharply to a conversion of 91 % at a Mg:P molar ratio of 1.3. The conversion then increases gradually to 99.5 % at a Mg:P molar ratio of 4 and at a pH of 8.7. This is the same condition at which the carbonate ions are converted to nesquehonite. The conversion of the carbonate ions after a Mg:P molar ratio of 4 and a pH of 8.7 starts and increases linearly for the entire Mg:P molar ratio range that was investigated. The conversion of the magnesium ions increases linearly to 84 % and at a Mg:P molar ratio of 0.65 after which it drops to 25 % at a Mg:P molar ratio of 4 and a pH value of 7.8 and 8.7 respectively. Thereafter, the conversion of the magnesium ions increases again up to a value of 81 % at Mg:P molar ratio of 11.

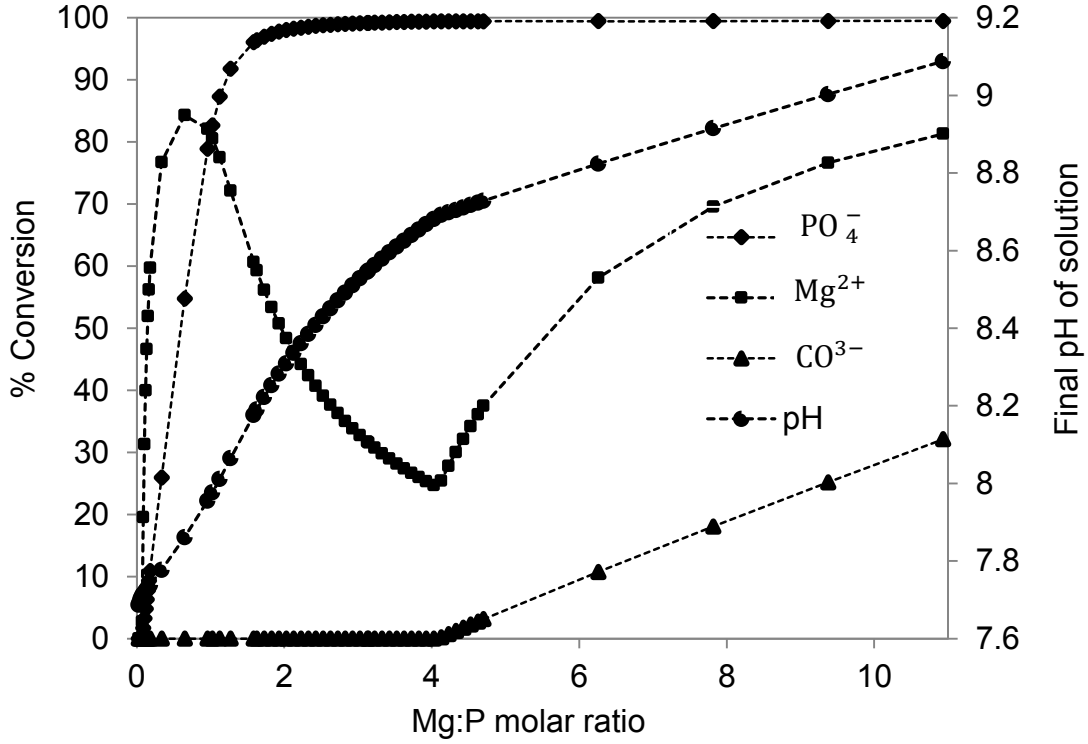

Figure 12: The percentage conversion of magnesium, phosphate and carbonate ions to struvite or nesquehonite with increase in Mg:P molar ratio.

The conversion of orthophosphate ions increases to almost 100% conversion due to the formation of struvite. Literature also shows that under these conditions, other magnesium phosphate compounds such as $MgHPO_4$, $MgH_2PO_4^+$and $MgPO_4^-$ form (Ronteltap et al., 2007). Magnesium is also converted in the formation of struvite. Initially the conversion of the magnesium ions increases, this is because the magnesium ion is the limiting reagent in the formation of struvite. The conversion of the carbonate ions and second increase incline of the conversion of the magnesium ions can be attributed to the formation of nesquehonite. For the Mg:P molar ratio range that was investigated, the conversion of magnesium does not reach 100 % due to the fact that it is in excess compared to the concentrations of the other reactants (orthosphospahte and carbonate) that mainly combines with to form compounds. There is also the likelihood of the formation of compounds such as calcium carbonate ($CaCO_3$) and hydroxylapatite ($Ca_5(PO_4)_3OH$) which may have consumed the phosphate and the carbonates in the solution before these ions could be used to precipitate magnesium based compounds (Ramaru, 2009).

5.1.2 Effect of pH on theoretical yield of struvite and nesquehonite

The pH of solution was then varied for four solutions at different Mg:P molar ratios in the thermodynamic model. This was done by keeping the magnesium ion concentration constant for each Mg:P molar ratio and changing the pH of the solution by balancing the resultant solution ionic charge with chloride and sodium ion. The same technique was used by Mehta and Batstone, (2013) in their thermodynamic modelling work. As aforementioned, chloride and sodium ions do not interfere in the precipitation of either struvite or nesquehonite and can be practically implemented by titrating hydrochloric acid (HCl) or sodium hydroxide $(NaOH)$ to achieve the preferred pH. The cases that were investigated were for Mg:P molar ratios of 1, 1.2, 7.8 and 21 in order to see how the recoveries of struvite and nesquehonite change with pH over a wide range of Mg:P molar ratios for a large range of the Mg:P molar ratio. If all the phosphate and the carbonate ions in the urine are precipitated out as struvite and nesquehonite, then the theoretical (for the measured initial orthophosphate and carbonate ion concentration in the urine sample) amount of struvite and nesquehonite that can be possibly precipitated is 0.0032 mol/L and 0.079 mol/L respectively, provided enough magnesium is supplied and there is no interference from other ions.

Figure 13 shows the yield of struvite and nesquehonite as a function of an increasing pH for the Mg:P molar ratio of 1. Yield is defined as the mass of the product as a fraction of the mass of the reactant. The yield of struvite increases from zero at pH 6.5 to 0.003 mol/l at pH 9.5. Thereafter, the yield decreases until no struvite is recovered which occurs at a pH of 12 and beyond. Nesquehonite is not formed at this molar ratio, even with an increase in pH.

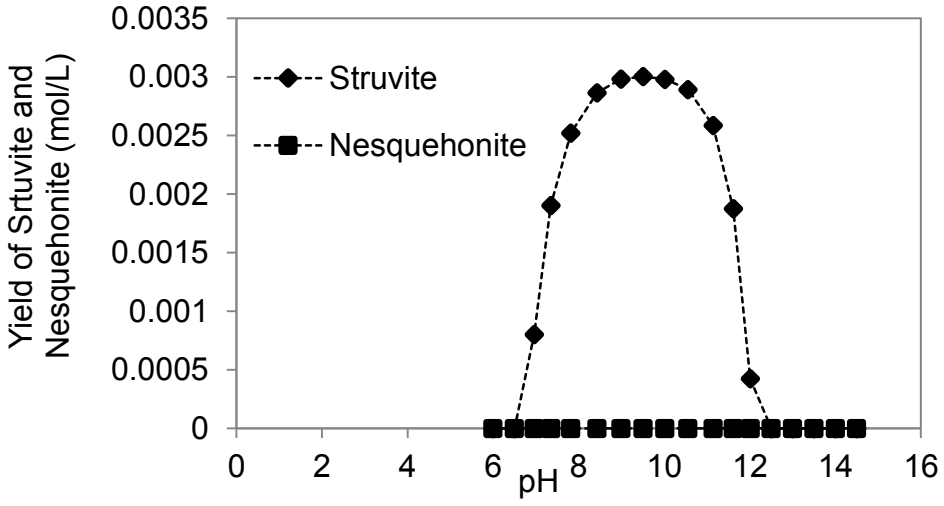

Figure 13: Yield of struvite and nesquehonite with increase in pH for the Mg:P molar ratio of 1.

Figure 14 shows that when the Mg:P molar ratio is increased to 1.2, similar trends for the yield of struvite and nesquehonite are observed as those obtained for the Mg:P molar ratio of 1 as shown in Figure 13. The yield of struvite increases from zero at a pH of 6.5 to 0.0031 mol/L at a pH of 9.5, thereafter it decreases to zero at pH 12 and beyond. The yield of nesquehonite remains at zeros at this Mg:P molar ratio even when the pH increases.

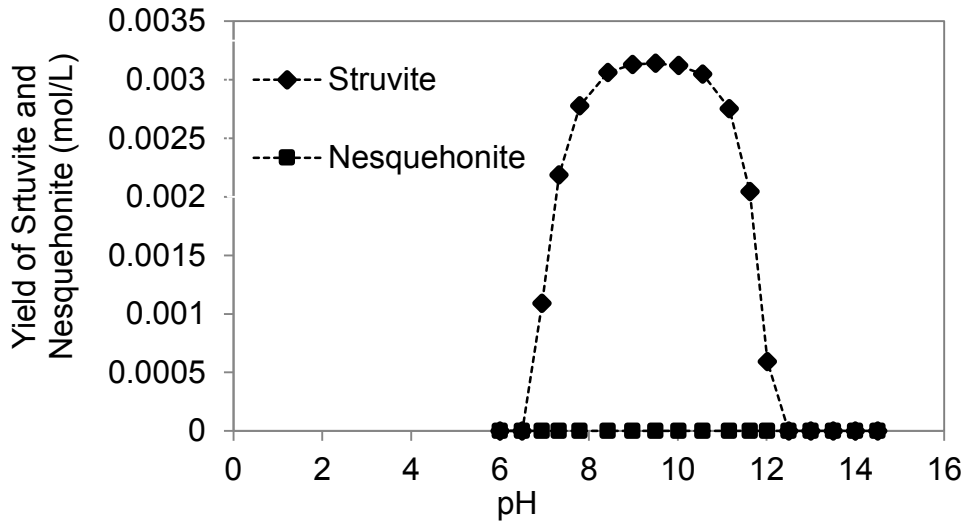

Figure 14: Yield of struvite and nesquehonite with increase in pH for the Mg:P molar ratio of 1.2.

For both results for Mg:P molar ratio of 1 and 1.2, the presence of magnesium, orthophosphate and ammonium ions and the speciation of the orthophosphate and ammonium as shown in Figure 6 and

Figure 7 in the pH range 6.5 to12 resulted in the formation of struvite. Nesquehonite is not formed and this may be due to insufficient magnesium ions to oversaturate the nesquehonite to precipitation even though other conditions such as pH and the speciation of the speciation of the carbonate ion permit. Also modelling always only considers the most stable compound and even if the compound would form in reality, thus the nesquehonite compound may not have been stable in those conditions. This implies that a seeded electrochemical cell, if kinetics are neglected, could be operated at a molar ratio of 1 and a pH of 9 to yield almost 100 % of the total struvite that can be potentially obtained with no nesquehonite. This then provided to be a good starting point for seeded electrochemical precipitation experiments.

Figure 15 shows the percentage conversion of the corresponding ions responsible in the formation of the compounds shown in Figure 13 i.e. magnesium, orthophosphate and carbonate ions with increasing pH at a Mg:P molar ratio of 1. Conversion is defined

as the difference between the initial and final concentration, as a fraction of the initial concentration. The conversion of the orthophosphate and magnesium ion increases from zero at pH 6.5 to a maximum of 94 % and 91 % at pH 9.5 respectively, thereafter they decrease to zero at pH 12.5 and beyond. The percentage conversion of the carbonate ions remains at zero throughout the entire pH range that was investigated.

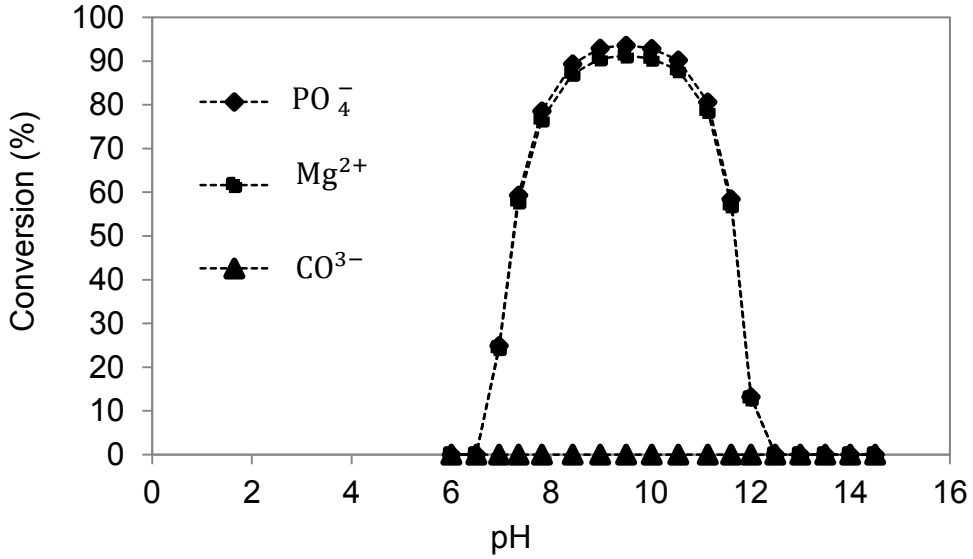

Figure 15: The percentage conversion of magnesium, phosphate and carbonate ions to struvite or nesquehonite with increase in pH for the Mg:P molar ratio of 1.

Figure 16 shows that when the Mg:P molar ratio is increased to 1.2 and the pH is increased, the percentage conversion of orthophosphate and magnesium increases from zero at a pH of 6.5 reaches a maximum of 98 % and 77 % respectively at a pH of 9.5, thereafter it decreases to zero at pH 12.5 and beyond. The conversion of carbonate ions remained at zero for the entire pH range that was investigated.

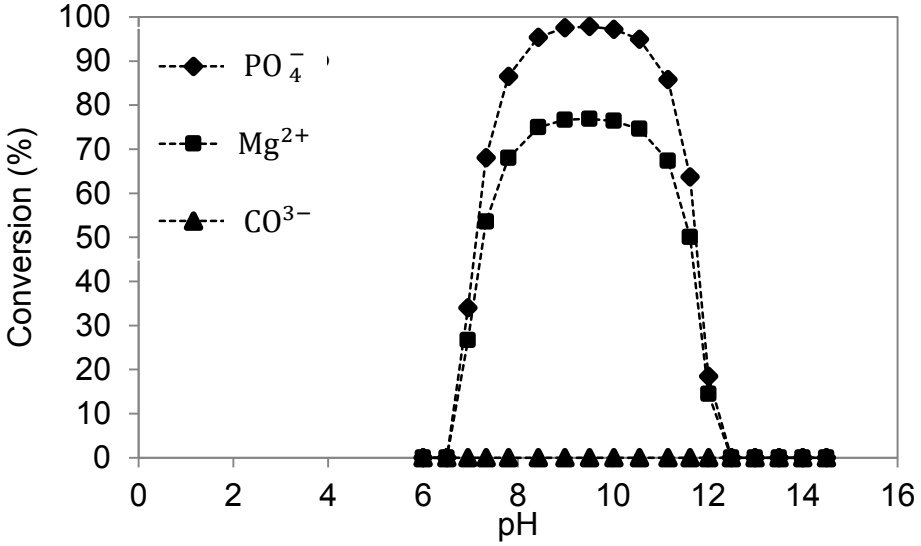

Figure 16: The percentage conversion of magnesium, phosphate and carbonate ions to struvite or nesquehonite with increase in pH for the Mg:P molar ratio of 1.2.

The conversions of orthophosphate and magnesium can be attributed to the speciation of the orthophosphate and ammonium and the formation of struvite as shown in Figure 13 and Figure 14; all the orthophosphate and magnesium is converted to struvite. The slight increase in the yield of struvite for the Mg:P molar ratio of 1.2 compared to that obtained at a Mg:P molar ratio of 1 as shown in Figure 13 and Figure 14 respectively, is due to more magnesium ions in the solution for the available orthophosphate to form struvite. Thus the decrease in the magnesium conversion from 91 % to 77 % as shown in Figure 15 and Figure 16 respectively.

According to the thermodynamic modelling, the potential of the formation and deposition of nesquehonite on the electrodes is unlikely at these conditions due to its instability, even though there are free magnesium and carbonate ions in solution. The zero change in the conversion of carbonate ions in both conditions further supports that nesquehonite does not form. It can be further postulated that at these conditions, other carbonate compounds such as calcium carbonate and anhydrous magnesium carbonate are also not likely to form.

Figure 17 shows that when the Mg:P molar ratio is increased to 7.8 the yield of struvite increases from zero at a pH of 6.5 and reaches a maximum of 0.0032 mol/L at a pH of 8.9, which is the maximum theoretical yield, given the initial orthophosphate concentration in the urine sample. Thereafter it decreases to zero at a pH of 12.6. It is also observed that the 100 % struvite recovery at this Mg:P molar ratio is attained at a lower pH value; 8.9 compared to pH 9.5 when the Mg:P molar ratio is 1 and 1.2. The

yield of nesquehonite at this Mg:P molar ratio increases from zero at a pH of 7.8 and increases to a maximum of 0.019 mol/L at a pH value of 10.6 then decreases to zero at a pH of 13.5 and beyond.

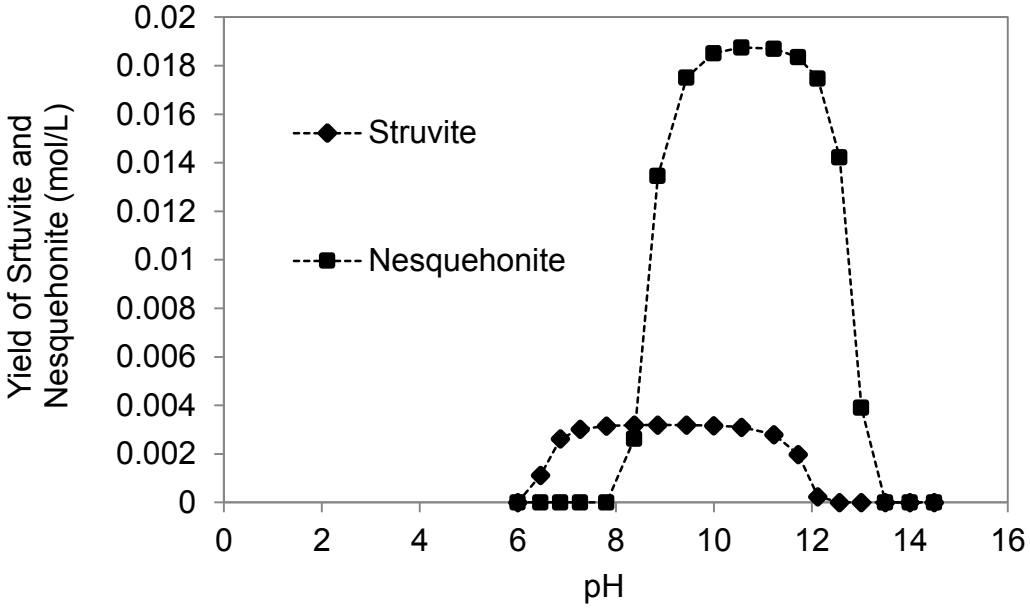

Figure 17: Yield of struvite and nesquehonite with increase in pH for the Mg:P molar ratio of 7.8.

Figure 18 shows the yield of struvite and nesquehonite when the Mg:P molar ratio is increased to 21. The yield of struvite increases from zero at a pH of 6 and reaches the maximum of 0.0032 mol/L at a pH of 8.5, thereafter it decreases to zero at a pH of 12.5 and beyond. That of nesquehonite also increases from zero at a pH of 8, increases to 0.062 mol/L at a pH value of 10.5 and then decreases to zero thereafter at a pH 13.5 and beyond.

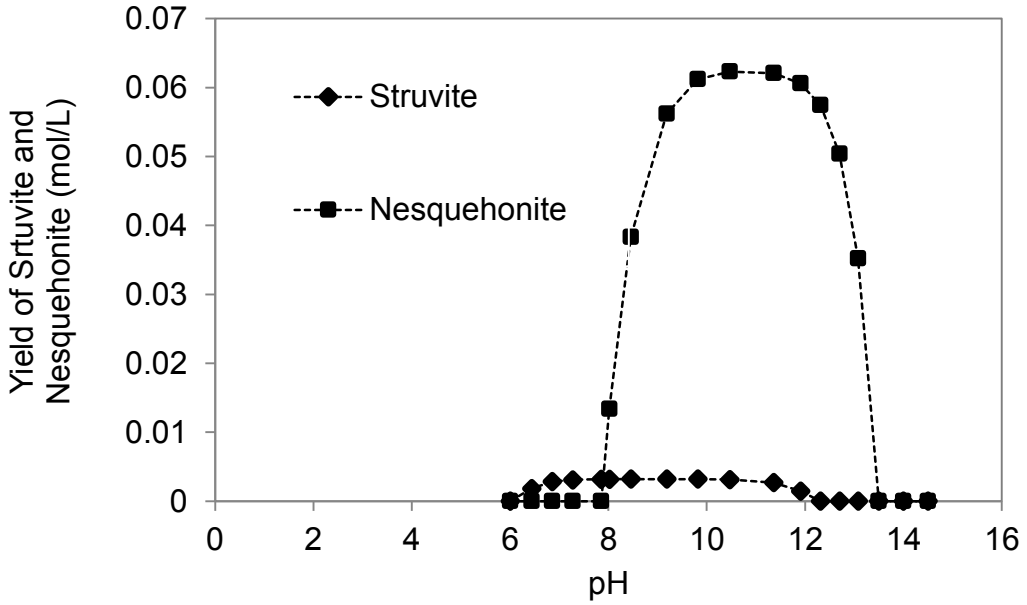

Figure 18: Yield of struvite and nesquehonite with increase in pH for the Mg:P molar ratio of 21.

Struvite recoveries at Mg:P molar ratio of 7.8 and 21 both reach 100% and in both cases nesquehonite is also recovered; with Mg:P molar ratio producing higher nesquehonite recoveries due to the increase in the magnesium ions in solution.

The high struvite yields at lower pH values can be attributed to the presence of a sufficient amount of reactants (orthophosphate, ammonium and magnesium ions) and pH ideal for the formation of struvite. The pH ideal for struvite precipitation seems to be in the range of 6 and 13. Nesquehonite is also formed at this Mg:P molar ratio due to the presence of magnesium ions in abundance, carbonate ions and ideal pH. These high Mg:P molar ratio conditions, however, are not ideal for the electrochemical precipitation of struvite because, not only would the quality of the struvite that is collected be compromised, but high electrode potentials would also be needed to dissolve the magnesium electrode into ions. Also, system failures due to the high degrees of passivation (caused by the accumulation of the nesquehonite on the anode surface) would also occur (Kruk et al., 2014).

Figure 19 shows the percentage conversion of individual ions: magnesium, orthophosphate and carbonate ions with an increasing pH at Mg:P molar ratio of 7.8. The conversion of the orthophosphate increases from zero at a pH of 6 and increases to 100 % at a pH of 8.9. It then decreases to zero at pH 12.5 and beyond. The percentage conversion of the magnesium ion also increases from zero at a pH of 6 and increases to a maximum of 87 % at a pH of 10.7 after which it decreases to zero at a pH of 13.5 and beyond. That of the carbonate ion increases from zero at a pH of

7.8 and increases to a maximum of 24 % at a pH of 10.5 after which it decreases to zero at a pH of 13.5 and beyond.

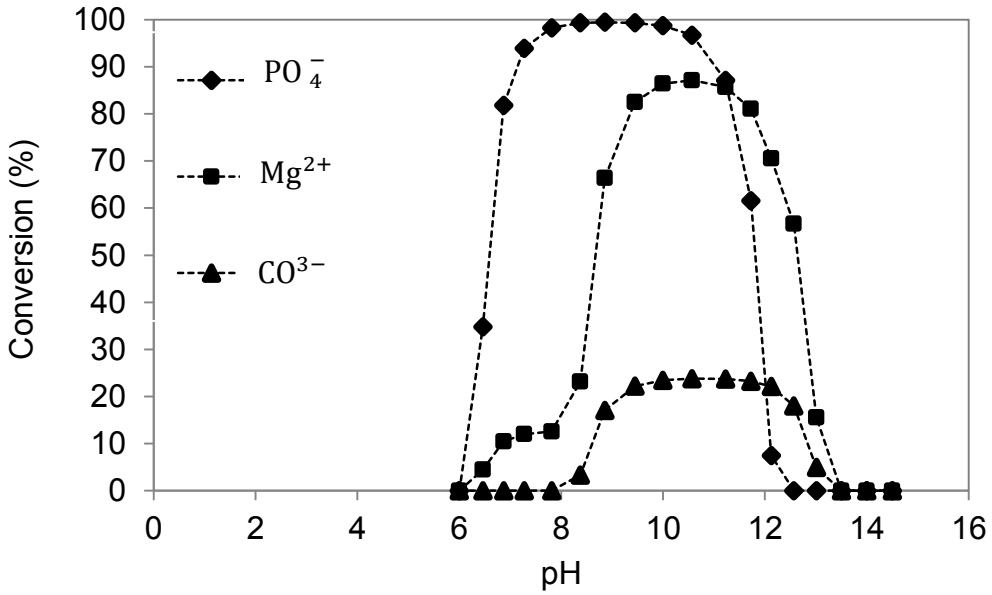

Figure 19: The percentage recovery of magnesium, phosphate and carbonate ions to struvite or nesquehonite with increase in pH for the Mg:P molar ratio of 7.8.

Figure 20 shows the percentage conversion of individual ions: magnesium, orthophosphate and carbonate ions with an increasing pH at Mg:P molar ratio of 21. The conversion of the orthophosphate increases from zero at a pH of 6 and increases to 100 % at a pH of 8.9. The conversion then decreases to zero at a pH of 12.5 and beyond. The percentage conversion of the magnesium ion also increases from zero at a pH of 6 and increases to a maximum of 87 % at a pH of 10.7 after which it decrease to zero at a pH of 13.5 and beyond. That of the carbonate ion increases from zero at a pH of 7.8 and increases to a maximum of 24 % at a pH of 10.5 after which it decreases to zero at a pH of 13.5 and beyond.

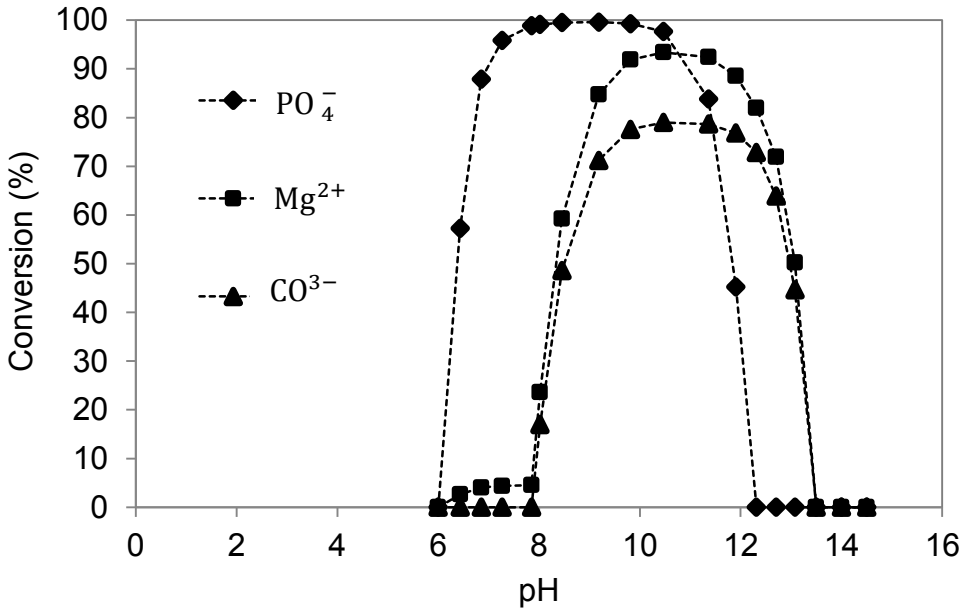

Figure 20: The percentage recovery of magnesium, phosphate and carbonate ions to struvite or nesquehonite with increase in pH for the Mg:P molar ratio of 21.

For both Mg:P molar ratios 7.8 and 21, the conversion of the orthophosphate and magnesium ions can be attributed to the formation of struvite at maximum yields as shown in Figure 17 and Figure 18. That of the carbonate ion can be attributed to the formation of nesquehonite and that the speciation of the orthophosphate and ammonium ion and the carbonate ion is favourable for the formation of struvite and nesquehonite at the pH range (6-13) at which the maximum conversion of these ions occurs.

In summary; assessing all four Mg:P molar ratios with regards to the maximum yields of struvite, when the Mg:P molar ratio is 1 or 1.2 (relatively low), the yield of struvite peaks at higher pH values (9.5) than when the Mg:P molar ratio is 7.8 and 21 (relatively high), the pH peaks at 8.9. The pH ideal for struvite precipitation seems to be in the range of 6 and 13. However, for these relatively high Mg:P molar ratios, struvite yields peak when nesquehonite has already started to form at approximately equimolar quantities as shown in Figure 17 and Figure 18. This means that the purity of struvite will be compromised and the build-up of nesquehonite on the electrode will compromise the functionality of the electrolytic cell and the efficiency of the entire electrochemical precipitation system.

5.1.3 Experimental recoveries of struvite and nesquehonite with change in magnesium ion concentration

Table 9 shows the initial composition and the initial and final pH of the urine that was used for the simple batch experiment for the validation of the thermodynamic model, Treatments E1 and E2.

Table 9: Average composition for the initial concentration and initial and final pH of the urine used in the simple batch experiment, Treatment E1 and Treatment E2. The urine from source separated urine storage tanks at Eawag main building (Forum Chriesbach).

Element	**Average composition for the urine sample for Treatment E1 (Mg:P =1.2)**	**Average composition for the urine sample for Treatment E2 (Mg:P =21)**
	mg/L	**mg/L**
COD	1102 ± 153	1180 ± 43.6
TIC	1150 ± 250	1137 ± 250
Mg	2.1 ± 0.5	2.3 ± 0.5
PO_4-P	98.5 ± 1.53	100.5 ± 0.99
NH_4-N	1830 ± 20.8	1790 ± 26.5
SO_4	236 ± 3.06	233 ± 3.51
Na	747 ± 6.1	733 ± 10.1
K	701±14.8	692 ± 9.17
Ca	30.7±2.52	29.7 ± 5.03
Average initial pH	8.90 ± 0.05	8.91 ± 0.03
Average final pH	8.91 ± 0.04	10.1 ± 0.03

The initial and final pH predicted by the thermodynamic model S1 did not change and was 8.90 and that of S2 was 8.93 and 9.98 respectively. These were similar to the initial and final pH that was recorder in Treatment E1 and E2 as shown in Table 9. Thus, the thermodynamic model was fairly accurate in predicting the final pH of the simple batch experiment for Treatment E1 and E2. For both treatments the final pH in both was higher than the initial pH due to the dosage of 1M sodium hydroxide solution. The higher final pH in Treatment E2 is attributed to the higher sodium hydroxide dosage.

The final concentrations of the urine after precipitation were measured and the conversions of magnesium, ortho-phosphate, ammonium and carbonate amongst other components in the urine were calculated. The results are shown in Figure 21 and Figure 22 for Treatments E1 and E2 respectively.

All components in the urine for both treatments undergo conversions with larger conversions being reported for Treatment E2. Determination of the conversions of ammonium and carbonate (TIC) ions was a challenge because the concentrations of these ions in the source separated urine are relatively higher than the other ions hence the urine sample had to be diluted in order to measure those concentrations and this increased the error in those measurements. Also, during the formation of struvite and nesquehonite, only small fractions of ammonium and carbonate (TIC), were consumed (in comparison to orthophosphate and magnesium). These small fractions sometimes fell in the range of the standard deviations of the concentration measurements due to sources of error (± 5%) including dilution. As such, it was mostly assumed that the ammonium that was converted was in equimolar quantities as the amount of struvite that was precipitated.

Figure 21 shows that the conversions of orthophosphate and magnesium were 68 % and 93 % respectively and those of ammonium and TIC were 3.4 % and 3.6 % respectively due to the formation of struvite and nesquehonite. The conversions of orthophosphate and magnesium were lower than those predicted by the thermodynamic model in Figure 16 due to reaction kinetics as Treatment E1 was only run for 2 hours and not infinitely as would have been simulated by the thermodynamic model. Low conversions for COD, sulphate, sodium, potassium and calcium were reported due to the formation of minute concentrations of compounds containing those ions. Ronteltap et al. (2010) also postulated that the due to the relatively low sulphate concentration in collected urine, sulphate complexes such as $[MgSO_4]_{aq}$ and $[NH_4SO_4]^-$ are not expected to form in high concentrations, however low concentrations of compounds such as calcium carbonate and calcium phosphate may form during the precipitation of struvite from source separated urine. The error associated with the experimental results was small and thus the experimental method is reproducible.

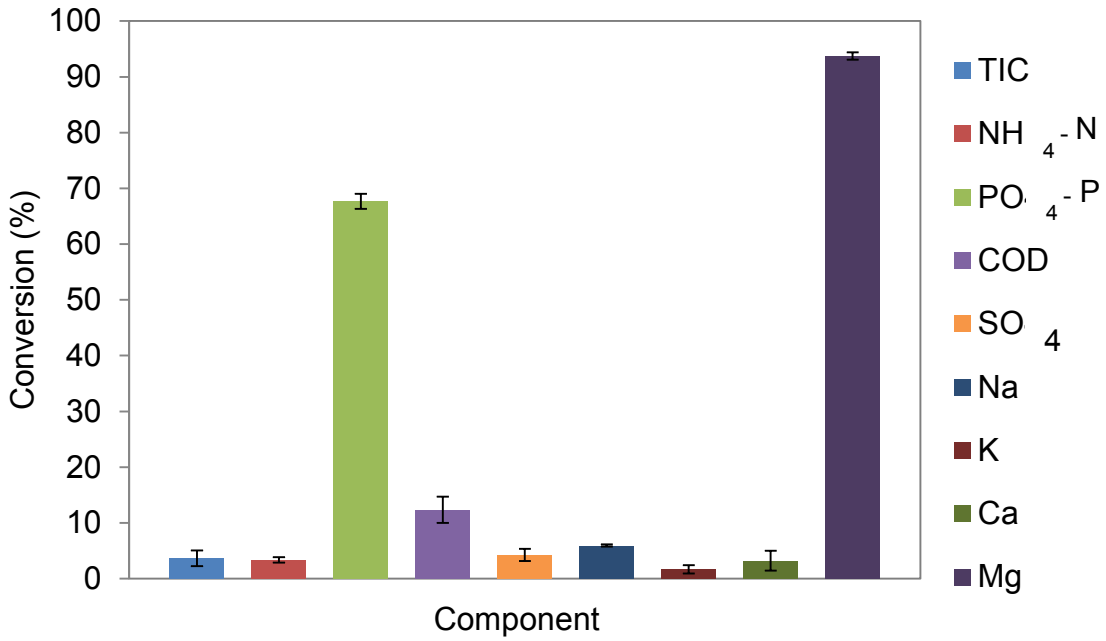

Figure 21: Percentage conversions for Treatment E1.

The higher conversions for orthophosphate, magnesium, ammonium and carbonate as reported in Figure 22 for Treatment E2 are due to the higher Mg:P molar ratio producing more struvite and nesquehonite as predicted by the thermodynamic model in Figure 20. The remainder of the components in the urine like calcium were also converted to other complexes especially with calcium such as calcium phosphate and calcium carbonate (Ronteltap et al., 2007).

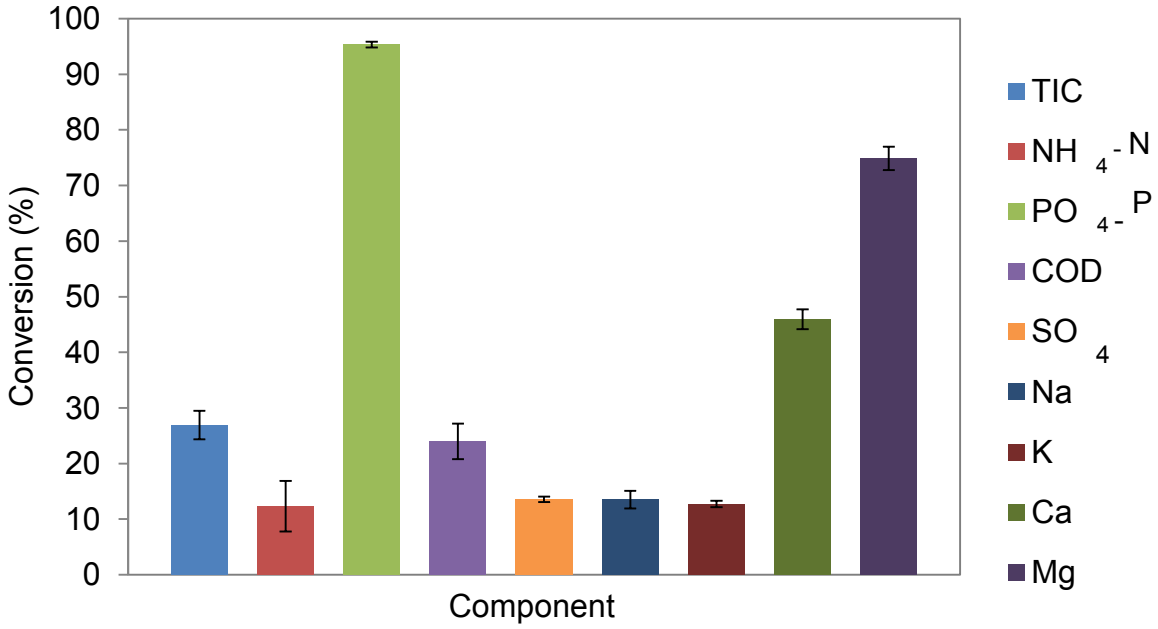

Figure 22: Percentage conversion for Treatment E2.

As magnesium ions remain in solution and pH increases other compounds such as huntite ($CaMg(CO_3)_4$) and dolomite ($CaMg(CO_3)_2$) may have formed (see Appendix I for positive saturation indexes).

The thermodynamic model shows the precipitation of the most stable compounds would be under equilibrium conditions and because reaction kinetics have been ignored, the formation of intermediate precipitates have been neglected. As aforementioned, the precipitation of only the struvite and nesquehonite was modelled in this set of simulations hence saturation indexes were used to decipher whether or not other complexes apart from struvite and nesquehonite are likely to precipitate.

Figure 23 shows the comparison of the thermodynamic simulation results and experimental results for Simulation S1 and Treatment E1 respectively. For both S1 and E1, there were no conversions for TIC, COD, sulphate, sodium, potassium and calcium were reported for the E1 as shown in Figure 21 and Figure 23. This is also supported by the negative saturation indexes for complexes such as $CaSO_4$ and $Na_2SO_4 \cdot 10H_2O$ as shown in Appendix I (Simulation S1). The error bars give an idea of how the measurements in the repeats deviated from the average value. The error associated with the experimental results is small and thus the experimental method is reproducible. There is no error associated with the simulations because the simulation is based on having a charge balance for the respective ions.

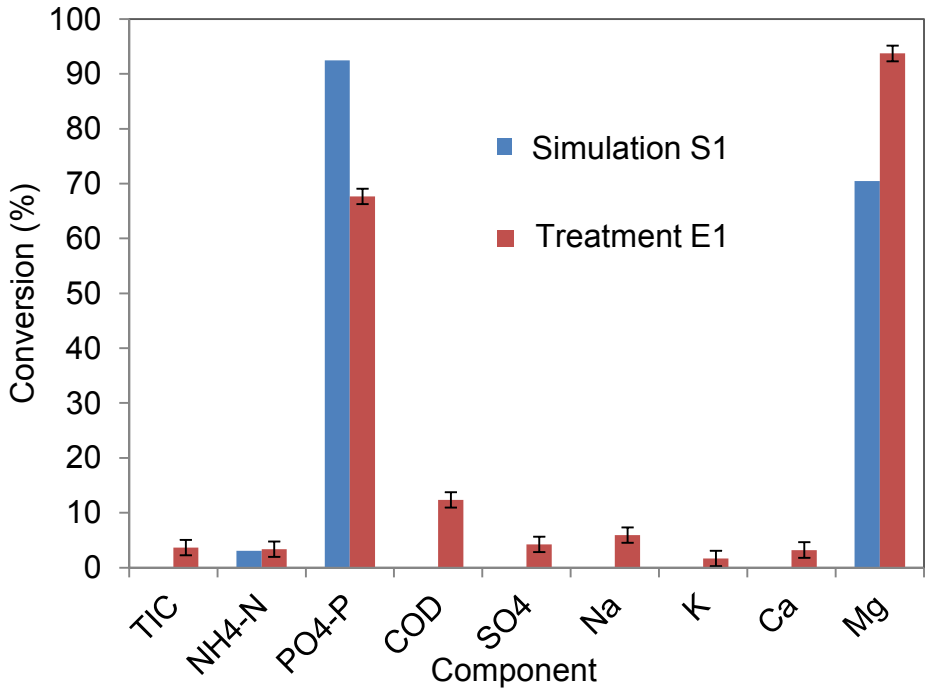

Figure 23: Percentage conversions for Simulation E1 and Experiment E1 (Mg:P molar ratio of 1.2).

Figure 24 shows the comparison of the conversions in Simulation S2 and Treatment E2. The higher conversions obtained from the experimental work are likely due to the formation of other complexes (with COD, sulphate, sodium, potassium and calcium) apart from struvite and nesquehonite. Similarly, for Treatment E1, these were not converted in the thermodynamic model and their formation was predicted by the saturation indexes in Appendix I (Simulation S1). The high conversions of TIC (carbonates), ammonium, orthophosphate and magnesium are comparable for both Simulation S2 and Treatment E2. Appendix I (Simulation S1) also shows that the saturation indexes of complex compounds such as calcite ($CaCO_3$), dolomite ($CaMg(CO_3)_2$), huntite ($CaMg(CO_3)_4$) and hydroxyapatite ($Ca_5(PO_4)_3OH$) may have contributed to the relatively high calcium conversions. Complexes that contain sulphate, sodium and potassium were not likely to precipitate.

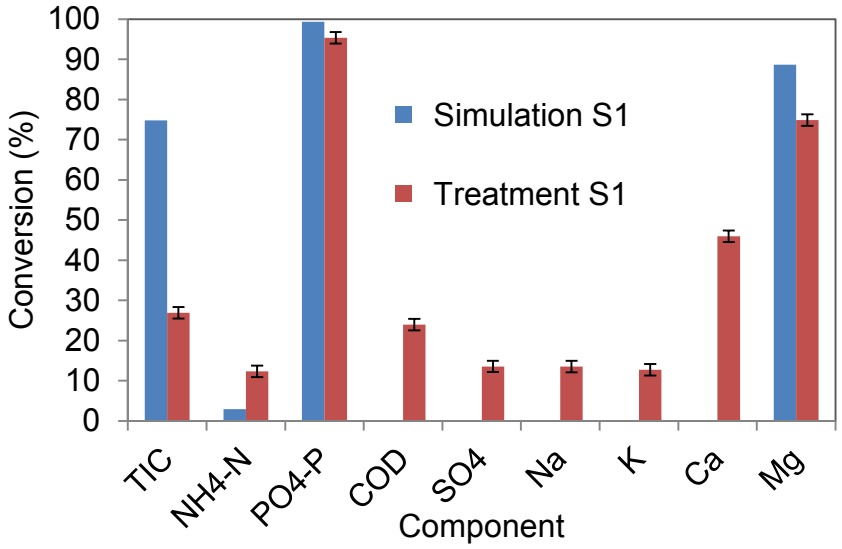

Figure 24: Percentage conversions for Simulation E2 and Experiment E2 (Mg:P molar ratio of 21).

In summary, the validation of the thermodynamic modelling results in S1 and S2 by the simple batch experiment by comparing the conversion of the orthophosphate, carbonate and magnesium ions which are the constituent compounds of struvite and nesquehonite compare with small deviations which are due to errors such as dilution. The conversion of other compounds in the experiments may have been due to the precipitation of some calcium containing compound as above mentioned and inevitably some error in measuring. Sources of error include the measuring equipment, dilution accuracy and human error. The error bars also show that the repeat runs deviated from the average value by a small value that the experimental method is reproducible. There is no error associated with the simulations because the simulation is based on having a charge balance for the respective ions.

5.1.4 X-Ray analysis of precipitates produced in Treatment E1 and E2

The precipitates formed in experiment E1[a] and E2[a] were collected and analysed by x-ray diffraction to give a qualitative identification of the compound that was formed. The spectrum for E1[b], E1[c], E2[b] and E2[c] are included in Appendix II. The spectra that were generated were compared to the spectrum for pure struvite and nesquehonite to draw clear comparisons.

Figure 25 shows the spectrum for the precipitate sample from Treatment E1[a], pure struvite and nesquehonite. The spectrum peaks for the sample produced in Treatment E1[a] correspond well with those for pure struvite and not with nesquehonite. It can thus be postulated that the precipitate sample E1[a] is mostly made up of struvite as predicted by the thermodynamic model S1.

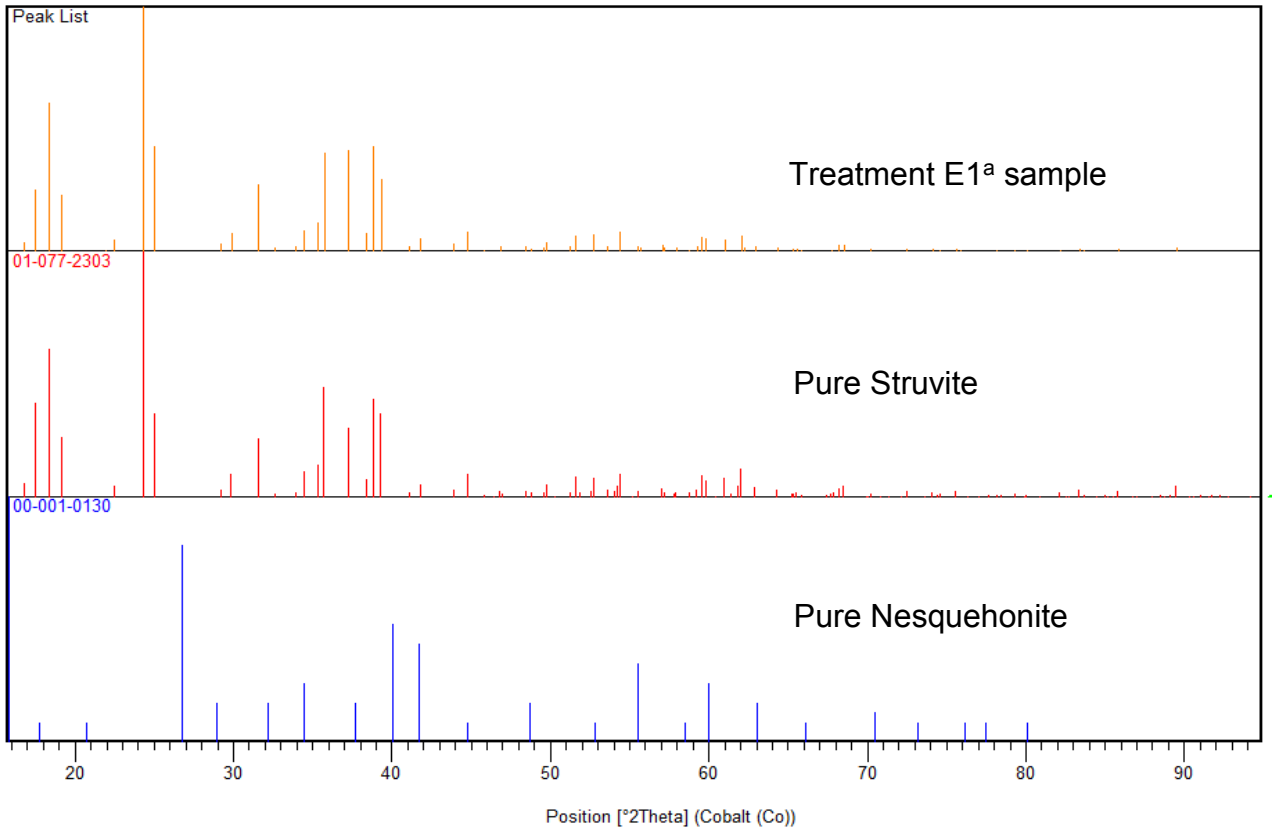

Figure 25: Spectrum for the precipitate sample from experiment E1[a] compared against that of pure struvite and nesquehonite.

Figure 26 shows the spectrum for the precipitate sample from Treatment E2[a], pure struvite and nesquehonite. The spectrum peaks for the sample produced in Treatment E2[a] correspond with both those of pure struvite and with nesquehonite. It can thus be postulated that the precipitate sample E2[a] is made up of both struvite and nesquehonite as predicted by the thermodynamic model S1.

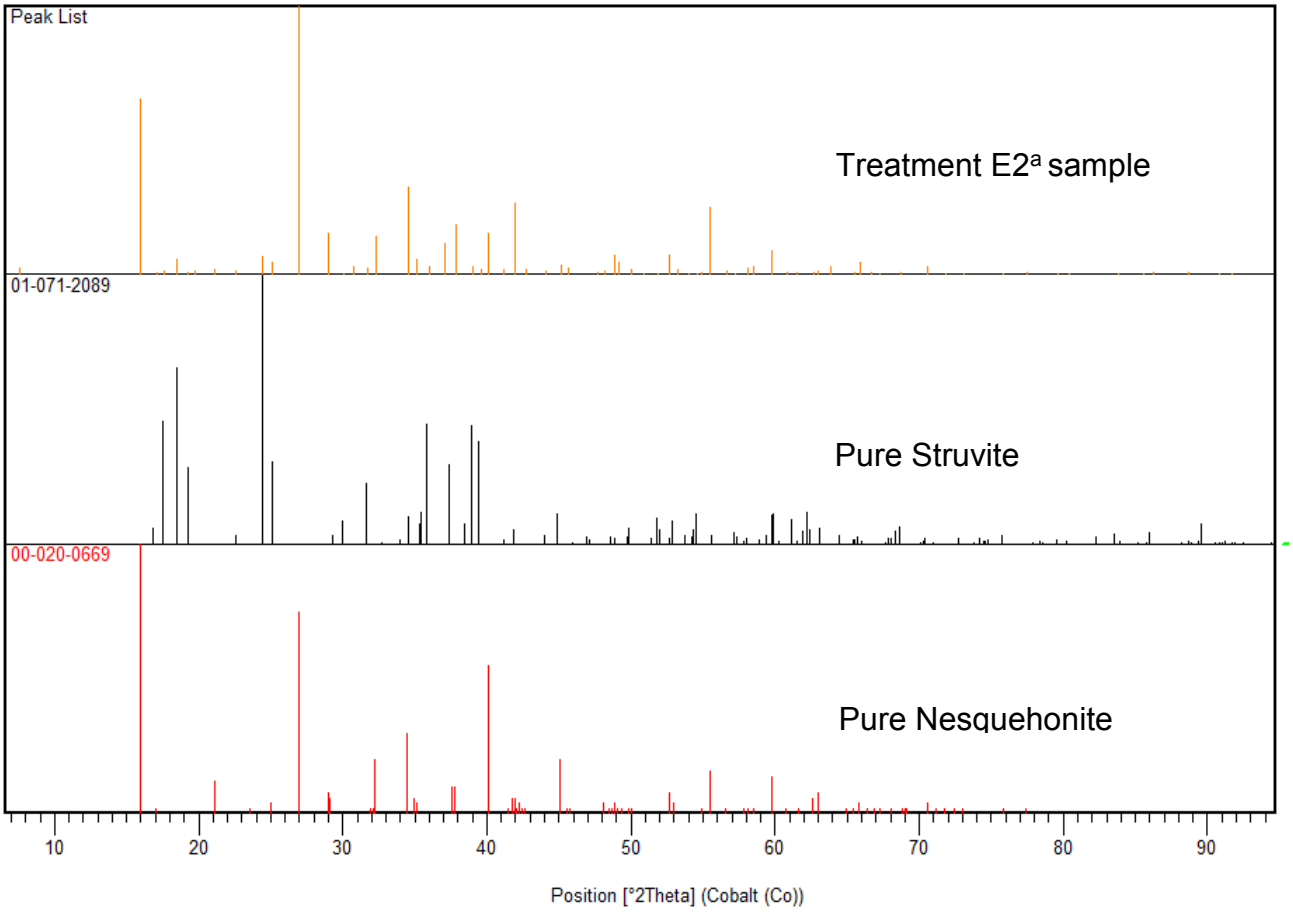

Figure 26: Spectrum for the precipitate sample from experiment E2ª compared against that pure struvite and nesquehonite.

5.2 Unseeded and seeded electrochemical precipitation

5.2.1 Comparison of the yields of the unseeded and seeded electrochemical batch experiment with the yields predicted by the thermodynamic model.

After conducting the validation of the thermodynamic model with Treatments E1 and E2, an electrochemical experiment was run with a Mg:P molar ratio of 1.2 by setting the potentiostat galvanostatically at a current density of 70 A/m^2 for two hours using a 15 cm^2 magnesium electrode. The results were then compared to the predictions of the thermodynamic model. Seeding cannot be modelled thermodynamically hence, one simulation at these optimum conditions was considered for the comparison.

Table 10 shows the average values for the initial concentration of the urine used in the electrochemical experiment for Treatments E3 to E7 and those of the corresponding thermodynamic model, S1. These treatments were performed in duplicates and the first and second run were denoted by [a] and [b] respectively. It should be noted that there were some differences between the initial composition of the urine used experimentally with respect to carbonate, magnesium and phosphate ions and that which was used for the thermodynamic model shown in Table 2. This is because the urine was collected on different days.

Table 10: Average Initial concentration of the urine used in the electrochemical experiments, Experiment E3 to E7 and those of the corresponding thermodynamic model. The urine taken from the source separated urine storage tanks at Eawag main building (Forum Chriesbach).

Element	**Urine sample for treatment E3 – E7**					**Thermodynamic model S1**
	E3	**E4**	**E5**	**E6**	**E7**	
pH	9.19±0.01	9.20 ± 0.04	9.24 ± 0.02	9.15± 0.02	9.06± 0.02	8.90
	mg/L	**mg/L**	**mg/L**	**mg/L**	**mg/L**	**mg/L**
TIC	1014± 26.4	1092 ± 21.6	1042 ± 20.0	1110 ± 21.4	1064 ± 26.0	948
Mg^{2+}	2.6± 0.5	2.2 ± 0.5	1.8± 0.5	3.1± 0.5	1.7± 0.5	2.1
PO_4-P	102.1± 0.50	108.9 ± 0.10	96.3 ± 0.50	99.3 ± 0.10	98.1 ± 0.20	99

Table 11 summarises the conditions for the treatments for the electrochemical experiment that were conducted as well as a comparison of the final pH values of the experimental and simulation solutions. The initial pH values of the urine for Treatments E3 to E7 were similar with an average initial and final pH of 9.17 and 9.38 respectively. In theory, these pH conditions are ideal for this investigation because they are in the range suitable for 98 % conversion of the orthophosphate as predicted by the thermodynamic model at a Mg:P molar ratio of 1.2 shown in Figure 16.

Table 11: Summary of the conditions for the treatments for the electrochemical experiment, E3, E4, E5, E6 and E7 and a comparison of the final pH values of the treatments and the thermodynamic model.

Treatment Number	**Type of seeds**	**Mass of seeds**	**Stirring rate**	**Initial pH**	**Final pH**	**Thermodynamic model S1 Final pH**
E3[a], E3[b] (control treatment)	No seeds	-	120 rpm	9.19 ± 0.01	9.50 ± 0.02	9.50
E4[a], E4[b]	VUNA struvite	0.8 g	120 rpm	9.20 ± 0.04	9.38 ± 0.03	9.50
E5[a], E5[b]	VUNA struvite	0.8 g	500 rpm	9.24 ± 0.02	9.42 ± 0.02	9.50
E6[a], E6[b]	Electrochemically precipitated struvite	0.8 g	120 rpm	9.15 ± 0.02	9.33 ± 0.03	9.50
E7[a], E7[b]	Electrochemically precipitated struvite	0.8 g	500 rpm	9.06 ± 0.02	9.29 ± 0.04	9.50

Figure 27 shows the percentage conversions of the carbonate, orthophosphate and magnesium ions in the electrochemical struvite precipitation batch reactor compared to those of the simulation (Mg:P=1.2) generated in Figure 16. The percentage conversions of these ions in the different treatments are fairly similar. The carbonate conversions measured for Treatments E3 to E7 are the lowest. The highest conversion measured for the carbonate is 3.6 % in Treatment E5 where the VUNA seeds were used at a stirring rate of 500 rpm. This is not what the thermodynamic model predicted and may have been as a result of the formation of carbonate containing compounds such as nesquehonite. The highest final pH amongst the seeded treatments was also measured in this experiment.

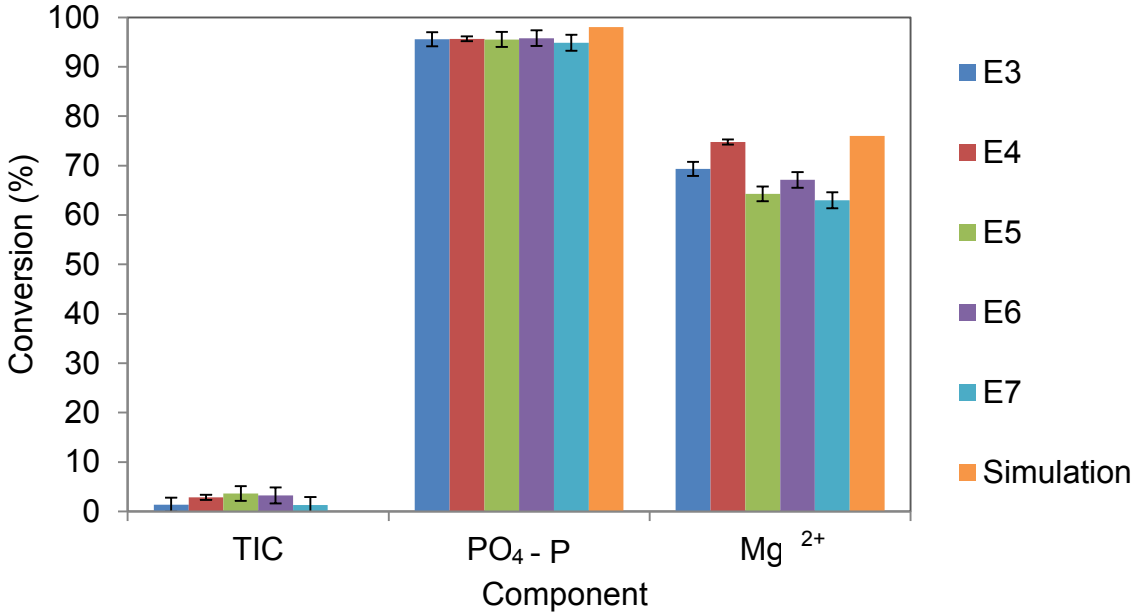

Figure 27: Conversion of carbonate, orthophosphate and magnesium ions in the electrochemical precipitation of struvite batch reactor for Treatments E3, E4, E5, E6 and E7 compared to those of the thermodynamic model.

The orthophosphate percentage conversions for all treatments (including the non-seeded treatment) were fairly similar and all above 94 % compared to 98 % as predicted by the thermodynamic model. This shows that the aspect of seeding does not affect the rate of phosphate recovery. The percentage conversions of magnesium ion were also fairly similar with the highest measured as 75 % for Treatment E4 and considerable carbonate conversions were also noted. The magnesium conversions also compared well with the thermodynamic modelling results. The results also show that the type of seeds and the rate of stirring rates that were investigated do not have significant effects on the rate of recovery of the orthophosphate in the urine.

Small differences of the thermodynamic predictions and the experimental results of the seeded electrochemical precipitation of struvite treatments were observed with respect to the conversions of the orthophosphate in urine and the electrochemically dosed magnesium. The main difference was in the prediction of the conversions in the carbonate ion and consequently the likelihood of the formation of nesquehonite at Mg:P molar ratio of 1.2 and pH of 9.5, due to the inaccuracies associated with measuring TIC. The error associated with the experimental results is small and thus the experimental method is reproducible and no error associated with the simulations.

Table 12 shows the quantitative analysis of the precipitates formed in suspension in the electrochemical precipitation of struvite batch reactor for Treatments E3, E4, E5, E6 and E7. The precipitates were dried, ground and dissolved in concentrated acid. The average concentration of the magnesium, orthophosphate and the ammonium ion in each treatment sample were measured and the molar concentrations were compared against the $\mathrm{PO_4 - P}$ in the sample bearing in mind that struvite exists in a 1:1:1 molar ratio of its constituent ions ($\mathrm{Mg^{2+}}$, $\mathrm{PO_4 - P}$ and $\mathrm{NH_4 - N}$). An assumption was made that, samples with higher magnesium ion molar concentration compared to the other constituent ions was due to the formation of nesquehonite.

It can be seen from Table 12 that the precipitates that were collected in suspension were struvite and the constituent ions were generally in a molar ratio of 1:1:1. It can thus be postulated that most of the magnesium in the suspended precipitates formed struvite and not nesquehonite.

Table 12: The quantitative analysis of the precipitates formed in the electrochemical precipitation of struvite batch reactor for Experiment E3, E4, E5, E6 and E7. The average concentration of the magnesium, orthophosphate and the ammonium ion in each experiment sample.

Experiment	$\mathbf{Mg^{2+}}$	$\mathbf{PO_4 - P}$	$\mathbf{NH_4 - N}$
E3[a], E3[b] (control Treatment)	1.05 ± 0.02	1.00	1.03 ± 0.20
E4[a], E4[b]	1.06 ± 0.01	1.00	1.08 ± 0.34
E5[a], E5[b]	1.04 ± 0.02	1.00	1.09 ± 0.27
E6[a], E6[b]	1.20 ± 0.04	1.00	0.97± 0.51
E7[a], E7[b]	1.16 ± 0.07	1.00	1.01± 0.32

Figure 28 shows how the electrode looked like before and after Treatment E3. Similar observations were made for Treatments E4 to E7, a formation of a layer on the electrode as a result of passivation on the magnesium anode.

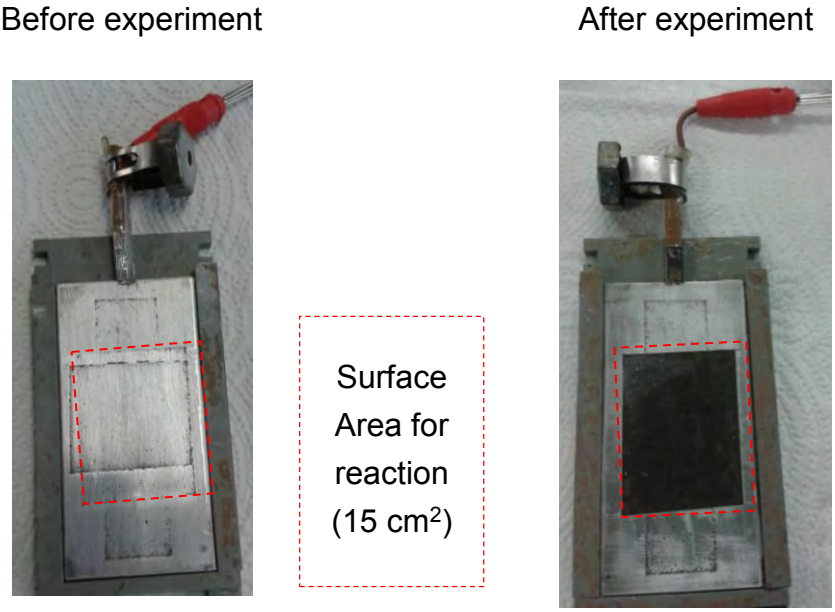

Figure 28: Images of the magnesium electrode before and after Treatment E3.

SEM and XRD methods of analysis were used to qualitatively analyse the layer that had formed on the anode surface. Upon analysis of this layer under the SEM, the structure of the compound was not easily identifiable. Figure 29 shows the SEM image of the layer.

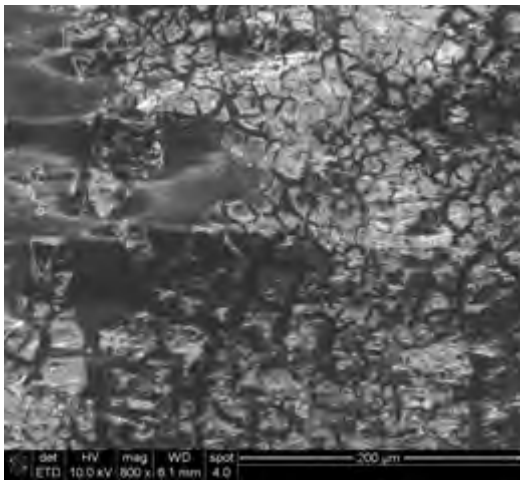

Figure 29: SEM image of the magnesium electrode after Treatment E3.

It can thus be postulated that because magnesium ions are continuously expelled from the anode into the solution in the electrochemical precipitation reactor, there is a region of high supersaturation of magnesium ions on the anode surface. The chemical reactions that take place on the surface of the electrode are based on Equation 15

and 16. These reactions lead to the formation of a high magnesium ion concentration and pH region which is favourable for the formation of nesquehonite however, the thermodynamic modelling predicts this as the model assumes a well-mixed system.

The XRD results then confirmed that the layer that formed on the surface of the electrode indeed contained some nesquehonite. Figure 30 shows the XRD spectrum of the layer. Both struvite and nesquehonite can be accounted for with multiple other peaks which may have been due to impurities on the magnesium anode plate.

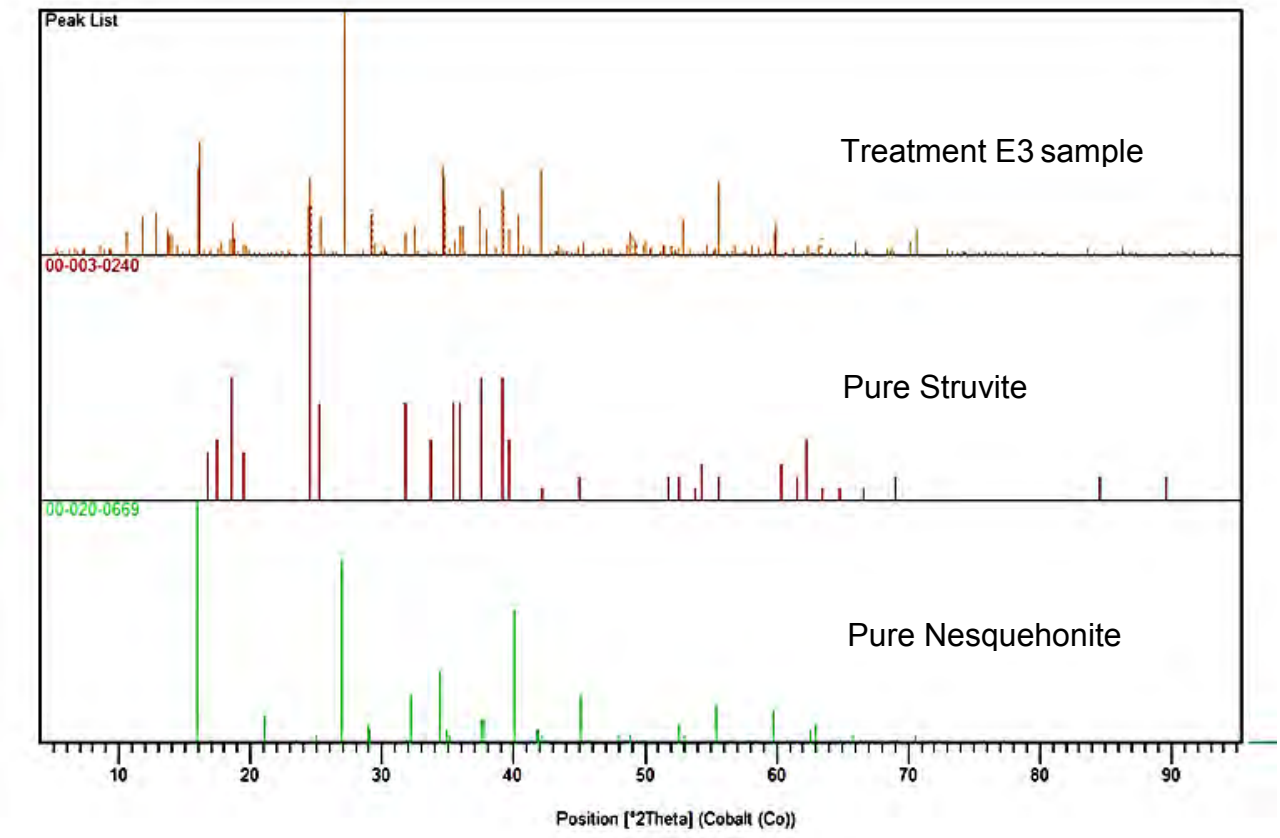

Figure 30: XRD spectrum of the magnesium electrode after Treatment E3.

5.2.2 Magnesium electrode potential and current flow

Figure 31 shows how the magnesium electrode potential varied with time for the duration of the experiment. The initial magnesium electrode potential when the power was switched on and the current was allowed to flow was -1.5, -1.3, -1.6, -1.4 and -0.8 V for Treatments E3, E4, E5, E6 and E7 respectively. This was due to differences in the electrolyte (urine) and electrode resistances because for each treatment, a different urine sample (because urine was collected on different days) and magnesium electrode samples were used. As the experiment progressed at a fixed current density, the magnesium electrode potential for all the treatments increased gradually to a maximum of 0.4 V in Treatment E3 and E4 and up to 0.34 V in Treatment E6. Slightly

lower values were observed for Treatment E5 and E7 with maximum magnesium electrode potentials of 0.1 and 0.02 V. Hug (2010) postulated that the ideal operational magnesium electrode potential would be at least -0.8 V because lower electrode potentials showed an unstable current in their batch experiments. However, in their experiment, current density was not controlled.

The magnesium electrode potential increased because a constant current flow had to be maintained despite an increase in the resistance on the electrode surface. The resistance on the electrode was caused by passivation (build-up of a layer) due to the interaction of the electrode with the environment in which it was placed. Figure 31 shows that this resistance also increases gradually over time. The implications of this would be the wastage to electricity, an eventual system failure due to the build-up of mass on the electrodes, damaging the system and the contamination of the struvite produced in the solution.

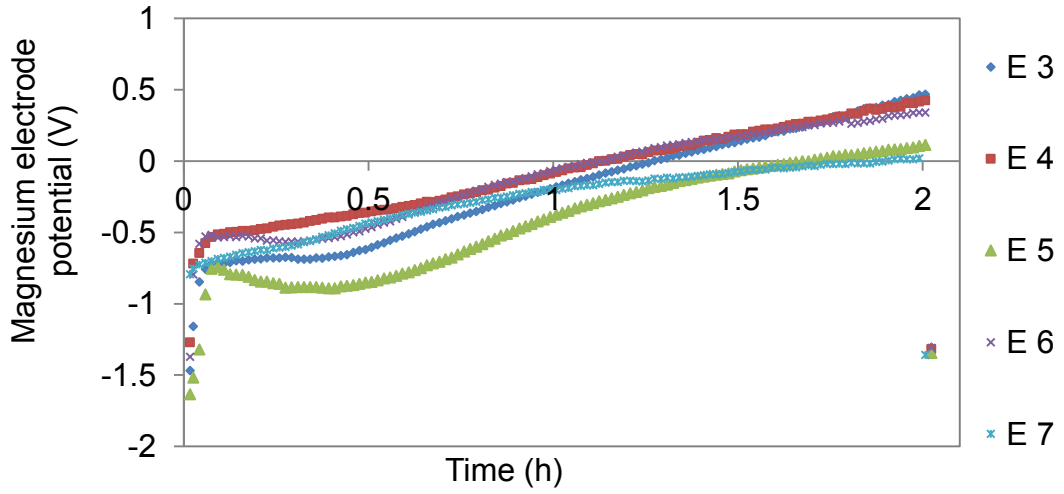

Figure 31: The magnesium electrode potential for experiments E3 to E7 at a fixed current density and current flow at Mg:P molar ratio 1.2.

Figure 32 shows that the current flow in Treatment E3 to E7 increased sharply when the power was applied to the cell in order to pass current as set on the potentiostat. The current flow then remained constant throughout the treatments and remained at an average value of 0.103 A as this was the chosen set point to ensure that a Mg:P molar ratio of 1.2 was achieved for the duration of 2 hours. This confirms that the apparatus were working properly.

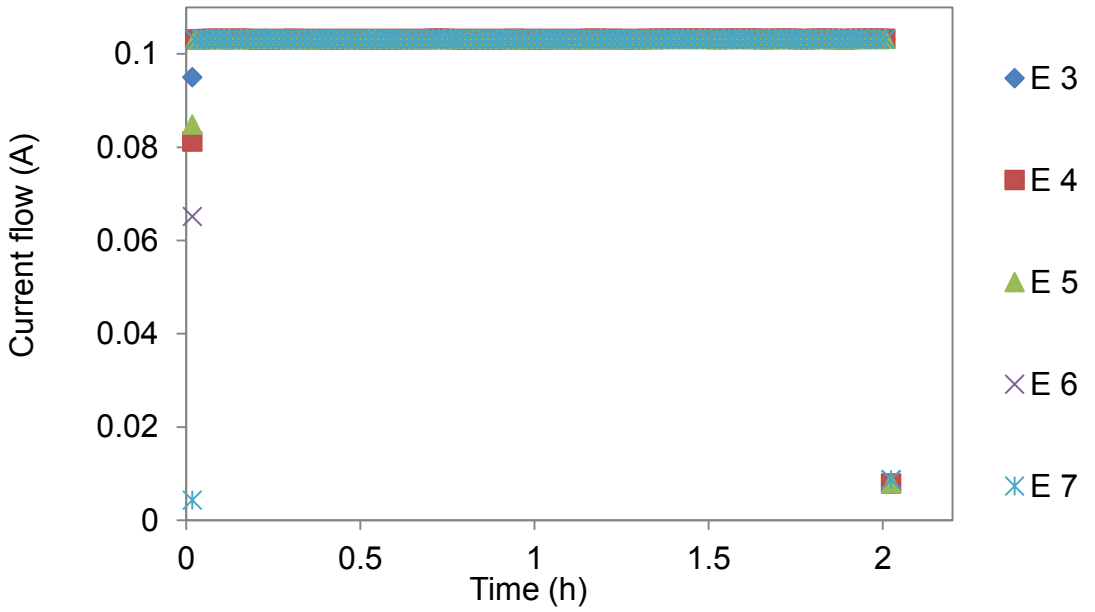

Figure 32: The current flow for Treatments E3 to E7 at varying magnesium electrode potentials.

Figure 33 shows the cell voltages for Treatments E3 to E7 when the power was applied to the cell and the treatment started until the end. The cell potential increases gradually throughout, which can be translated as more electric power was needed for the cell. This is because of the increase in the magnesium electrode potential as discussed and shown above in Figure 31.

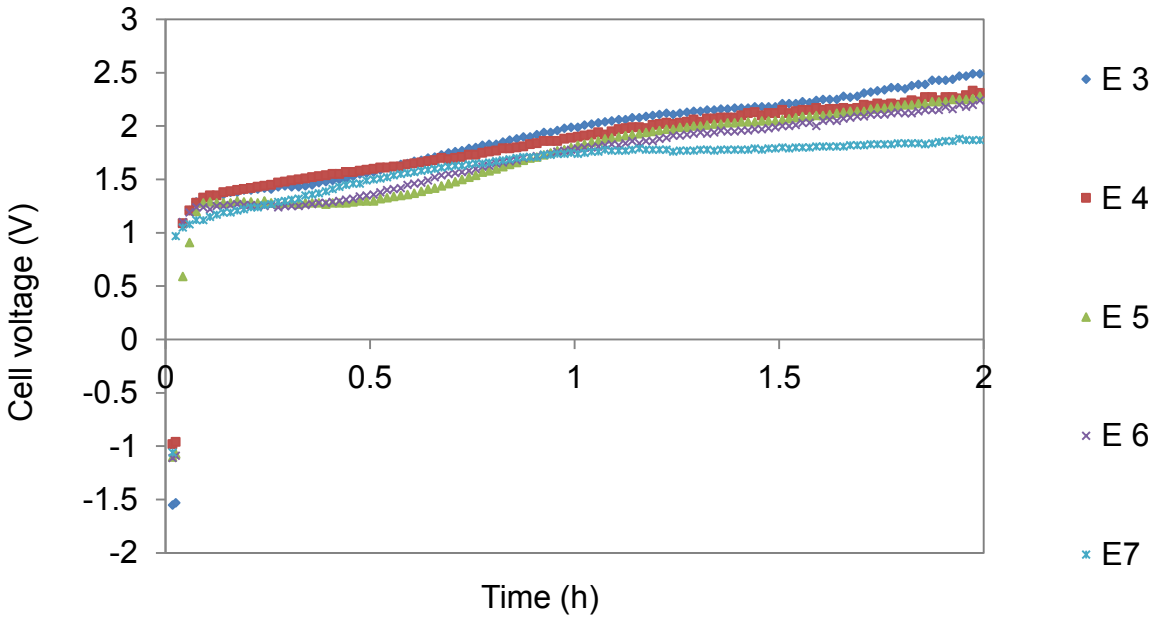

Figure 33: The cell voltage of the electrochemical cell for E3 to E7 at varying magnesium electrode potentials and constant current flow.

5.3 Product characteristics of struvite produced in electrochemical precipitation reactor

Analyses include products from both batch and continuous reactor setups.

5.3.1 Size distribution with current density

The investigation of current density was carried out in order to determine how the struvite product is affected by the change in the supersaturation of magnesium ions in solution. According to Faraday's law, the higher the current density, the more supersaturated the solution became with magnesium ions. Figure 34 shows the particle size distribution for the struvite precipitates that were produced at different current densities. It is important to note that these distributions were derived from a volume basis and that all the particles were assumed to be spherical. Figure 35 shows the corresponding cumulative particle size distributions for the particles and shows the d_{50} ratio of the various particle samples.

Figure 34 shows that across the current densities that were investigated, the distributions are evenly spread between particle diameters of 0.5 and 1000 µm. The particle size distributions also show that particles of 20 µm in diameter make up more than 5 % of the total particle volume and this is true for all the current densities that were investigated. The narrowest size distribution is recorded for 90 A/m^2 with the diameters ranging from 0.3 to 550 µm and the highest particle volume percentage of about 7 % of the total particle volume being made up of particles of 10µm in diameter. For current density of 30 to 60 Am^2, particles of 100 µm made up approximately 4 % of the total volume of the particles that were measured and about 1 % with a diameter of 150 µm. Figure 36 shows that the average d_{50} for the various particle samples is at or below 20 µm. Literature shows that when a solution is highly supersaturated, primary nucleation occurs and numerous small particles are produced, whereas larger particles are produced at lower supersaturation levels (Ronteltap, 2010; Mullin, 1972). The results presented in Figure 34 and Figure 35 show that a current density of 90 A/m^2 is high and not suitable if large particle diameters greater than 100 µm are to be achieved. Low current densities are ideal for producing large particles.

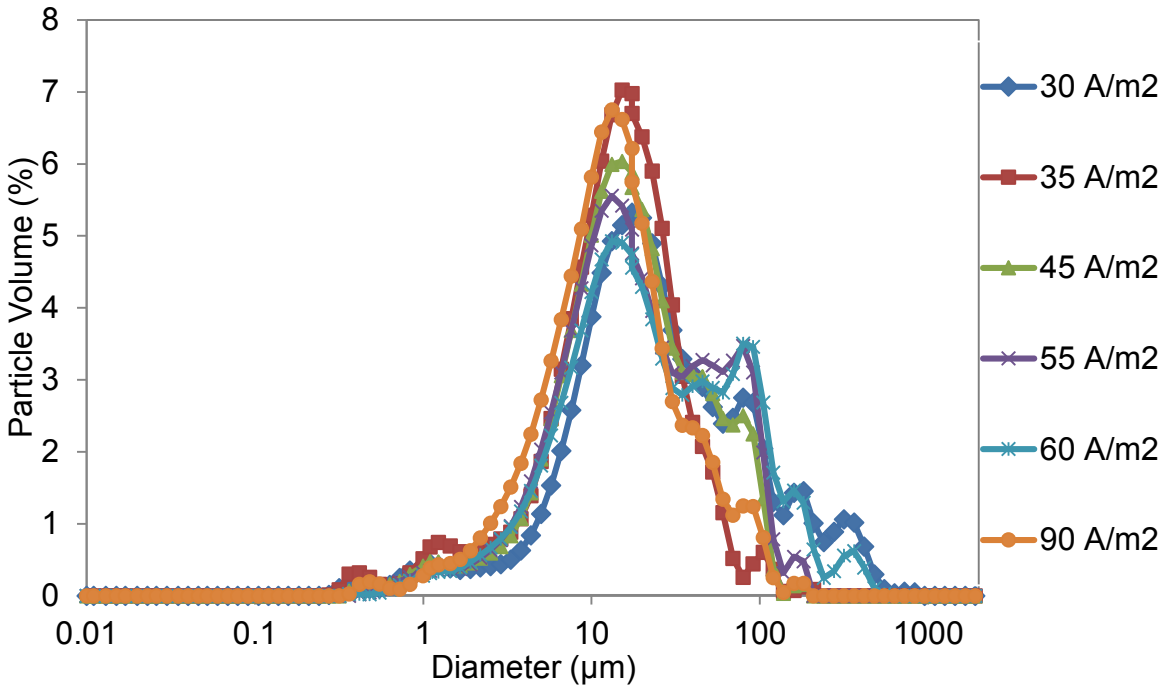

Figure 34: Particle size distribution for the precipitates produced at current density 30, 35, 45, 55, 60 and 90 A/m^2.

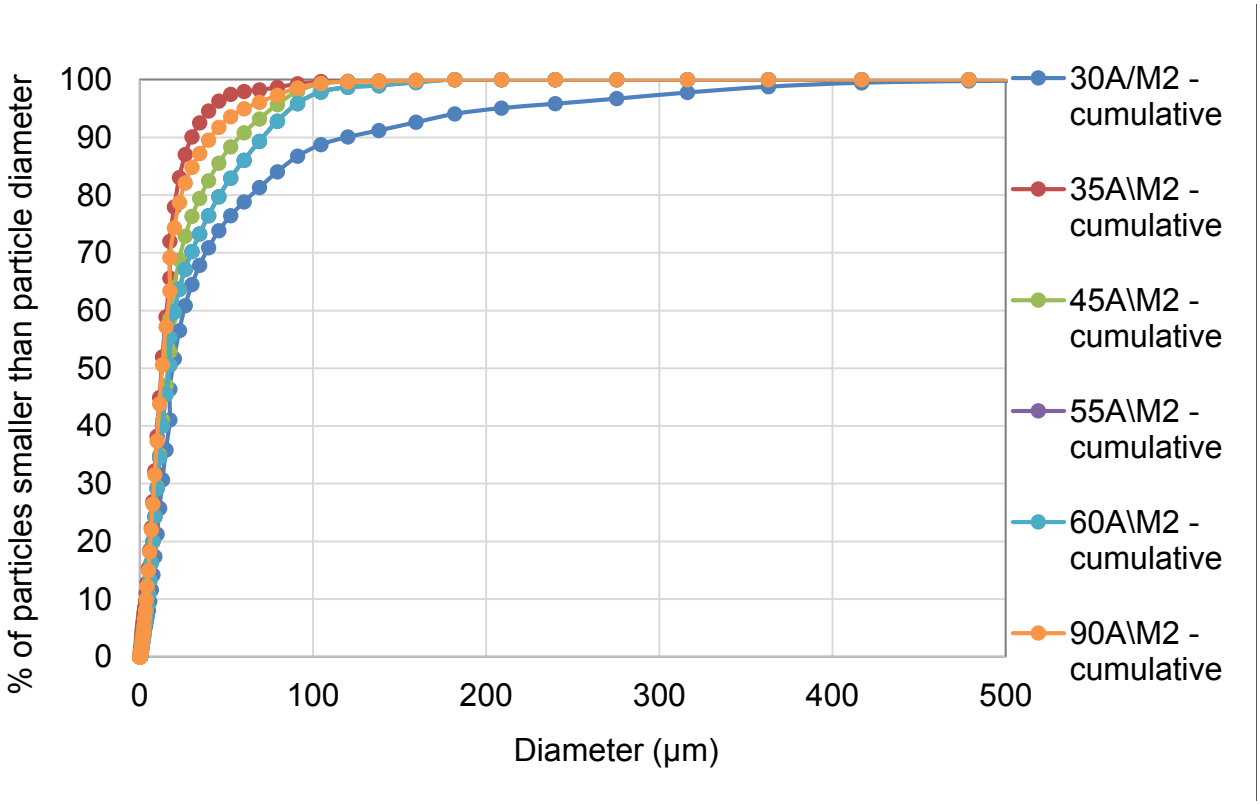

Figure 35: Cumulative particle size distribution for the precipitates produced at current density 30, 35, 45, 55, 60 and 90 A/m^2.

5.3.2 Size distribution for the particles produced in Treatment E3, E4, E5, E6 and E7 (batch mode, shown in Table 5)

Treatments E3, E4, E5, E6 and E7 were carried out at a current density of 70 A/m^2 in the electrochemical batch as outlined in Section 3.3. The current density of 70 A/m^2 was inspired by the analysis that was carried out in Section 4.3.1 on the influence of current density on size of resultant struvite particles produced and also keeping in mind that passivation occurs at higher current densities. Electrochemically precipitated struvite seeds were produced in Treatment E3 and used in Treatment E6 and E7. VUNA Struvite was used as seeds in Treatment E4 and E5. Figure 36 shows the particle size distribution for the struvite precipitates that were produced at the end of Treatment E3 to E7 and that of the VUNA seeds. The particle distribution for all the particles that were analysed varies from 0.4 to 120 µm in diameter. Analysis of the VUNA struvite particles shows that the highest particle volume percentage of about 7 % of the total volume of particles is made up of particles that are approximately 20 µm in diameter. It can also be noted that the particles produced in Treatment E4 and E5 undergo some growth when compared to the original seeds (VUNA struvite), with the highest particle volume percentage of 8 and 8.5 % respectively. Figure 37 shows the corresponding cumulative particle size distributions for the particles and shows that the average d_{50} is at or below 20 µm for E3, E6 and E7 and at or below 50 µm for E4, E5 and struvite.

Analysis of the particles produced in Treatment E3 shows that the highest particle volume percentage of about 5 % of the total volume of particles is made up of particles that are approximately 10 µm in diameter. It can also be noted that the particles produced in Treatment E6 and E7 also exhibit slight growth from the original particles from Treatment E3. The highest particle volume percentage for Treatment E6 and E7 is 5 and 13 % respectively.

The growth of the particles in Treatment E4 and E5 from the original size of the VUNA struvite is due to secondary nucleation. This explanation is also true for the growth observed in the particles from Treatment E6 and E7 from the original size of the particles/seeds produced in Treatment E3.

The stirring rate in Treatment E4 and E6 was 120 rpm and was 500 rpm for Treatment E5 and E7. It can thus be postulated that when seeding is implemented, larger particles are produced when the system is well mixed.

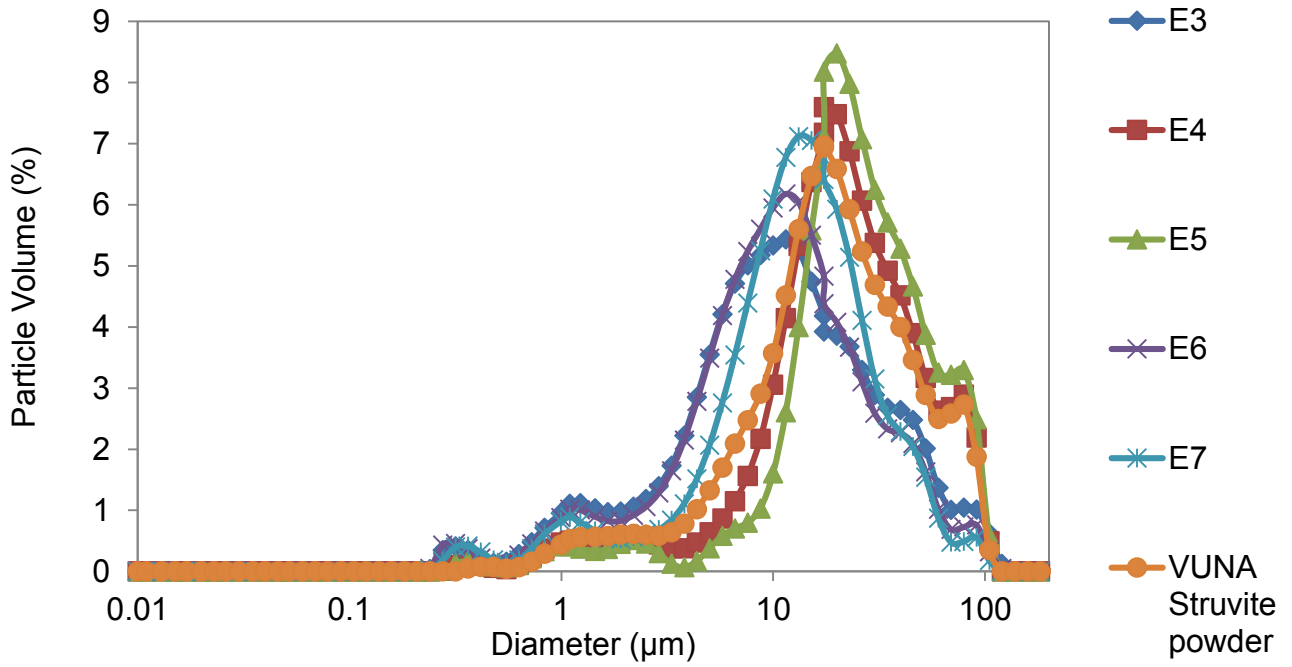

Figure 36: Particle size distribution for the VUNA struvite and the precipitates that were produced in Treatment E3, E4, E5, E6 and E7.

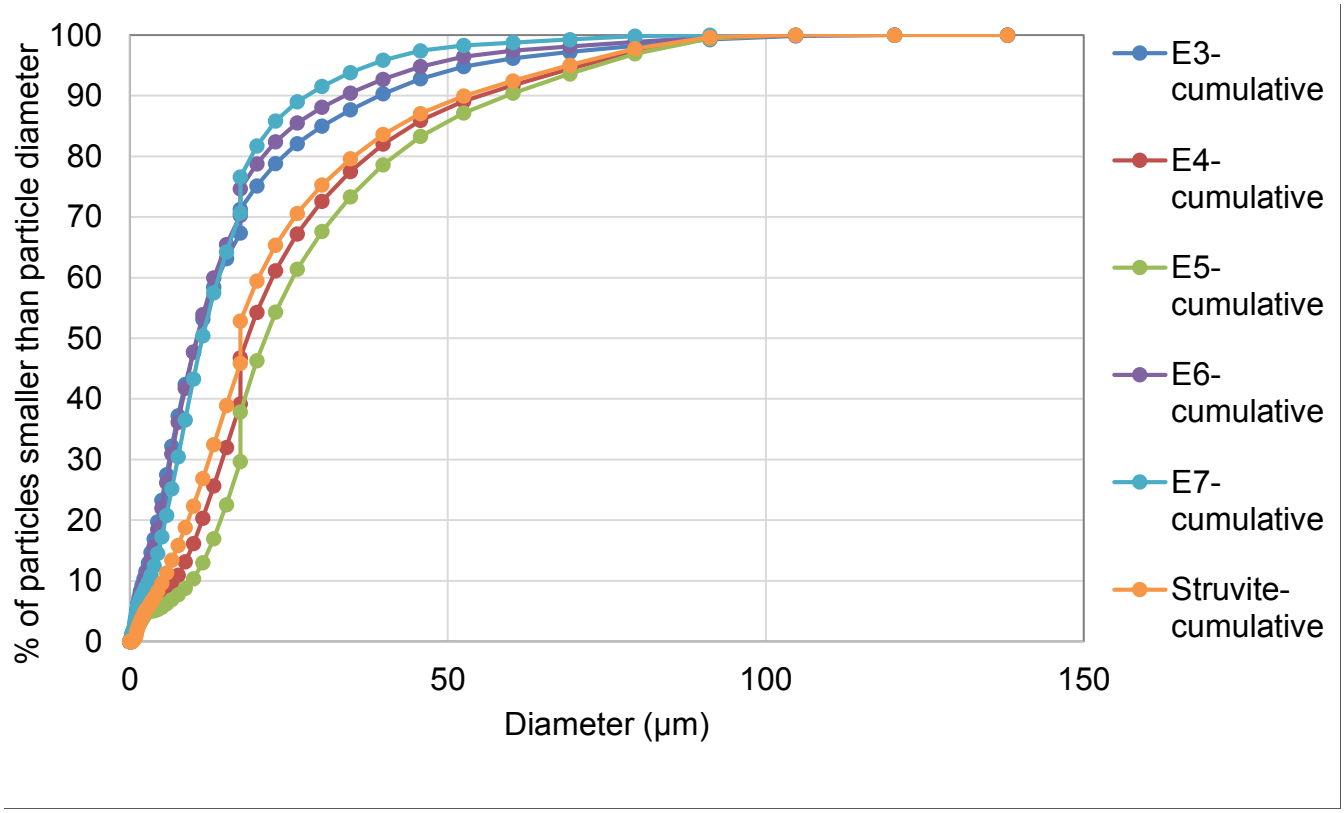

Figure 37: Cumulative particle size distribution for the VUNA struvite and the precipitates that were produced in Treatment E3, E4, E5, E6 and E7.

Figure 38 shows the particle size distribution of the struvite precipitates that were produced in the seeded continuously stirred reactor over a period of 8 hours (shown in Table 7). The particle distribution for all the particles that were analysed varies from 0.3 to 120 µm in diameter. The highest particle volume percentage for all the samples is about 7 % of particles of a diameter of 20 µm. It can also be noted that the particle size distribution curve shifts to the right with increase in residence time due to particle growth. Figure 39 shows the corresponding cumulative particle size distributions for the particles and shows that the average d_{50} is at or below 20 µm for the various particle samples that were collected over time.

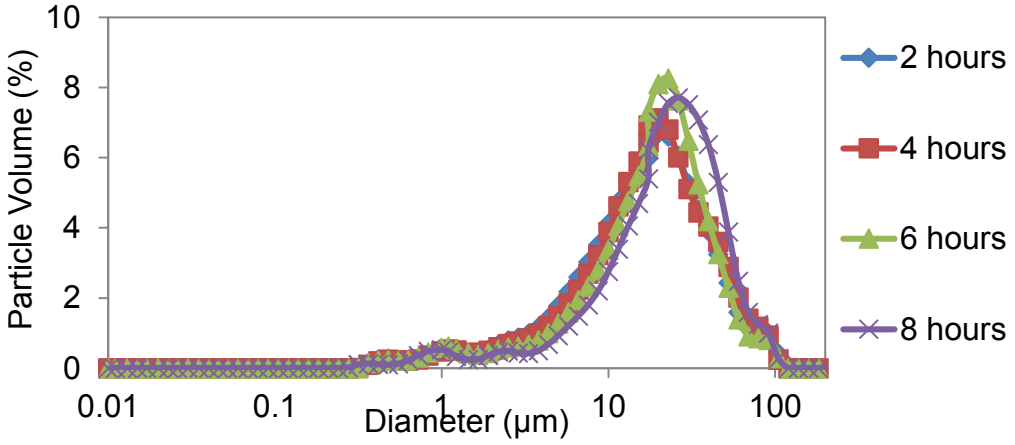

Figure 38: Particle size distribution for the precipitates that were produced in the seeded continuously stirred electrochemical precipitation of struvite, Treatment E9 at various times for the duration of the Treatment.

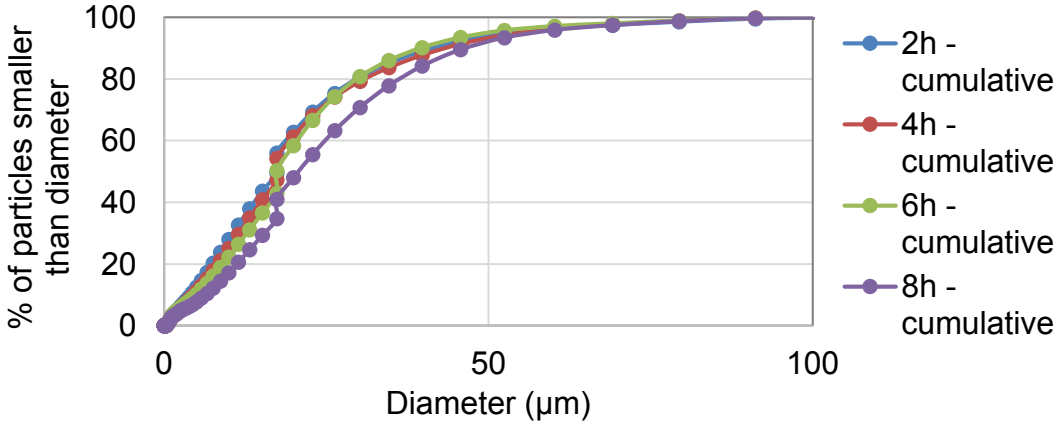

Figure 39: Cumulative particle size distribution for the precipitates that were produced in the seeded continuously stirred electrochemical precipitation of struvite, Treatment E9 at various times for the duration of the Treatment.

5.3.3 Investigation of particle sizes and morphology

Scanning Electron Microscopy (SEM) was used to analyse the morphology and to track the particle growth of the particles with time. Figure 40 shows the morphology of the VUNA seeds (a), the resultant seeds produced at the end of Treatment E4 (b) and E5 (c) after seeding with the VUNA seeds. The particles in all cases exhibit the typical coffin like structures of struvite. As shown in Figure 40, there is no notable difference in the appearance of the particle in the three different images in size and shape. This method of particle analysis was not as clear as the particle size distributions shown in Figure 36 due to the small increase of size from particle in image a to b and c, however the shape of the particles clearly shows that the coffin like structures that are common with struvite particles were maintained.

a b c

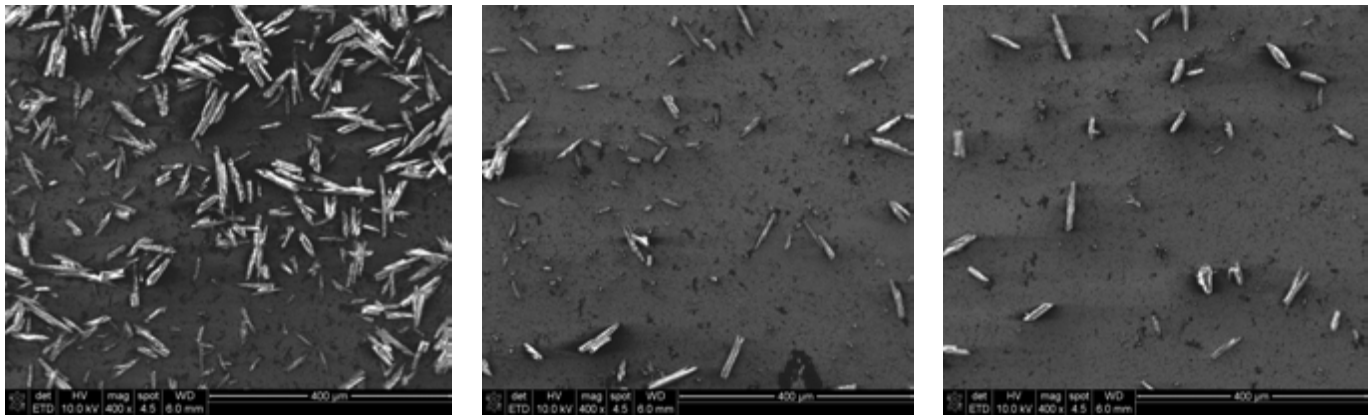

Figure 40: SEM images of the VUNA struvite (image a) and the particles that were produced at the end of Treatment E4 (image b) and Treatment E5 (image c).

Figure 41 shows the SEM images for the particles that were produced at the end of Treatment E3, E6 and E7. The particles displayed in image d (from Treatment E3) were used as seeds in Treatment E6 and E7 and shown in images e and f respectively. Tiny coffin like structures and spheres can be observed with sizes of approximately 20 µm in length on average. Image e and f show that there is growth from the particles shown in image d through to e and f. Images e and f show that the particles produced are also coffin like and spherical in structure of approximately 30 µm in length on average. Literature states that the typical shapes for struvite particles vary from coffin-like structures (Wierzbicki et al. 1997), to needle-like structure but are assumed to be spherical when the crystal size measurements is measured with a Mastersizer X (Malvern Instruments Ltd., Worcestershire, United Kingdom), (Ronteltap et al., 2009).

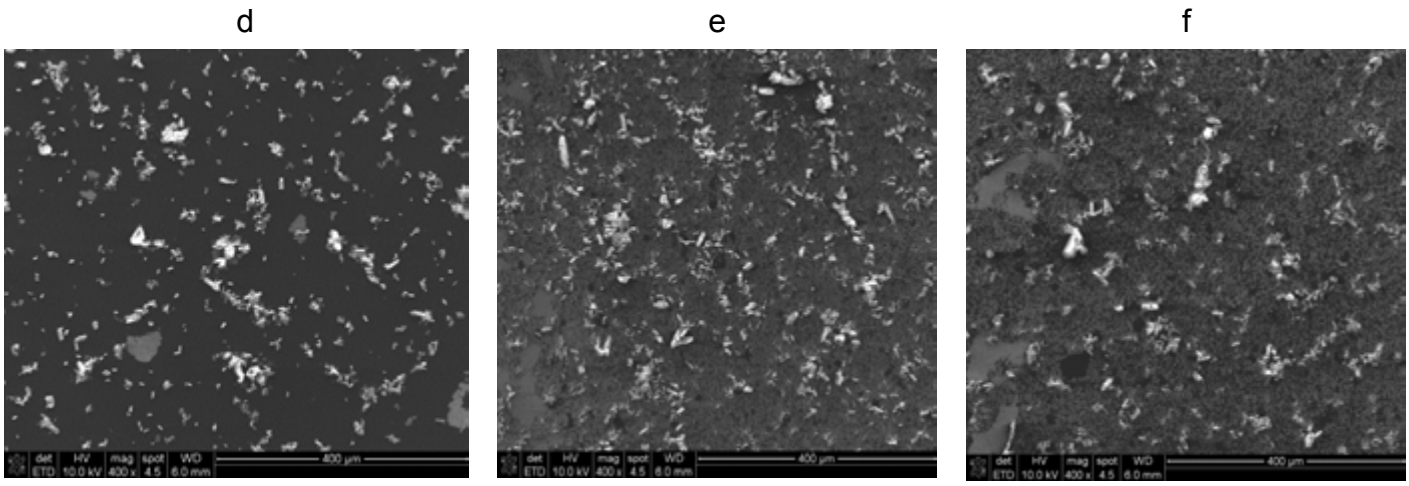

Figure 41: SEM images of the particles that were produced at the end of experiment E3 (image d), experiment E6 (image e) and experiment E7 (image f).

Figure 42 shows the SEM images for the particles that were produced in the seeded continuously stirred electrochemical precipitation of struvite. Image g shows the particles that were first withdrawn from the reactor after 0.5 h. Images h, i, j through to k shows the particles that were collected from the reactor after 2, 4, 6 and 8h respectively. It can be noted that there is some growth of the particles from image g to image k due secondary nucleation with average particle sizes increasing from approximately 10 μm to approximately 15 μm. The growth of the struvite particle is slow due to the fast precipitation of the struvite hence the dominant mechanism of nucleation is primary rather than secondary nucleation. The general shape exhibited by the particles is generally spherical in all the images with other coffin like and randomly shaped particles.

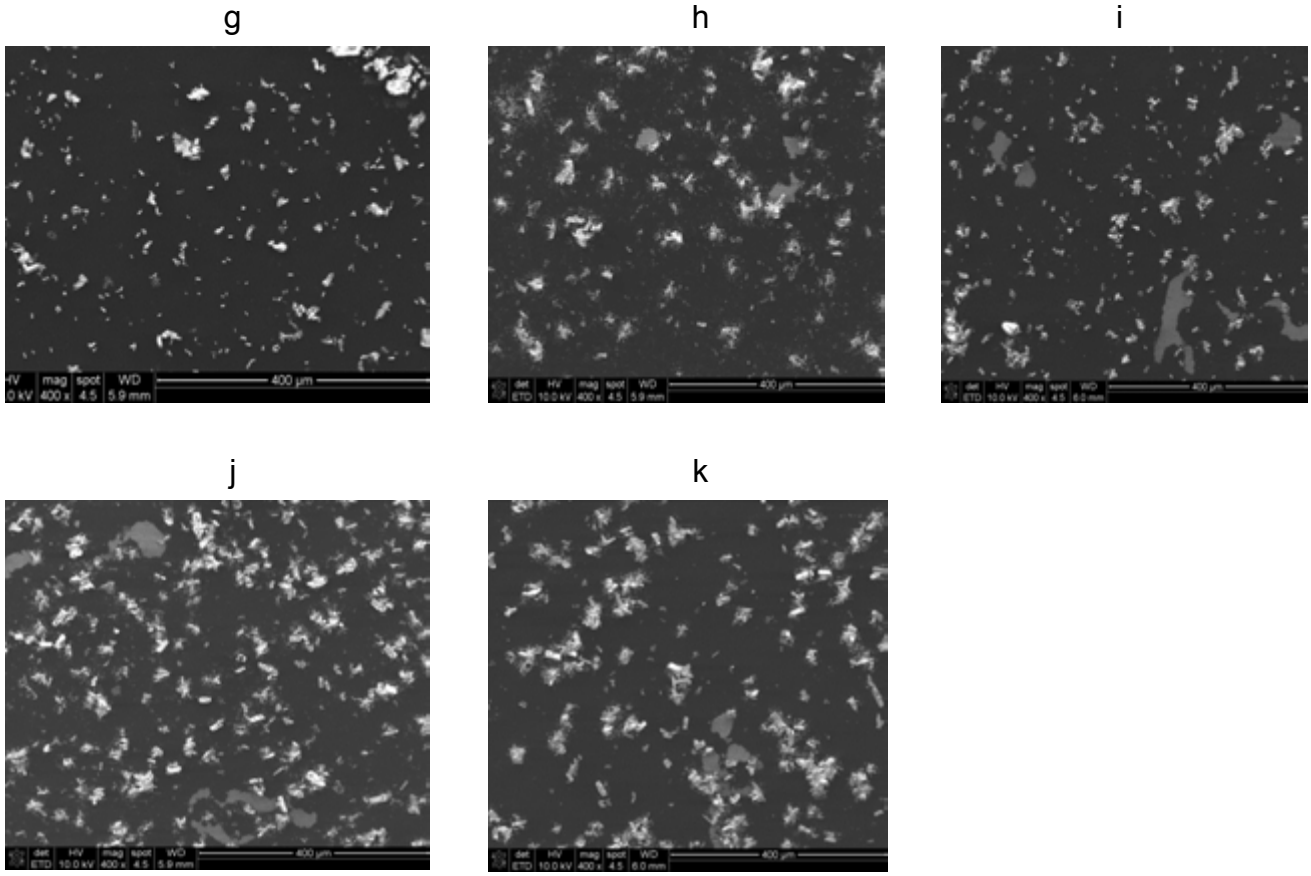

Figure 42: SEM images of the particles that were produced in the seeded continuously stirred electrochemical precipitation of struvite after 0.5 h (image g), 2 h (image h), 4 h (image i), 6 h (image j) and 8 h (image k).

In summary the particles that were produced from the electrochemical reactor mostly exhibited a spherical shape and this was clearly seen for the SEM images. However, the SEM method of analysis was not ideal for tracking the sizes of the particles. Particle size distribution with the Mastersizer X was ideal for assessing and tracking the sizes of the particles but not the shapes of the particles, thus the combination of the using SEM and particle size distribution with Mastersizer X worked really well. The particle sizes produced from the electrochemical reactors run in both batch and continuous mode showed some increases in sizes and exhibition of spherical and coffin like structure with and without seeding in batch mode and when the reactor was run continuously with a recycle.

5.4 Economic assessment

The cost of struvite precipitation in the seeded electrochemical precipitation reactor using a magnesium sacrificial anode was evaluated and compared against the cost of struvite precipitation by chemical dosage of magnesium with $MgCl_2$.The electricity and magnesium electrode costs were evaluated for the seeded electrochemical precipitation method while only the $MgCl_2$ chemical costs for the chemical dosage method was used. Transport costs were neglected as they were assumed to be the same for both methods. It was also assumed that these resources were readily and easily available. Table 13 shows the input parameters that were used to calculate the costs for the two methods. Appendix IV shows the details of the calculations.

The results the electrochemical precipitation method costs about ZAR 3.47 while the chemical dosing method costs about ZAR 3.87 per kg of struvite produced. These costs are comparable with the electrochemical precipitation method being slightly cheaper. The other advantage of the electrochemical precipitation method, apart from the fact that pure struvite can be produced safely if the production of nesquehonite is eliminated.

The major costs with the seeded electrochemical precipitation reactor lie in cost of the metal anode.

Table 13: The input parameters used for the costing of the two methods of producing struvite (prices quoted 2014).

Description	Unit	Value	Source/comment
Price of magnesium chloride	R/kg	8.30	Protea Chemicals, 2014
Price of electricity	R/kWh	1.00	City of Cape town electricity tariffs, 2014
Price of magnesium metal	R/kg USD	27.00 2.4	Magnesium alloy Mg (90% Mg minimum), from Investment Mine (Mining markets and Investment)

6 Conclusions

This chapter covers the conclusions to the work presented in Chapter five and shows how the approach, results and discussions of this study help to answer the key questions and objections that were raised in Chapter 4. Section 6.1 and 6.2 conclude on the thermodynamic modelling, the investigation of the formation of nesquehonite and the aspect of seeding and it influences, respectively. Section 6.3 concludes on the economics of the process and finally in Section 6.4, the hypotheses are reviewed and concluded. The holistic conclusion of the study is also presented and demonstrations which improvements to the electrochemical precipitation of struvite from source separated urine have been made and the contribution that this dissertation has made to this field of study.

6.1 Comparison of thermodynamic modelling of struvite with electrochemical experiments of struvite

The electrochemical precipitation of struvite from source separated urine is a functional lab scale and feasible method of producing struvite with high yields. The electrochemical batch reactor that was developed by Hug and Udert (2013) was modified to a seeded electrochemical reactor and was also run in continuous mode all to improve the process of the electrochemical precipitation of struvite from source separated urine. In the midst of the improvements, the seeded electrochemical precipitation of struvite maintained the feasibility that Hug and Udert (2013) demonstrated and achieved phosphorous recoveries of up to 96 %.

The validation of the thermodynamic model of struvite precipitation with batch experiments by dosing magnesium chloride gave a good starting point to design and investigate the seeded electrochemical precipitation of struvite batch reactor for the particular urine stream that was investigated. The thermodynamic model predicted that the formation of struvite and nesquehonite is strongly dependant on the Mg:P molar ratio, pH and the presence of other urine constituent ions in adequate quantities. It is also showed that the precipitation of struvite in stored urine is easily triggered by slight increases in magnesium concentration because of its favourable pH and availability of ammonium and phosphate ions. The model predicted that phosphorous conversion to struvite from stored urine can reach up to 98 % when the Mg:P molar ratio is 1.2 and the pH is kept at 9.5 (Udert et al. 2003).

When comparing the thermodynamic model results with those of the seeded electrochemical precipitation results, it was concluded that for a Mg:P molar ratio of 1.2 and a pH of 9.5, the results are comparable with regards to the recovery of the orthophosphate from urine and the conversion of magnesium. However, there were notable discrepancies with regards to the final pH and the conversion of the carbonate ions due to the formation of nesquehonite. This was due to the conditions and the chemical reactions on the surface of the anode which could not be predicted by the thermodynamic model. The results also showed that the precipitates that formed in suspension were mostly struvite and most of the nesquehonite that formed built up on the anode surface and did not largely affect the quality of the struvite collected.

6.2 Investigation on the formation of nesquehonite and the feasibility of the aspect of seeding in the electrochemical reactor and its influence on the struvite crystal characteristics

Recoveries above 90 % were also obtainable at higher Mg:P molar ratios of up to 21 and at a pH range of 9 to 10. However, nesquehonite ($MgCO_3.3H_2O$) also started to form at Mg:P molar ratios greater than 7.8 and between pH 6 and 12 due to the presence of carbonates in the solution. Theoretically, the implication of this was; a compromise in the quality of the struvite produced and practically; the likelihood of the formation of a passivation layer on the magnesium anode. As such, the magnesium ion concentration must be carefully controlled and kept high enough to recover 98% of the orthophosphate present in the urine but low enough to avoid the formation of nesquehonite. According to the thermodynamic modelling, in order to achieve a phosphorus recovery of more than 95% and pure struvite, the Mg:P molar ratio has to be maintained at 1.2 and at a pH between 8.5 and 10.5.

In the electrochemical precipitation experiments, directly controlling the concentration of magnesium was more practical than directly controlling the pH (by titrating an acid or a base for the duration of the experiment) because a current can be defined such that the dissolution of the magnesium electrode is regulated. As such, for the electrochemical experiments the magnesium concentration was defined by the Mg:P molar ratio of 1.2 and a phosphate recovery of 96% was achieved in these experiments.

Seeding of the electrochemical reactor was then employed by introducing externally produced seeds (VUNA seeds) and electrochemically produced seeds into the reactor to create a nucleus for precipitation and possibly promote

crystal growth and rate of phosphate recovery. The results of the seeded electrochemical precipitation of struvite at different seeding conditions shows that the aspect of seeding does not affect the rate of phosphate recovery and the rate at which equilibrium is reached. This is due to the fact that the precipitation of struvite occurs extremely fast and seeding does not aid in the kinetics or the thermodynamics of the process. There is also the formation of the layer of nesquehonite over time and this led to increases in the magnesium electrode potential which translated to increases in the cell potential up to 2.3 V.

The effect of current density on the size of the resultant particles is such that at high current densities (90 Am/^{2}) the solution becomes highly saturated and precipitates out numerous tiny particles due to primary nucleation. At lower current densities (30 to 60 A/m^2) the particles produced are larger than those produced at a current density of 90 A/m^2. This is shown by the largest particles produced at a current density of 90 A/m^2, measuring up to 200 µm in diameter whilst the largest particles produced at 30 A/m^2, measured up to 550 µm.

The particles produced from the seeded electrochemical batch system that is outlined in Section 5.3 shows that seeding plays a role in particle growth and that the type of seeds (electrochemically or chemically dosed with magnesium) used are not an influencing factor to particle growth. Particle growth from 10 to 20 µm was observed for the system that was seeded with seeds that were produced electrochemically. It was also observed that stirring influences the particle growth positively with well mixed systems producing larger particles.

Residence time affects the growth of the struvite particle in the reactor in that the longer a particle stays in a continuously stirred reactor, the bigger it becomes. The growth of the struvite particles is slow due to the high rate of precipitation of struvite. It is recommended that the residence time be increased in order to increase the crystal size further.

6.3 Investigation of the economics of the of the SEP

The cost of struvite precipitation in the seeded electrochemical precipitation reactor using a magnesium sacrificial anode was evaluated and compared against the cost of struvite precipitation by chemical dosage of magnesium with $\mathrm{MgCl_2}$. The electricity and magnesium electrode costs were evaluated for the seeded electrochemical precipitation method while only the $\mathrm{MgCl_2}$ chemical costs for the chemical dosage method were considered. Transport costs were neglected as they were assumed to be the same for both. The economic

evaluation showed that it is cheaper to produce struvite using the electrochemical precipitation method with sacrificial magnesium anode, than with chemical dosing method using $MgCl_2$. The electrochemical precipitation method costs about ZAR 3.47 per kg of struvite produced while the chemical dosing method costs about ZAR 3.87 per kg of struvite produced.

6.4 Summary of conclusion

In summary the hypothesis that the thermodynamic model predicts the recovery rates of phosphorous for the electrochemical precipitation experimental processes with and without seeding the same, is accepted. The reason being that seeding influences the rate at which phosphorous is consumed and not the extent to which it is consumed. It is thus true that the process of phosphorous recovery depends on the kinetics of the process and not the thermodynamic equilibrium of the process. The running time for the experiments was sufficient for all the phosphorous to be recovered, given that the thermodynamic model assumes that the process runs for infinity.

The second hypothesis that nearly all the phosphorous in urine can be recovered electrochemically by introducing magnesium ions slowly enough in the form of struvite and avoid the formation of nesquehonite is also confirmed. This is because nesquehonite only forms when a significantly high level of supersaturation of magnesium ions occurs, at high pH. This was shown by the results of the purity of struvite that was collected in the experiments. Nesquehonite only formed on the surface of the cathode wall where the supersaturation of magnesium was high and the pH of the solution on that area was ideal for the formation of nesquehonite.

The third hypothesis that seeding can help both to make larger struvite particles and to speed up the process without increasing the risk of supersaturation and thus nesquehonite formation was also confirmed. There was also an indication of slow crystal growth with the recycling of struvite seed in the continuous electrochemical reactor that was well mixed. The well mixed system ensured that within the solution, there were no localised points of magnesium supersaturation.

This dissertation has thus shown that the electrochemical precipitation of struvite from source separated urine can be improved in terms of the functionality of the system and the quality of product by i)seeding ii) stirring.

The minimum concentration of magnesium ions and the ideal pH necessary to recover most of the phosphorous from source separated urine without triggering the precipitation of nesquehonite is a Mg:P molar ratio of 1.2 in the electrochemical experiments and pH 9. Running the electrochemical precipitation reactor continuously and recycling the struvite particles that are produced, back into the reactor increases the resultant size of the of struvite particles, and should thus allow for particle size control in such a seeded electrochemical precipitation system.

7 Recommendations

It is recommended that the influence of seeding on particle properties, such as size and how residence time influences them, be investigated further to discover the extent to which the struvite crystals can grow. In the batch setup, the rate of magnesium dissolution can be varied so as to achieve different residence times. Other aspects that could be investigated with regards to seeding are: the seed loading, seeding time, size of the seeds, the state of the seed material (dry or in suspension) and the point of addition in the crystalliser. These parameters, as literature suggests, are vital when implementing the aspect of seeding.

Another aspect that can be investigated is the use of an ion exchange membrane which separates the anode and the cathode compartments. The concept may offer the advantage of flexible designs through control of retention time by varying the volume of the reactor, suspension seeds concentration and seeds specific area. Membranes that eliminate carbonate ions from the cathode side could also be ideal in preventing passivation on the cathode wall. Ultimately, since the cost comparison between chemical precipitation and electrochemical precipitation are almost similar, it is recommended that this technology be investigated further. It is also important to note that chemical precipitation is a somewhat proven technique for struvite production while electrochemical precipitation of struvite is still relatively new and hence very investigations have been done with regards to crystal growth of struvite, even though the core technology (electroprecipitation) has existed for some time now. Therefore, there is likely more room for improvement and optimization in an electrochemical precipitation process while this might not be the case for chemical precipitation of struvite.

8 Bibliography

Morse, G. K., Brett, S. W., Guy, J. A., & Lester , J. N. (1997, October 27). Review: Phosphorus removal and recovery technologies. *The Science of the Total Environment*.

Abma, W. R., Driessen, W., Haarhuis, R., & Loosdrecht, M. C. (2009). Upgrading of sewage treatment plants by sustainable & cost-effective separate treatment of industrial wastewater. *IWE Nutrient Management in Wastewater Treatment Processes.*

Adam, C. (2009). *SUSAN: Sustainable and Safe Re-use of Municipal Sewage Sludge for Nutrient Recovery*. Activity Report, Global Change and Ecosystems.

AFRISCO. (2012). *AFRISCO Organic Standards*. Retrieved August 2013, from AFRISCO Certified Organic: http://www.afrisco.net/

Balmer, P. (2003). Phosphorus recovery, an overview of potential and possibilities. *IWA Specialist conference. Wastewater Sludge as a Resource.* Trondheim: IWA S.

Barak, P., & Stafford, A. (2006). Struvite: A recovered and Recycled Phosphorus Fertilizer. *Aglime & Pest Management Conference*, *45*, pp. 199-204.

Barbeau, D., Kresge, B., & Bowers, K. (2009). West Boise WWTF Use of Struvite Crystallization Technology as Part of the Phosphorus Removal Plan. *PNCWA 2009.* PNCWA.

Bayer Technology Services. (n.d.). *Waste water treatment.* Retrieved from Bayer technology: http://www.bayertechnology.com/uploads/media/en07_LOPROX_1305_290909.pdf

Bergmans, B. (2011). *Struvite recovery from digested sludge.* Thesis, Delft University of Technology, Civil Engineering.

Bhuyan, M. I., Mavinic, D. S., & Koch, F. A. (2008). Phosphorus recovery from wastewater through struvite formation in fluidized bed reactors: A sustainable approach. *Water Science and Technology*(57), 175-181.

Bilyk, K., Taylor, R., Piit, P., & Wankmuller, D. (2010). *PROCESS AND ECONOMIC BENEFITS OF SIDESTREAM TREATMENT.* Hazen and Sawyer:, Environmental Engineers and Scientists. Hazen and Sawyer:.

Brent, A. C., Musango, J., Mokheseng , M. B., & Amigun , B. (2011). *Systems dynamics modelling to assess the sustainability of renewable energy technologies in developing countries.* entre for Renewable and Sustainable Energy Studies, School of Public Leadership, Stellenbosch University, South Africa. 2 Sustainable Energy Futures, Natural Resources and the Environment, Council for Scientific and Industrial Research, South Africa.

Bridger, G. L., Salutsky, M. L., & Starostka, R. W. (1962). Micornutrient Sources, Metals Ammonium Phospahte as fertilizers. *Journal of Agriculture and Food Chemistry, 10*(3), 181-188.

Britton, A., Prasad, R., Balzer, B., & Cubbage, L. (2009). Pilot testing and economic evaluation of struvite recovery from dewatering centrate at HRSD's Nansemond WWTP. *Nutrient Recovery from Wastewater Streams Vancouver, 2009.* Vancouver.

Brown, J. (2011). *http://www.cropking.com*. Retrieved October 22, 2012, from Crop King: http://www.cropking.com/articlehfs

Cabeza Perez, R., Steingrobe, B., Romer, W., & Claassen, N. (2009). Plant availability of P fertilzers recycled from sewage sludge and meat and bone meal in field and pot experiments. *International Conference on Nutrient Recovery from Wastewater Streams:.* Vancouver: IWA publishing.

CEEP. (2013). *Current*. Retrieved February 27, 2013, from CEEP Centre European d'Etudes des Polyphosphates: http://www.ceep-phosphates.org/Documents/shwList.asp?NID=1&HID=34

City of Yakima. (2014). *Yakima Regional Wastewater Treatment*. Retrieved july 28, 2014, from City of Yakima: http://www.yakimawa.gov/services/wastewater-treatment-plant/

Clancy, K. (2012). *Sodium Affected Soils.* Retrieved November 3, 2012, from fusionfert: http://www.fusionfert.com/itn/articles/sodium.pdf

Constantine, T. (2008). An Overview of Ammonia and Nitrogen Removal in Wastewater Treatment. *CH2M HILL Canada.* CH2M HILL Canada.

Cordell, D., Drangert, J.-O., & White, S. (2008, May 27). The story of phosphorus: Global food security and food for thought. *Global Environmental Change, 19*, 292 - 305.

Cordell, D., Rosemarin, A., Schroder, J. J., & Smit, A. L. (2011, March). Towards global phosphorus security: A systems framework for phosphorus recovery and reuse options. *Chemosphere, 84*(6), 747 - 758.

Cornel, P., & Schaum, P. (2009). Phosphorus recovery from wastewater: needs, technologies and costs. *Water Science & Technology, 59*(6).

Crutchik , D., & Garrido, J. M. (2011). Struvite crystallization versus amorphous magnesium and calcium phosphate precipitation during the treatment of a saline industrial wastewater. *Water Science and Technology, 64*(12).

de- Bashan, L. E., & Bashan, Y. (2004, July 6). Recent advances in removing phosphorus from wastewater and its future use as fertilizer (1997–2003) . *Water Research, 38*, 422 - 4246.

deBarbadillo, C., Benisch, M., Barnard, J., & Neethling, J. B. (2012). *Sustainable Operating Practices fro Achieving Low Phosphorus Effluents.* WERF Nutrient Challenge Program. WERF.

deBarbadillo, C., Levesque, S., & Maxwell, M. (n.d.). *Strategies for meeting ultra-low phosphorus limits: State of the art technologies and case studies.* Kansas City: Black & Veatch Corporation.

de-Bashan, L. E., & Bashan, Y. (2003). Fertilzier potential of phosphorus recovered from wastewter treatment. *First International Meeting on Microbial Phosphate Solubilization*, (pp. 179-184). Mexico.

Department of Agriculture, Forestry and Fisheries. (2005). *National Policy on Organic Production.* Department of Agriculture, Forestry and Fisheries.

differencebetween. (2011). *Diferrence between crystallization and vs precipitation*. Retrieved July 2013, from differencebetween: : http://www.differencebetween.com/difference-between-crystallization-and-vs-precipitation/#ixzz2PPCOPT4A

Dittrich, C., Rath, W., Montag, D., & Pinnekamp, J. (2009). Phosphorus recovery from sewage sludge ash by a wet-chemical process. *International Conference on Nutrient Recovery form wastewater streams.* Vancouver: IWA.

Eawag Research. (2011). *VUNA - Nutrient Harvesting in South Africa*. (E. Research, Producer) Retrieved October 31, 2013, from Eawag Research: http://www.eawag.ch/forschung/eng/gruppen/vuna/index_EN

Etter, B. (2009). *Struvite recovery from urine at community scale in Nepal .* Eawag , EPFL . Nepal: Eawag .

Etter, B., Tilley, E., Khadka, R., & Udert, K. M. (2011). Lost Cost Struvite production using source-separated urine in Nepal. *Water Research, 45*, 852-862.

FAO. (2005). *Fertilizer use by crop in South Africa.* Land and Plant Nutrition Management Service, Land and Water Development Division, Rome.

Folkstad, B. (2008, June). *Analysing Interviews: Possibilities and Challenges.* Retrieved August 27, 2013, from Euroshpere Workshops: http://eurospheres.org/files/2010/08/Eurosphere_Working_Paper_13_Folkestad.pdf

Foskor. (2014). *Product Prices*. Retrieved March 10, 2014, from Foskor: http://www.foskor.co.za/cd_products.php

Ganrot, Z. (2005). *Urine processing for efficient nutrient recovery and reuse in agriculture.* Gotebirg University, Environmental Science and Conservation. Goteborg: Gotebirg University.

Ganrot, Z. (2005). *Urine processing for efficient nutrient recovery and reuse in agriculture.* Goteborg University, Environmental Science and Conservation. Goteborg: Goteborg University.

Ganrot, Z. (n.d.). *Fertilizer products from human urine .* Melica Environmental Consulting, Göteborg.

Gecko Fert. (2013). *Two types of phosphates*. Retrieved January 23, 2014, from Organic phosphate fertilizer: http://www.geckofert.co.za/e02types.html

Gell, K., Ruijter, F. J., Kuntke, P., de Graaf, M., & Smit, A. L. (2011). Effectiveness of Struvite from Black Water nadn Urine as a Phosphorus Fertilizer. *Journal of Agricultural Science* .

Ghosh, G. K., Mohan, K. S., & Sarkar, A. K. (1996). Characterization of soil-fertilzer P reaction products and their evaluation as sources of P for gram. *Nutrient Cycling in Agroecosystems, 46*(1), 71-79.

Giesen, A., Erwee, H., Wilson, R., Botha, M., & Fourie, S. (2009). Experience with crystallization as sustainabale, zero - waste technolgoy for treatment of wastewater. *Internationla Mine Water Conference* (pp. 401-406). Pretoria: Document transformation technologies.

Goldblatt, A. (2011). *Agriculture: Facts & Trends, South Africa.* WWF.

Gordon, J. (n.d.). *Precipitation and Crystallization Processes.* Los Alamos National Laboratory.

Goto, I. (1998). Application of phosphorus recovered from sewage plants . *Environmental Conservation Engineering, 27*, 418-422.

Green, c., Johnson, P., Allen, V., & Crossland, S. (2004). *Treatment Technologies for Phosphorus Removal from water derived from cattle feedyards.* Texas Tech University, Plant and Soil Science Department and Agriculture & Applied Economics Department, Texas.

Hampton Roads Sanitation District. (2010, May 27). Ostara Increases Plant Efficiencies for Hampton Roads Sanitation District in Innovative Public/Private Partnership Launching. *Virginia Wastewater Treatment Plant First In Chesapeake Bay Watershed to Recover Nutrients and Transform them into "Green" commercial fertilizer*.

Hasson, G., Sidorenko, G., & Semiat, R. (2008). Calcium carbonate hardness removal by a novel electrochemical seeds system. *Desalination*(15), 1207-1212.

Heinzmann, B., & Engel, G. (2007). Two-stage high rate digestion and phosphorus recovery. *Water Practice & Technology, 2*(1).

Henze, M., van Loosdrecht, M., Ekama, G. A., & Brdjanovic, D. (2008). *Biological Wastewater Treatment* (Vol. 2). IWA publishing.

Hermann, L. (2009). P-recovery from sewage sludge ashes by thermochemical treatment. Presentation in BALTIC 21. *Phosphorus Recycling and Good Agricultural Management Practice.*

HRSD. (2009, Septmeber 23). *Nutreint recovery at HRSD, Nansemond WWTP: Nutrient Recovery system equipment agreement.* HRSD.

Hug, A., & Udert, K. M. (2013). Struvite precipitation from urine with electrochemical magnesium dosage. *Water Research*(47), 289-299.

IFA. (n.d.). Retrieved October 22, 2012, from http://www.fertilizer.org

IFDC. (2012, November). *Promoting Affordable Sources of Plant Nutrients in Africa Through Innovative Composting Alternatives*. Retrieved April 24, 2013, from IFDC: http://www.ifdc.org/Training/Recent_Training_Programs/Promoting_Affordable_Sources_of_Plant_Nutrients_in

Infomine. (2014). *Historical Phosphate Rock Prices and Price Chart*. Retrieved March 20, 2014, from Infomine: http://www.infomine.com/investment/metal-prices/phosphate-rock/all/

IPCC. (2000). *Summary for Policymakers: Methodological and Technolgical Issues in Technology Transfer.* Intergovernmental panel on climate change, Working Group 3. Intergovernmental panel on climate change.

Ipipotash. (2011). *Ipipotash.* Retrieved November 3, 2012, from http://www.ipipotash.org/udocs/Chap-2_K_and_cl_in_soils.pdf

IPNI. (n.d.). *Nutrient source specifications.* Retrieved November 21, 2013, from International Plant Nutrition Institute: https://www.ipni.net/publication/nss.nsf/0/2F200FA9C8C946F0852579AF00762904/$FILE/NSS-09%20Monoammonium%20Phosphate.pdf

Jenkins, D., & Hermanowicz, S. W. (1991). Principals of Chemical Phosphate Removal. In R. Sedlak, & R. Sedlak (Ed.), *Phosphorus and Nitrogen Removal from Municipal Wastewater, Principles and Practice* (Vol. 2). New York.

Johnson, A. E., & Richards, I. R. (2003). Effectiveness of different precipitated phosphates as phosphorus sources for plants. *Soil Use and Management, 19*(1), 45-49.

Kalmykova, Y., Harder, R., Borgestedt, H., & Svanang, I. (2012). Pathwats and Management of Phosphorus in Urban Areas. *Journal of Industrial Ecology, 16*(6).

Kilimohai Organic. (2007). *East African Organic Products Satandards.* Kilimohai Organic.

Kopec, D. M. (1994, October). *Easing the Roller Coaster Ride with Slow Release Fertilizers.* Retrieved from Turf: turf.arizona.edu/tips1094.html

Kroiss, H., Rechberger, H., & Egle, L. (2011). Phosphorus in Water Quality and Waste Management. In M. S. Kumar (Ed.), *Intergrated Waste Mangament* (Vol. 2, pp. 183- 218). Austria: Intech.

Kujawa-Roeleveld, K., & Zeeman, G. (2006). Anaerobic Treatment in Decentralized and Source-Separation-Based Sanitation Concepts. *Reviews in Environmental Science and Biotechnology, 5*(1), 115-139.

Kvale, S. (1996). *Interviews: An introduction to Qualitative Research Interviewing.* California: SAGE.

Lienert, J., Larsen, (2004). Introducing urine separation in Switzerland: NOVAQUATIS, an interdisciplinary research project. 2nd International Symposium on Ecological Sanitation Lübeck Deutsche Gesellschaft für Technische Zusammenarbeit (GTZ) GmbH, 891-899.

Le Corre , K. S., Valsami-Jones , E., Hobbs , P., & Parsons , S. A. (2009, May 28). Phosphorus Recovery from Wastewater by Struvite Crystallization: A Review. *Critical Reviews in Environmental Science and Technology*.

Lenntech. (2005). *Phosphorus removal from wastewater*. Retrieved January 10, 2014, from Lenntech: http://www.lenntech.com/phosphorous-removal.htm

Levlin, E. (2004). *Reovery of phosphate from sewage slduge and separatin of metals via ion exchange.* Royal insitute of technology, Land and water resource engieering, Stockholm.

Li, X. Z., & Zhao, Q. L. (2003). Recovery of ammonium-nitrogen from landfill leachate as a multi-butrient fertilizer. *Ecological Engineering, 20*(2), 171-181.

Liberti, L., Petruzzelli, D., & De Florio, L. (2001). REM-NUt ION Exchange Plus Struvite Precipitation Process. *Holland Conference.*

Liu, y., Villalba, G., Ayres, R. U., & Schroder, H. (2008). Global Phosphorus Flows and Environmental Impacts from a Consumption Perspective. *Journal of Industrial Ecol, 12*(2).

Margate, R. Z., & Magat, S. S. (2012). *Phillipine coconut authority.* Retrieved November 2, 2012, from Phillipine coconut authority: www.pca.da.gov.ph/pdf/techno/salt.pdf

Max - Neef, M. A. (2005, January). Foundations of transdisciplinarity. *Ecological Economics, 53*(16).

Mels, A., Castellano, D., Braadbaart, O., Veenstra, S., Dijkstra, I., & Meulman, B. (2009). *Sanitation servies for informal settlements of Cape Town.* Desalination, Cape Town.

Montag, D. (2008). *Phosphorus recovery in wastewater treatment - Development of a procedure for integration into municipal wastewater treatment plants. .* Dissertation.

Montag, D. (2009). The PASH process for P-recovery and overview of the. *Recycling management of plant nutrients, especially phosphorus.* Berlin: German Funding Programme.

Morris, M., Kelly, V. A., Kopicki, R. J., & Byerlee, D. (2007). *Fertilizer Use in African Agriculture.* The World Bank, Agriculture and Rural Development. Washington: The World Bank.

Mostert, A. (2013). *Fertilizer Consumption in South Africa 2013*. Retrieved November 13, 2013, from Fertilizer Soicety of South Africa: http://www.fssa.org.za/Statistics/Fertilizer_Consumption_in_South_%20Africa_1955-2017.pdf

Motevallian, S. S., & Tabesh, M. (2009). *A Framework for Sustainability Assessment of Urban Water Systems Using a Participatory Approach.* Thesis, University of Tehran, Infrastructures, School of Civil Engineering, , Tehran.

Muga, H., & Mihelcic , J. R. (2007, March 27). Sustainability of wastewater treatment technologies. *Journal of Environmental Management , 88*.

Muller, J. A., Gunther, L., Dockhorn, T., Dichtl, N., Phan, L. C., Urban, I., . . . Bayerle, N. (2007). *Nutrient Recycling from Sewage Sludge using the Seaborne Process.* Insitute of Sanitary and Environmental Engineering, Gifhorn.

Musango, J., Brent, A. C., Armigon, B., Prestorious, L., & Muiller, H. (2012, November). A system dynamics approach to technology sustainability assessment: The case of biodiesel developments in South Africa. *Technovation, 32*, 639 -651.

Musango, K. J., & Brent, A. C. (2010, November). A conceptual framework for energy technology sustainability assessment. *Energy for Sustainable Development*, 84 -91.

Muzanenhamo, P., & Sikosana, M. (2012). *Phosphate recovery from wastewater treatement effluent using ion exchange resins.* University of Cape Town, Chemical Engineering. Cape Town: Unversity of Cape Town.

Nattorp, A. (2013). Recovery Technologies products. *Phosphorus recycling from prototype to market.* Northwestern: Univeristy of Applied Sciences and Arts.

Nawa, Y. (2001). *P-recovery in Japan – the PHOSNIX process.* Retrieved January 13, 2014, from JKI: http://www.jki.bund.de/fileadmin/dam_uploads/_koordinierend/bs_naehrstofftage/baltic21/8_poster%20UNITIKA.pdf

Neethling, J. B. (2013). Phosphorus removal challenges and opportunities. *IWEA Nutrient Removal and Recovery Workshop.* Addison, IL: HDR Engineering.

Neethling, J. B. (2013). Phosphorus Removal Challenges and Opportunities. *IWEA Nutrient REmoval and Recovery Workshop.* Addison: HDR Engineering.

Neethling, J. B., Smith, S., Moller, G., Lancaster, C., Pincine, A. B., & Zhang, H. (2009). *Tertiay phosphorus Removal.* WERF. WERF.

Nguyen, T. A., Ngo, H. H., Guo, W., & Nguyen, T. V. (2013). Phosphorus removal from Aqueous Solutions by Agriculture By -products: A Critical Review. *Journal of Water Sustainability, 2*(3), 193-207.

Nieminen, J. (2010). *PHOSPHORUS RECOVERY AND RECYCLING FROM MUNICIPAL WASTEWATER SLUDGE.* Aalto University, Civel and Environmental Engineering. Aalto University.

Nieminen, J. (2010). *PHOSPHORUS RECOVERY AND RECYCLING FROM MUNICIPAL WASTEWATER SLUDGE.* Aalto University, Civel and Environmental Engineering. Aalto University.

OSTARA. (2013). Retrieved February 10, 2014, from OSTARA.com: http://www.ostara.com/sites/default/files/pdfs/Saskatoon_Ostara_Case%20Study.pdf

Overview of the technology transfer process: RERC Technology Transfer. (n.d.).

Panasiuk, O. (201). *Phosphorus Removal and Recovery from Wastewater using Magnetite.* Master of Science, Royal Institute of Technology, Stockholm.

PAQUES. (n.d.). *PAQUES Products*. (PAQUES, Producer) Retrieved April 2, 2013, from PAQUES: en.paques.nl/pageid=199/PHOSPAQ%99.html

Pawar, J. (2012, June). *LOPROX: Alternative pre-treatment of spent caustic waste water by wet air oxidation.* Retrieved from Induswater: http://induswater.ncl.res.in/Resources/Presentations/Jyoti-Pawar-Bayer%20(2).pdf

Petzet, S., & Cornel, P. (2013). Phosphate Recovery from Wastewater. In R. E. Hester, & R. M. Harrison, *Waste as a Resource.* Cambridge, UK: RSCPublishing.

Putnam, D. (1971). *Composition and concentrative properties of human urine.* National Aeronautics and Space Administration , Langley Research Centre. Washington: NASA.

Richert, A., Grensch, R., Jonsson, H., Stenstrom, T.-A., & Dagerskog, L. (2010). *Practical Guidance on the Use of Urine in Crop Production.* Stockhlom Environment Instiute, EcoSanRes . Stockhlom: Sustainable Sanitation Alliance.

Rocks for Crops. (2001). South Africa. In *Rocks for Crops* (pp. 257-268).

Romer, W. (2006). Plant availability of P from recycling products and phosphate fertilizers in a growth chamber trial with rye seedlings. *Journal of Plant Nutrition and Soil Science, 169*(6), 826-832.

Ronteltap, M., Maurer, M., & Gujer, W. (2007). The behaviour of pharmaceuticals and heavy metals during struvite precipitation in urine. *Water Research, 41*(9), 1859-1868.

Roseberg, R. J., & Christensen, N. W. (1986). Chloride, soil Solution osmotic potenetila and soil pH effects on nitirfication. *Soil Science Society of America, 50*(4), 941 - 945.

Rossle, W. H., & Pretorius , W. A. (2001). Preview of characterisation requirements for in-line prefermenters Paper 1: Wastewater characterisation. *WaterSA, 27*(3), 405-412.

Rundgren, G., & Lustig, P. (2005). *Feasibility study for the establishment of certification bodies for organic agriculture in Eastern and Southern Africa).* Retrieved February 13, 2014, from grolink: http://www.grolink.se/Resources/studies/719%20Afrocert%20Rapport%20Final.PDF

Rybicki, S. M. (1997). *New Technologies of phosphorus removal from wastewater.* Royal Institute of Technology., Advanced wastewater Treatment.

Sartorius, C., von Horn, J., & Tettenborn, F. (2011). *Phosphorus Recovery from Wastewater - State-of-the-art and Futre Potential.* Fraunhofer Institute for Systems and Innovation Research , Nutrient Recovery and Mangement . Karlsruhe : Water Environment Federation.

Scheidig, K., Schaaf, M., & Mallon, J. (2009). Profitable recovery of phosphorus from sewage sludge and meat & bone meal by the Mephrec process-a new means of thermal sludge and ash treatment. *Internationa Conference on Nutrient Recovery from Wastewater Streams* (pp. 563-566). London: IWA.

Schick, J., Kratz, S., Adam, C., & Schnug, E. (2009). Techniques for P-recovery from waste water and sewage sludge and fertilizer quality of P-recycling products. *P-recycling conference .* Berlin.

Schipper, W. J., & Korving, L. (2009). Full-scale plant test using sewage sludge ash as raw material for phopsphorus production. *Internation Conference on Nutrient Recovery from Wastewater Streams* (pp. 591-598). Vancouver: IWA.

Schipper, W. J., Klapwijk, A., Potjer, B., Rulkens, W. H., Temmink, B. G., Kiestra, F. D., & Lijmbach, A. C. (2001, September). Phosphate recycling in the phosphorus industry. *Environmental Technology*.

Schouw, N. L., Danteravanich, S., Mosbaek, H., & Tjell, J. C. (2009). Composition of human excreta: A case study from Southern Thailand. *Science Total Environ*, 155-166.

Schröder, , J. J., Cordell, D., Smit , A. L., & Rosemari, A. (2009). *Sustainable Use of Phosphorus.* Report 357, Plant Research International.

Seaborne. (n.d.). *Sewage Slduge to Fertilizer.* Retrieved from Seaborne-epm: http://www.seaborne-epm.de/englisch/3_Downloads/daten/info_project_gf_e.pdf

Sengupta, S. (2013). Macronutrient Removal and Recovery from Tertiary Treatment of Wastewater. In A. C. Society, *Novel Solutions to Water Pollution* (Vol. 1123, pp. 167-187).

Sims, C. (1999). *Profile: Foskor. Industrail minerals.* Foskor.

Sims, C. (1999). *Profile: Foskor. Industrial minerals.* Foskor.

Slibverwerking Noord - Brubant. (2013). *Phosphate recovery*. Retrieved February 27, 2013, from SNB: http://www.phosphaterecovery.com/the-phosphate-issue/how-much-phosphate-is-left/77

Smith, D. (Director). (2012). *The first full-scale Multiform Harvest system became operational at the Yakima WWTP in May 2012.* [Motion Picture]. US.

Smith, D. S., Takacs, I., Murthy, S., Daigger, G., & Szabo, A. (2008). Phosphate complexation model and its complications for chemical phosphorus removal. *Water Environemnent Research, 80*(428).

Smith, J. A., & Osborn, M. (2007). Interpretative Phenomenological Analysis. In J. Smith, *Qualitative Psychogy* (pp. 53 -80).

South African department of Transport. (2005). *North West Province Freight Transport Databank*. Retrieved February 10, 2014, from http://www.nwpg.gov.za/transport/nwftd/nw/industries/fertiliser_distribution/index_xml.html

Spuhler, D., & Gensch, R. (2011). *Sanitation Systems.* Retrieved May 28, 2013, from Sustainable sanitaiton and water management: http://www.sswm.info/print/1728?tid=707

Stratful, I., Scrimshaw, M. D., & Lester, J. N. (2004). Removal of struvite to prevent problems associated with its accumulation in wastewater treatment works. . *Water Environment Research, 76*, 437-443.

Strom, P. F. (2006). *Technologies to remove phosphorous from wastewater .* Rutgers University, Environmenta Science .

Terman, G. L., & Taylor, A. W. (1965). Sources of Nitorgen and phosphorus, Crop Respnse to Nitrogen abd Phosphorus in metal ammomium Phosphates. *Journal of Agricutlture and Food Chemistry*, 497-500.

The Money Converter. (2014, March 13). *The Money Converter*. Retrieved March 13, 2014, from http://themoneyconverter.com/ZAR/EUR.aspx

Trenkel, M. E. (1997). *Controlled-Release and Stabilized Fertilizers in Agriculture.* International Fertilzier Industry Association. Paris: International Fertilzier Industry Association.

UNEP. (2007, August). *Organic Agriculture in Africa .* Retrieved March 3, 2014, from UNEP: http://www.unep.org/training/programmes/Instructor%20Version/Part_2/Activities/Human_Societies/Agriculture/Supplemental/Organic_Agriculture_in_Africa.pdf

US. Environmental Proctection Agency. (2007). *Advancede Wastewater Treatment to achieve low concentration of phosphorus .* US. Environmental Proctection Agency.

USGS. (2013). *Mineral Commodity Summaries 2013.* U.S Geoligal Survey, U.S department of the interior. USGS.

Usman, K., Khan, S., Ghula,, S., Khan, M. U., Khan, N., Khan, M. A., & Khalil, S. K. (2012, Novmeber). Sewage Sludge: An important bilogical

resource for sustainable agriculture and its environmental implications. *American Journal of Plant Science*, 1708-1721.

Vinneras, B. (2001). *Faecal separation and urine deiversion for nutrient management of household biodegradable waste and wastewater.* Swedish University of Agriculture Sciences, Agriculture Engineering. Swedish University of Agriculture Sciences.

Vinneras, B. (2001). *Faecel separation and urine diversion for nutrient management of household biodegradable wastewater.* Thesis, Swedish University of Africultural Sciences, Agricultural Engineering.

Vinneras, B., & Jonsson, H. (2002, April 30). Faecal seperation for nutrient management - evalutaion of different separation techniques. *Urban Water, 4*, 321-329.

VUNA. (2013, December). Pathogens in urine. *Promoting sanitation and nutrient recovery through urine separation*.

VUNA. (2013, December). Urine Fertilizers: Greenhouse trials with struvite and nitrified urine. *Promoting sanitation and nutrient recovery through urine separation*.

Wang, D. B., Li, X. M., Ding, Y., & Zeng, G. M. (2009, November). Nitrogen and phosphorus recovery from wastewater and the supernate of dewatered sludge. *1*(3), 236-2242.

Washington state deaprtment of health. (2005). *Nitrogen reducein technolgies for onsite wastewater treatment systems.* Washington state deaprtment of health, Environmental Health and Safety. Washington state deaprtment of health.

Wastewater solutions group. (2012). *Container wastewater treatment plants.* Retrieved July 21, 2013, from Wastewater solutions group: www.wastewater.at

Water Environment Research Federation. (2009). *Sustainable Technologies for Achieveing Very Low Nitorgen and Phopsphorus Effluent Limits.*

Water Research commission. (1997). *Permissible Utilisation and Disposal of Sewage Sludge.* Pretoria: Water Research commission.

Weerasuiya, T. J., Pushpakumara, S., & Cooray, P. I. (1993). Acidulated pegmatitic mica: a promising multi-nutrient fertilizer. *Agroecosyst, 56*(67), 525-531.

Wefnet. (2009). *Chemical Phosporus removal.* Retrieved January 10, 2014, from Wefnet: http://www.wefnet.org/biological/NutrientRemoval/Chapter%2007%20Final%20Draft.pdf

Weigand, H., Bertau, M., Hubner, W., Bohndick, F., & Bruckert , A. (2012, January). RecoPhos: Full-scale fertilizer production from sewage sludge ash. *Waste management*.

Werner, C. (2006). *Closing the loop thorugh ecological sanitation.* Deutsche Gesellschaft für Technische Zusammenarbeit (GTZ) GmbH , Ecosan sector programme.

White, S., & Cordell, D. (2009, May). The story of phosphorous: Global food security. *Global environmental change, 19*(2), 292 -305.

Wilkinson, M. J., Crafford, J. G., Jonsson, H., & Duncker, L. (2009). *Cost Benefit Analysis of the Use of Humanure from Urine Diversion Toilets to Improve Subsistence Crops in the Rural Areas of South Africa.* CSIR - Built Environment and Swedish Univesity of Agricultureal Sciences, Energy and Technology. Pretoria: Sustento Development Services.

WIN - SA. (n.d.). *eThekwini's Water and Sanitation Programme: Lessons series, Lesson 2.* Lessons series, Water Information Network , Durban.

www.Oregon.gov. (n.d.). Retrieved from BioEnergy in Oregon: www.oregon.gov

Zhigang, L., & Qingliang, Z. (2008). . nhanci- ng phosphorus recovery by a new internal recycle seeding MAP reactor. . *Bioresource Technology, 99*, 6488-6493.

Zhou, A., & Tang, J. (2008). *Progress in the Study of Magnesium Ammonium Phosphate Crystallization Reactor.* University of Science and TEchnology Beijing, Metal mines.

9 Appendices

Appendix I

Saturation indexes

Simulation S1:

----------Saturation indices----------

Phase	SI**	log IAP	log K(298 K, 1 atm)	
Anhydrite	-2.85	-7.21	-4.36	CaSO4
Aragonite	0.95	-7.38	-8.34	CaCO3
Artinite	-4.14	5.46	9.60	MgCO3:Mg(OH)2:3H2O
Brucite	-4.30	12.54	16.84	Mg(OH)2
Calcite	1.10	-7.38	-8.48	CaCO3
CH4(g)	-121.81	-124.67	-2.86	CH4
CO2(g)	-1.48	-2.95	-1.47	CO2
Dolomite	2.62	-14.47	-17.09	CaMg(CO3)2
Dolomite(d)	2.07	-14.47	-16.54	CaMg(CO3)2
Eitelite	-2.95	3.41	6.36	NaMg0.5CO3
Epsomite	-4.79	-6.93	-2.14	MgSO4:7H2O
Gypsum	-2.64	-7.22	-4.58	CaSO4:2H2O
H2(g)	-36.53	-39.68	-3.15	H2
H2O(g)	-1.51	-0.00	1.51	H2O
Halite	-4.76	-3.18	1.58	NaCl
Huntite	1.34	-28.63	-29.97	CaMg3(CO3)4

Hydromagnesite -7.03 -15.79 -8.76 Mg5(CO3)4(OH)2:4H2O

Hydroxyapatite 6.94 -50.56 -57.50 Ca5(PO4)3OH

Magnesite 0.95 -7.08 -8.03 MgCO3

Mirabilite -5.49 -6.60 -1.11 Na2SO4:10H2O

Nahcolite -2.31 -2.86 -0.55 NaHCO3

Natron -5.46 -6.77 -1.31 Na2CO3:10H2O

Nesquehonite -1.47 -7.09 -5.62 MgCO3:3H2O

NH3(g) -4.12 -2.35 1.77 NH3

O2(g) -10.13 -13.03 -2.89 O2

Periclase -9.04 12.54 21.58 MgO

Portlandite -10.56 12.24 22.80 Ca(OH)2

Struvite 0.00 -13.15 -13.15 MgNH4PO4

Thenardite -6.40 -6.58 -0.18 Na2SO4

Thermonatrite -6.88 -6.76 0.13 Na2CO3:H2O

Trona -8.83 -9.62 -0.80 NaHCO3:Na2CO3:2H2O

Simulation S2:

----------Saturation indices----------

Phase SI** log IAP log K(298 K, 1 atm)

Anhydrite -3.02 -7.38 -4.36 CaSO4

Aragonite 1.52 -6.81 -8.34 CaCO3

Artinite 1.50 11.10 9.60 MgCO3:Mg(OH)2:3H2O

Brucite -0.12 16.72 16.84 Mg(OH)2

Calcite	1.67	-6.81	-8.48	CaCO3
CH4(g)	-122.05	-124.91	-2.86	CH4
CO2(g)	-4.18	-5.65	-1.47	CO2
Dolomite	4.67	-12.42	-17.09	CaMg(CO3)2
Dolomite(d)	4.12	-12.42	-16.54	CaMg(CO3)2
Eitelite	-1.18	5.18	6.36	NaMg0.5CO3
Epsomite	-4.07	-6.21	-2.14	MgSO4:7H2O
Gypsum	-2.81	-7.39	-4.58	CaSO4:2H2O
H2(g)	-35.91	-39.06	-3.15	H2
H2O(g)	-1.51	-0.00	1.51	H2O
Halite	-3.43	-1.85	1.58	NaCl
Huntite	6.33	-23.64	-29.97	CaMg3(CO3)4
Hydromagnesite	3.02	-5.74	-8.76	Mg5(CO3)4(OH)2:4H2O
Hydroxyapatite	7.24	-50.26	-57.50	Ca5(PO4)3OH
Magnesite	2.42	-5.61	-8.03	MgCO3
Mirabilite	-4.18	-5.29	-1.11	Na2SO4:10H2O
Nahcolite	-2.63	-3.18	-0.55	NaHCO3
Natron	-3.41	-4.72	-1.31	Na2CO3:10H2O
Nesquehonite	0.00	-5.62	-5.62	MgCO3:3H2O
NH3(g)	-2.93	-1.16	1.77	NH3
O2(g)	-11.37	-14.26	-2.89	O2
Periclase	-4.86	16.72	21.58	MgO
Portlandite	-7.28	15.52	22.80	Ca(OH)2

Struvite	0.00	-13.15	-13.15	MgNH4PO4
Thenardite	-5.08	-5.26	-0.18	Na2SO4
Thermonatrite	-4.82	-4.69	0.13	Na2CO3:H2O
Trona	-7.08	-7.88	-0.80	NaHCO3:Na2CO3:2H2O

Appendix II

XRD Spectrum for experiment E1[b], E1[c], E2[b] and E2[c]

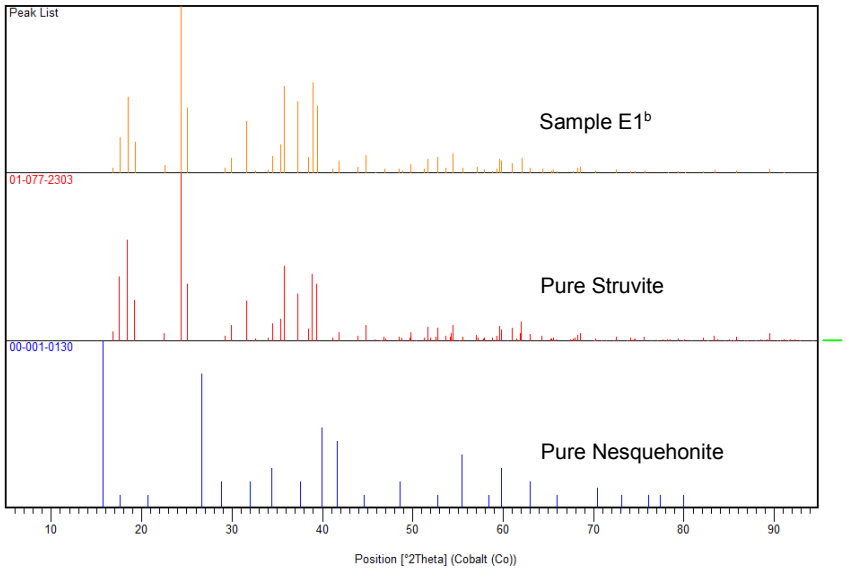

Figure 43: Spectrum for the precipitate sample from experiment E2[b] compared against that pure struvite and nesquehonite.

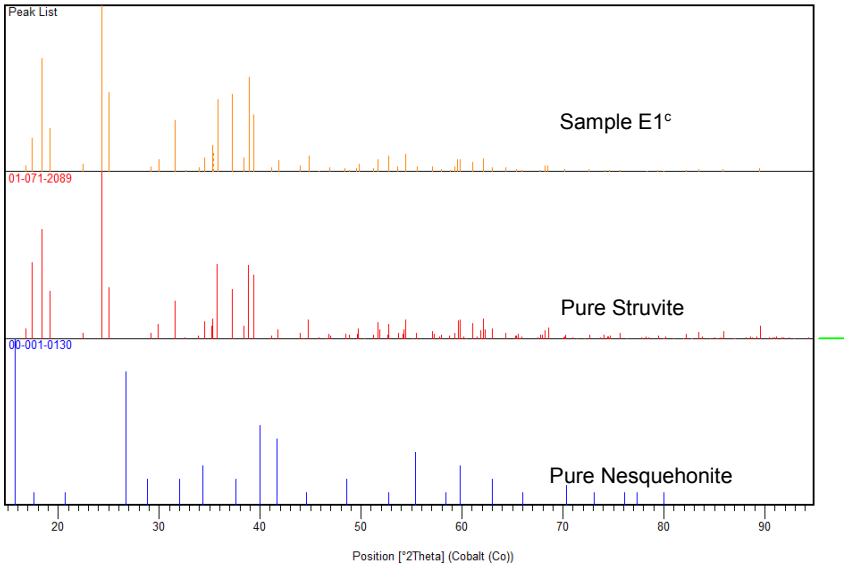

Figure 44: Spectrum for the precipitate sample from experiment E2[c] compared against that pure struvite and nesquehonite.

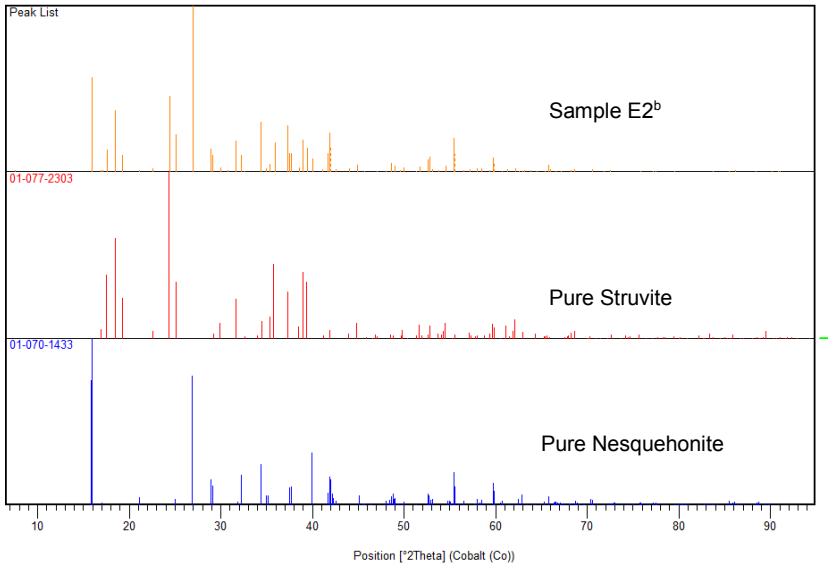

Figure 45: Spectrum for the precipitate sample from experiment E3^{b} compared against that pure struvite and nesquehonite.

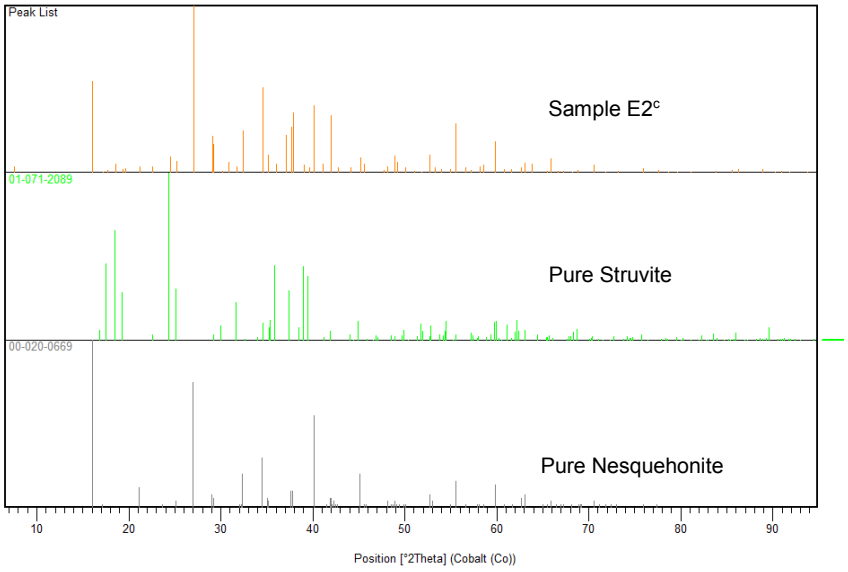

Figure 46: Spectrum for the precipitate sample from experiment E3^{c} compared against that pure struvite and nesquehonite.

Appendix III

Characterisation of the VUNA struvite seeds

Table 14 sows the the quantitative characterisation of the VUNA struvite seeds. The VUNA seeds were produced by MgCl2 dosing in 2013.

Table 14: The quantitative analysis of the VUNA struvite seeds.

Type of seeds	Mg^{2+}	$PO_4 - P$	$NH_4 - N$
VUNA	1.02 ± 0.05	1.00	1.05 ± 0.05

Figure 47 shows the SEM image of the VUNA seeds.

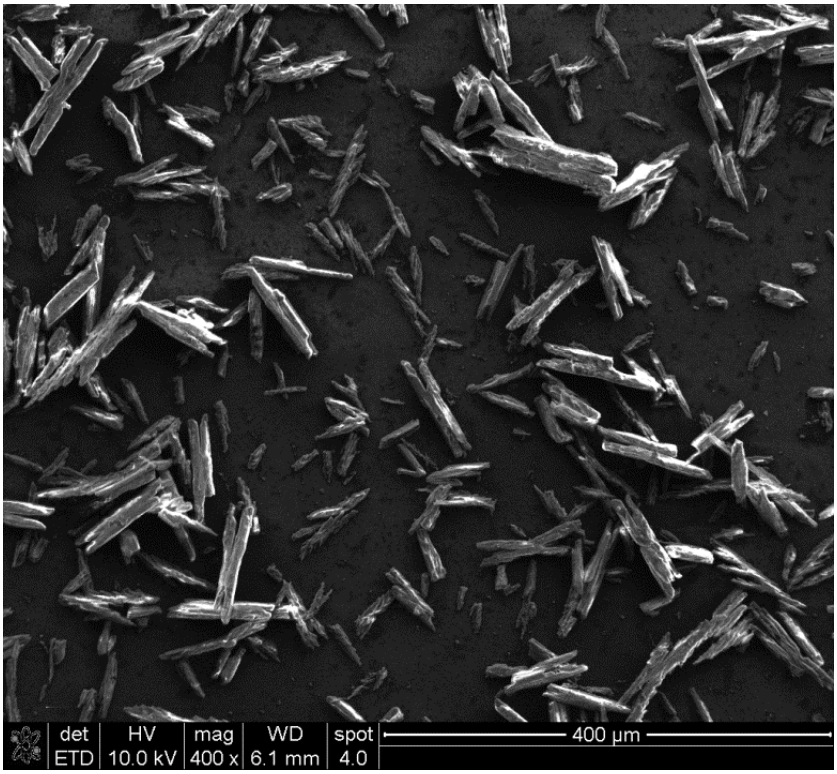

Figure 47: SEM image if the VUNA seeds used for experiment E4[a], E4[b]and E5[a], E5[b].

Appendix IV

Economic evaluation of electrochemical and chemical dosing precipitation of struvite

The amount of magnesium needed to precipitate out 96 % of the phosphorous as achieved in an electrochemical precipitation cell using magnesium sacrificial anode as in experiment E3 was calculated as follows:

$$m_{Mg,dissolves}(t) = \left(m_p(t_0) - m_p(t)\right).\frac{M_{Mg}}{M_p} + m_{Mg}(t) - m_{Mg}(t_0) \quad (34)$$

$$m_{Mg,dissolves}(g) = (102.1 - 4.1).\frac{24.3}{31} + 33.4 - 2.6 = 108.2mg = 0.108g \quad (35)$$

$$m_{Faraday} = \frac{M_{Mg}}{z}.\frac{Q}{F} = \frac{M}{z}.\frac{It}{F} = \frac{24.3}{2}.\frac{0.103 \times 2 \times 3600}{96485} = 0.093g \quad (36)$$

$$Coulombicefficiency = \frac{m_{Mg,dissolves}}{m_{Mg,Faraday}} \times 100 = \frac{0.108}{0.093} \times 100 = 115.3\% \quad (37)$$

Cost of magnesium source:

$$\text{Mass of magnesium needed per litre of urine} = 0.108g = 0.000108kg \quad (38)$$

$$\text{Price of magnesium per kg} = US\$\ 2.24 = ZAR\ 27.00 \quad (39)$$

$$\text{Price of magnesium per litre of urine} = ZAR\ 0.003 \quad (40)$$

$$\text{Price of magnesium per } m^3 \text{ of urine} = ZAR\ 3.00 \quad (41)$$

$$\text{Price of magnesium per kg of struvite} = ZAR\ 3.77 \quad (42)$$

If the electrochemical cell is run for 2 hours with a current of 0.103 A at a cell voltage of 2.3 V per litre of feed. Cost of electricity:

$$\text{Electric energy} = \int_0^t V_{cell} I \, dt = V_{cell} I (t_1 - t_2) = 2.3 \times 0.103 \times 2 \quad (43)$$

$$\text{Electric energy} = 0.474 \text{ WhL}^{-1} \text{ of urine} = 473.8 \text{ Whm}^{-3} \text{of urine} \quad (44)$$

$$= 0.474 \text{kWm}^{-3} \text{of urine}$$

$$\text{Price of electric energy per kWh} = \text{ZAR } 1.00 \quad (45)$$

$$\text{Price of electric energy per m}^3 \text{ of urine} = \text{ZAR } 0.474 \quad (46)$$

$$\text{Total expense of the elctrochemical precipitation of struvite} \quad (47)$$
$$= \text{ZAR } (0.47 + 3.00) = \text{ZAR } 3.47 \text{ per m}^3 \text{of urine}$$

$$= \text{ZAR } 3.47 \text{ per kg of struvite}$$

The amount of magnesium needed to precipitate out 96 % of the phosphorous using in a chemical dosing method of precipitation with $MgCl_2$ at Mg:P molar ratio of 1.2

$$\text{Mass of magnesium need for 96 \% per litre of urine}$$
$$= 0.96 \times \left(n_p(t_0) - n_p(t)\right) \times 1.2) \times M_{MgCl_2}$$
$$= (\, 0.96 \times (0.00316) \times 1.2) \times 95.2 \;\; = 0.362\text{g} \quad (48)$$
$$= 0.000362 \text{ kg}$$

$$\text{Price of magnesium chloride per kg} = \text{ZAR } 8.30 \quad (49)$$

$$\text{Price of magnesium chloride per kg of struvite} \quad (50)$$
$$= \text{ZAR } 3.87$$

$$\text{Total expenses of the conventional precipitation of struvite} \quad (51)$$

$$= \text{ZAR } 3.87 \text{ per kg of struvite}$$

Appendix V:

Specifications of the thermodynamic model (wateq4f.dat)

The file named wateq4f.dat contains thermodynamic data for the aqueous species and gas and mineral phases that are essentially the same as WATEQ4F (Ball and Nordstrom, 1991). In addition to data for the elements in the database file, phreeqc.dat, the database file wateq4f.dat contains data for the elements: arsenic, cesium, iodine, nickel, rubidium, selenium, silver, and uranium.

We used the PHREEQC Interactive software (Version 2.15.0; Parkhurst and Appelo, 1999) to calculate the saturation of struvite and nesquehonite. The basic database wateq4f.dat was extended with terms for acetate (data taken from the minteq.dat database) and struvite (solubility constant pK =13.15; Taylor et al., 1963). Acetate was used as a model substance for chemical oxygen demand (COD). We used the concentrations given in Table 1 as the initial conditions and fitted the ion balance by adjusting the acetate concentration.

The saturation index SI is given by:

$$SI = \frac{log_{10}(IAP)}{log_{10}(k_{sp})}$$

IAP ion activity product; Ksp solubility product of the respective mineral

Appendix VII

Setup of the seeded continuously stirred electrochemical precipitation of struvite reactor system

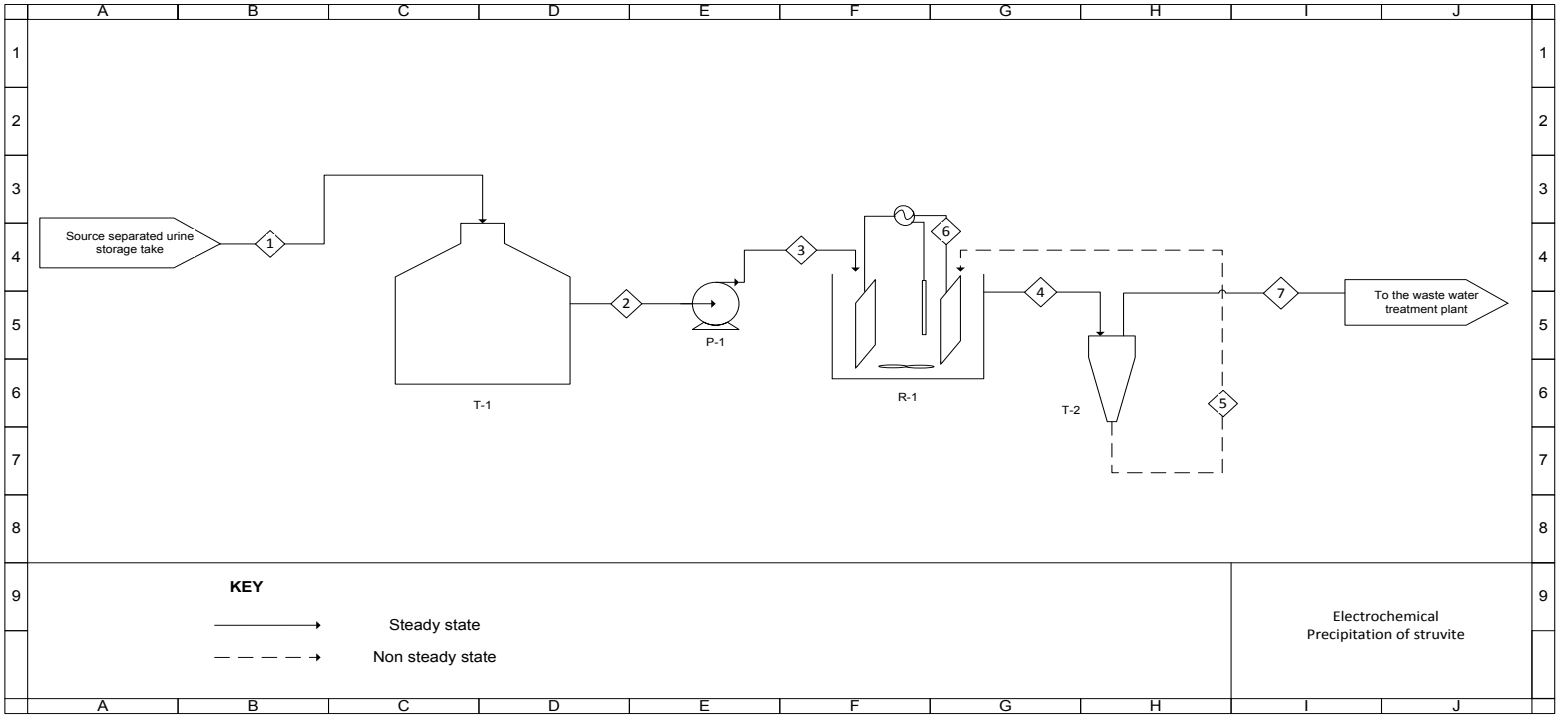

Figure 48: Setup of the seeded continuously stirred electrochemical precipitation of struvite reactor system

Appendix VIII

Ethics form

EBE Faculty: Assessment of Ethics in Research Projects

Any person planning to undertake research in the Faculty of Engineering and the Built Environment at the University of Cape Town is required to complete this form before collecting or analysing data. When completed it should be submitted to the supervisor (where applicable) and from there to the Head of Department. If any of the questions below have been answered YES, and the applicant is NOT a fourth year student, the Head should forward this form for approval by the Faculty EIR committee: submit to Ms Zakiya Chikte (Zakiya.chikte@uct.ac.za); New EBE Building, Ph 021 650 5739).

Please note – It is important to keep a signed copy of this form as students must include a copy of the completed form with the dissertation/thesis when it is submitted for examination.

Name of Principal Researcher/Student: NICOLE MALANDA Department: CHEMICAL ENGINEERING

If a Student: Degree: MSC. CHEMICAL ENGINEERING Supervisor: HARRO VON BLOTTNITZ

If a Research Contract indicate source of funding/sponsorship: WATER RESEARCH COMMISSION

Research Project Title: AN INVESTIGATION OF IMPROVEMENTS TO ELECTROCHEMICAL

PRECIPITATION OF STRUVITE FROM SOURCE SEPARATED URINE

Overview of ethics issues in your research project:

Question 1: Is there a possibility that your research could cause harm to a third party (i.e. a person not involved in your project)?	YES	NO ✔
Question 2: Is your research making use of human subjects as sources of data? If your answer is YES, please complete Addendum 2.	YES	NO ✔
Question 3: Does your research involve the participation of or provision of services to communities? If your answer is YES, please complete Addendum 3.	YES	NO ✔
Question 4: If your research is sponsored, is there any potential for conflicts of interest? If your answer is YES, please complete Addendum 4.	YES	NO ✔

If you have answered YES to any of the above questions, please append a copy of your research proposal, as well as any interview schedules or questionnaires (Addendum 1) and please complete further addenda as appropriate.

I hereby undertake to carry out my research in such a way that

- there is no apparent legal objection to the nature or the method of research; and
- the research will not compromise staff or students or the other responsibilities of the University;
- the stated objective will be achieved, and the findings will have a high degree of validity;
- limitations and alternative interpretations will be considered;
- the findings could be subject to peer review and publicly available; and

- I will comply with the conventions of copyright and avoid any practice that would constitute plagiarism.

Signed by:

	Full name and signature	Date
Principal Researcher/Student: NICOLE MULENGA MALANDA	***Signed digitally by Nicole Mulenga Malanda (29/03/2016)*** ***Email: mlnnic004@myuct.ac.za*** 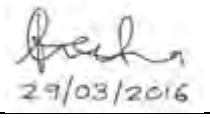	29/03/2016

This application is approved by:

Supervisor (if applicable): HARRO VON BLOTTNITZ	Harro von Blottnitz 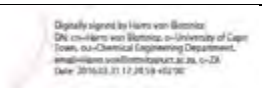	31/03/2016
HOD (or delegated nominee): Final authority for all assessments with NO to all questions and for all undergraduate research.		
Chair : Faculty EIR Committee For applicants other than undergraduate students who have answered YES to any of the above questions.		

ADDENDUM 1:
Please append a copy of the research proposal here, as well as any interview schedules or questionnaires:

ADDENDUM 2: To be completed if you answered YES to Question 2:
It is assumed that you have read the UCT Code for Research involving Human Subjects (available at http://web.uct.ac.za/depts/educate/download/uctcodeforresearchinvolvinghumansubjects.pdf) in order to be able to answer the questions in this addendum.

2.1 Does the research discriminate against participation by individuals, or differentiate between participants, on the grounds of gender, race or ethnic group, age range, religion, income, handicap, illness or any similar classification?	YES	NO
2.2 Does the research require the participation of socially or physically vulnerable people (children, aged, disabled, etc) or legally restricted groups?	YES	NO
2.3 Will you not be able to secure the informed consent of all participants in the research? (In the case of children, will you not be able to obtain the consent of their guardians or parents?)	YES	NO
2.4 Will any confidential data be collected or will identifiable records of individuals be kept?	YES	NO
2.5 In reporting on this research is there any possibility that you will not be able to keep the identities of the individuals involved anonymous?	YES	NO
2.6 Are there any foreseeable risks of physical, psychological or social harm to participants that might occur in the course of the research?	YES	NO
2.7 Does the research include making payments or giving gifts to any participants?	YES	NO

If you have answered YES to any of these questions, please describe how you plan to address these issues (append to form):

ADDENDUM 3: To be completed if you answered YES to Question 3:

3.1 Is the community expected to make decisions for, during or based on the research?	YES	NO
3.2 At the end of the research will any economic or social process be terminated or left unsupported, or equipment or facilities used in the research be recovered from the participants or community?	YES	NO
3.3 Will any service be provided at a level below the generally accepted standards?	YES	NO

If you have answered YES to any of these questions, please describe how you plan to address these issues (append to form)

ADDENDUM 4: To be completed if you answered YES to Question 4

4.1 Is there any existing or potential conflict of interest between a research sponsor, academic supervisor, other researchers or participants?	YES	NO
4.2 Will information that reveals the identity of participants be supplied to a research sponsor, other than with the permission of the individuals?	YES	NO

4.3 Does the proposed research potentially conflict with the research of any other individual or group within the University?	YES	NO

If you have answered YES to any of these questions, please describe how you plan to address these issues(append to form)